YAEC-1342

VERMONT YANKEE
CYCLE 10
CORE PERFORMANCE ANALYSIS

January 1983

Major Contributors:

B. G. Baharynejad	D. M. Kapitz
D. K. Beller	J. M. Kendall
K. J. Burns	K. E. St.John
J. T. Cronin	M. A. Sironen
G. E. Jarka	D. M. VerPlanck
	R. A. Woehlke

Approved by: R J Caccippouti 2/9/83
R. J. Caccippouti, Manager (Date)
Reactor Physics Group

Approved by: P.A. Bergeron 2/9/83
P. A. Bergeron, Manager (Date)
Transient Analysis Group

Approved by: Stephen P. Schultz 2/9/83
S. P. Schultz, Manager (Date)
Nuclear Evaluations and Support Group

Approved by: Ausaf Husain 2/9/83
A. Husain, Manager (Date)
LOCA Group

Approved by: Bruce C. Slifer 2/9/83
B. C. Slifer, Manager (Date)
Nuclear Engineering

DISCLAIMER OF RESPONSIBILITY

This document was prepared by Yankee Atomic Electric Company for its own use and on behalf of Vermont Yankee Nuclear Power Corporation. This document is believed to be completely true and accurate to the best of our knowledge and information. It is authorized for use specifically by Yankee Atomic Electric Company, Vermont Yankee Nuclear Power Corporation and/or the appropriate subdivisions within the Nuclear Regulatory Commission only.

With regard to any unauthorized use whatsoever, Yankee Atomic Electric Company, Vermont Yankee Nuclear Power Corporation and their officers, directors, agents and employees assume no liability nor make any warranty or representation with respect to the contents of this document or to its accuracy or completeness.

ABSTRACT

This report presents design information and calculational results pertinent to the operation of Cycle 10 of the Vermont Yankee Nuclear Power Station. These include the fuel design and core loading pattern descriptions; calculated reactor power distributions, power peaking, shutdown capability and reactivity functions; and the results of safety analyses performed to justify plant operation throughout Cycle 10.

TABLE OF CONTENTS

TABLE OF CONTENTS
(Continued)

LIST OF FIGURES

LIST OF FIGURES
(Continued)

LIST OF TABLES

ACKNOWLEDGEMENTS

The authors and principal contributors would like to acknowledge the contributions to this work by P. A. McGahan, K. E. Mitchell, J. Pappas, and the YAEC Word Processing Center. Their assistance in preparing figures and text for this document is recognized and greatly appreciated.

1.0 INTRODUCTION

This report provides information to support the operation of the Vermont Yankee Nuclear Power Station through the forthcoming fuel reload cycle (called Cycle 10). The refueling preceding Cycle 10 (called Reload 9) will involve the discharge of 108 irradiated fuel bundles and the insertion of 108 new fuel bundles. The resultant core will consist of 108 new fuel bundles and 260 irradiated fuel bundles of the pressurized retrofit 8X8 design (P8DPB289). All fuel bundles for Cycle 10 operation have been fabricated by General Electric (GE).

This report contains descriptions and analyses results pertaining to the mechanical, thermal-hydraulic, physics, and safety aspects of Cycle 10.

The cycle dependent operating limits as calculated for Cycle 10 are given in Appendix A.

2.0 RECENT REACTOR OPERATING HISTORY

2.1 Operating History of the Current Cycle

The current operating cycle is Cycle 9. The reactor was started up for this cycle on December 1, 1981 and is projected to be shut down for refueling on March 5, 1983. During this period, control rod sequence exchanges were performed on the following schedule:

	SEQUENCE from	SEQUENCE to
January 28, 1982	A1-1	B2-1
March 13, 1982	B2-1	A2-1
April 24, 1982	A2-1	B1-1
June 10, 1982	B1-1	A1-2
July 24, 1982	A1-2	B2-2
September 11, 1982	B2-2	A2-2
October 30, 1982	A2-2	B1-2

The reactor has been operated smoothly and at full power with the exception of normal maintenance and a few scrams. The control rod sequence exchanges in January, April and June were performed following scrams. The rest of the exchanges occurred at minimum flow, reduced power. The reactor started coastdown on December 16, 1982 with four rods at position 30. These were pulled out on January 14, 1983. The remainder of the cycle will be in the All-Rods-Out (ARO) condition.

2.2 Operating History of Recent Applicable Cycles

Fuel to be re-irradiated in Cycle 10 includes fuel bundles which were initially inserted into the reactor in Cycles 7, 8, and 9.

Cycle 7 reactor operation proceeded at full power with normal maintenance and operational maneuvers with the exception of a three day outage in February 1980 to implement plant modifications required by the NRC (TMI fix). A total of four control rod sequences were used during the cycle.

Cycle 8 operation [1] also proceeded at full power with normal maintenance and operational maneuvers. Four control rod sequences were used in Cycle 8. Two sequence exchanges were performed at minimum flow, reduced power. Following the exchange in March 1981, the reactor was operated at reduced power for five days to allow for special testing; including, recirculation pump trip testing and reactor stability testing.

3.0 RELOAD CORE DESIGN DESCRIPTION

3.1 Core Fuel Loading

Reload 9 (Cycle 10) will discharge 108 spent fuel assemblies out of a core total of 368. Thus, the Cycle 10 core will consist of 108 new assemblies and 260 irradiated assemblies. All assemblies have bypass flow holes in the lower tie plate. Table 3.1.1 characterizes the core by fuel type, batch size, and first cycle loaded. A description of the fuel is found in Reference 2.

3.2 Design Reference Core Loading Pattern

The Cycle 10 assembly locations are indicated by the map in Figure 3.2.1. For the sake of legibility only the lower right quadrant is shown. The other quadrants are mirror images with bundles of the same type having nearly identical exposures. The new bundles (inserted during Reload 9) have been identified as R9. Similarly, irradiated bundles are designated by the reload number in which they were first introduced into the core. If any changes are made to the loading pattern at the time of refueling, they will be checked and verified acceptable under 10CFR50.59. The final loading pattern with specific bundle serial numbers will be supplied with the Startup Test Report.

3.3 Assembly Exposure and Cycle 9 History

The assumed nominal exposure on the fuel bundles in the design reference loading pattern is given in Figure 3.2.1. To obtain this exposure distribution, previous cycles up to Cycle 9 were depleted with the SIMULATE model [3,4] using actual plant operating history. For Cycle 9, plant operating history was used through 8/19/82; that is, a core average exposure of 14.339 GWD/ST. Beyond 8/19/82 the exposure was accumulated using a best-estimate rodded depletion analysis to EOFPL9. This was followed by a projected coastdown to EOC9 on 3/5/83.

Table 3.3.1 gives the assumed nominal burnup on Cycle 9 and the BOC10 exposure that results from the shuffle. In this table, as in the rest of this report, the terms "End of Cycle (EOC)" and "End of Full Power Life (EOFPL)", as applied to Cycle 10, are used interchangeably.

TABLE 3.1.1

VY CYCLE 10 FUEL BUNDLE TYPES AND NUMBERS

	Fuel Designation	Cycle Loaded	Number	Possible Bundle ID's
IRRADIATED	P8DPB289	7	60	LJGXXX, LJHXXX, LJLXXX
	P8DPB289	8	80	LJPXXX, LJUXXX
	P8DPB289	9	120	LJTXXX, LJZXXX
NEW	P8DPB289	10	108	LY4XXX

NOTE: XXX stands for the last three digits of the bundle serial number.

TABLE 3.3.1

DESIGN BASIS VY CYCLE 9 AND CYCLE 10 EXPOSURES

Assumed Previous Cycle Core Average Exposure End of Cycle 9	18.19 GWD/ST
Assumed Reload Cycle Core Average Exposure Beginning of Cycle 10	10.48 GWD/ST
Haling Calculated Core Average Exposure at End of Cycle 10	17.70 GWD/ST
Cycle 10 Capability	7.22 GWD/ST

VERMONT YANKEE
CYCLE 10
BOC BUNDLE AVERAGE EXPOSURES

PLANT COORD	23	25	27	29	31	33	35	37	39	41	43
22	R6 19.75	R7 15.34	R9 0.00	R6 22.66	R8 8.47	R7 14.83	R9 0.00	R8 11.32	R9 0.00	R8 9.71	R6 23.06
20	R7 15.40	R9 0.00	R8 6.96	R9 0.00	R7 16.74	R9 0.00	R7 13.47	R9 0.00	R8 10.63	R8 10.16	R6 22.76
18	R9 0.00	R8 6.97	R7 17.57	R8 10.63	R9 0.00	R7 15.58	R9 0.00	R8 11.07	R9 0.00	R8 11.60	R6 23.28
16	R6 22.71	R9 0.00	R8 10.82	R9 0.00	R7 17.06	R9 0.00	R8 9.67	R9 0.00	R8 11.16	R6 22.80	
14	R8 8.44	R7 16.69	R9 0.00	R7 17.19	R8 8.26	R7 15.43	R9 0.00	R8 11.65	R7 17.36		
12	R7 14.67	R9 0.00	R7 15.54	R9 0.00	R7 15.50	R8 8.25	R7 15.03	R8 10.70	R6 22.89		
10	R9 0.00	R7 13.77	R9 0.00	R8 9.65	R9 0.00	R7 15.13	R9 0.00	R8 10.97	R6 23.15		
08	R8 11.29	R9 0.00	R8 11.16	R9 0.00	R8 11.62	R8 10.62	R8 11.16	R7 17.48			
06	R9 0.00	R8 10.84	R9 0.00	R8 11.22	R7 17.21	R6 22.78	R6 23.20				
04	R8 9.67	R8 10.16	R8 11.40	R6 22.76							
02	R6 22.98	R6 23.27	R6 23.13								

BUNDLE ID
EXPOSURE (GWD/ST)

R6 - P8DPB289, RELOAD 6
R7 - P8DPB289, RELOAD 7
R8 - P8DPB289, RELOAD 8
R9 - P8DPB289, RELOAD 9

FIGURE 3.2.1

VY CYCLE 10 DESIGN REFERENCE LOADING PATTERN, LOWER RIGHT QUADRANT

4.0 FUEL MECHANICAL AND THERMAL DESIGN

4.1 Mechanical Design

One hundred and eight (108) fresh fuel bundles fabricated by the General Electric Co. will be inserted into the Vermont Yankee reactor for Cycle 10 operation. The mechanical design parameters are identical to the General Electric fabricated bundles which were inserted and irradiated during Cycles 7, 8 and 9. Table 4.1.1 identifies the major design parameters. Further descriptions of the fuel rod mechanical design and mechanical design analyses are provided in Reference 2. These design analyses remain valid with respect to Cycle 10 reactor operation. Mechanical and chemical compatibility of the fuel assemblies with the in-service reactor environment is also addressed in Reference 2.

4.2 Thermal Design

The fuel thermal effects calculations were performed using the FROSSTEY computer code [5-7]. The FROSSTEY code calculates pellet-to-clad gap conductance and fuel temperatures from a combination of theoretical and empirical models which include fuel and cladding thermal expansion, fission gas release, pellet swelling, pellet densification, pellet cracking, and fuel and cladding thermal conductivity.

The thermal effects analysis included the calculation of fuel temperatures and fuel cladding gap conductance under nominal core steady state and peak linear heat generation rate conditions. Figure 4.2.1 provides the core-average response of gap conductance. These calculations integrate the responses of individual fuel batch average operating histories over the core average exposure range of Cycle 10. The gap conductance values are weighted axially by power distributions and radially by volume. The core-wide gap conductance values for the RETRAN system simulations, described in Sections 7.1 and 7.2, are from this data set at the particular exposure statepoints.

The gap conductance values input to the hot channel (RETRAN/TCPYA01) calculations were evaluated for the P8X8R fuel bundle type as a function of the assembly exposure. The calculation assumed a 1.4 chopped cosine axial power shape with the peak power node running at the MAPLHGR limit defined in Reference 8 for the P8X8R fuel type. Figure 4.2.2 provides the hot channel response of gap conductance. In Figure 4.2.2, "planar exposure" refers to the exposure of the node running at the MAPLHGR limit.

Gap conductance values for the hot channel analysis were extracted from Figure 4.2.2 using the maximum bundle exposure of any MCPR limiting bundle within the exposure interval of interest. The SIMULATE rodded depletion (Section 5.1.2) provides predictions of both limiting MCPR and the associated bundle exposure for the entire cycle.

Table 4.2.1 provides the core average and hot channel gap conductance values used in the transient analyses (Section 7.1).

Fuel rod local linear heat generation rates at fuel centerline incipient melt and 1% clad plastic strain as a function of local axial segment exposure for the gadolinia concentrations used in Vermont Yankee P8X8R fuel were previously reported in Reference 1.

4.3 Operating Experience

All fuel bundles scheduled to be reloaded in Cycle 10 have operated as expected in previous cycles of Vermont Yankee. Off-gas measurements are at normally low levels indicating that no fuel failures are present.

TABLE 4.1.1

NOMINAL FUEL MECHANICAL DESIGN PARAMETERS

	FUEL TYPE P8X8R
Fuel Pellets	
Fuel Material (sintered Pellets)	UO_2
Initial Enrichment, w/o U-235	2.89
Pellet Density, % theoretical	95.0
Pellet Diameter, inches	0.410
Fuel Rod	
Active Length, inches	150.0
Plenum Length, inches	9.5
Fuel Rod Pitch, inches	0.640
Diametral Gap (cold), inches	0.009
Fill Gas	Helium
Fill Gas Pressure, psig	[See Ref. 2]
Cladding	
Material	Zr-2
Outside Diameter, inches	0.483
Thickness, inches	0.032
Inside Diameter, inches	0.419
Fuel Channel	
Material	Zr-4
Inside Dimension, inches	5.278
Wall Thickness, inches	0.C80
Fuel Assembly	
Fuel Rod Array	8x8
Fuel Rods per Assembly	62
Spacer Grid Material	Zr-4

TABLE 4.2.1

GAP CONDUCTANCE VALUES USED IN VY CYCLE 10 TRANSIENT ANALYSES

Cycle Exposure Statepoint (MWD/ST)	Core Average Gap Conductance (BTU/Hr-Ft^2 - ^{o}F)	Hot Channel Bundle Exposure (MWD/ST)	Hot Channel Gap Conductance (BTU/Hr-Ft^2 - ^{o}F)
BOC10	750	9680$^{(1)}$	1370
EOC10-2000 MWD/ST	960	6580	1050
EOC10-1000 MWD/ST	975	7670	1140
EOC10	990	8650	1240

NOTE

(1) Between BOC and EOC-2000 MWD/ST, the highest exposure limiting hot channel bundle is once-burned.

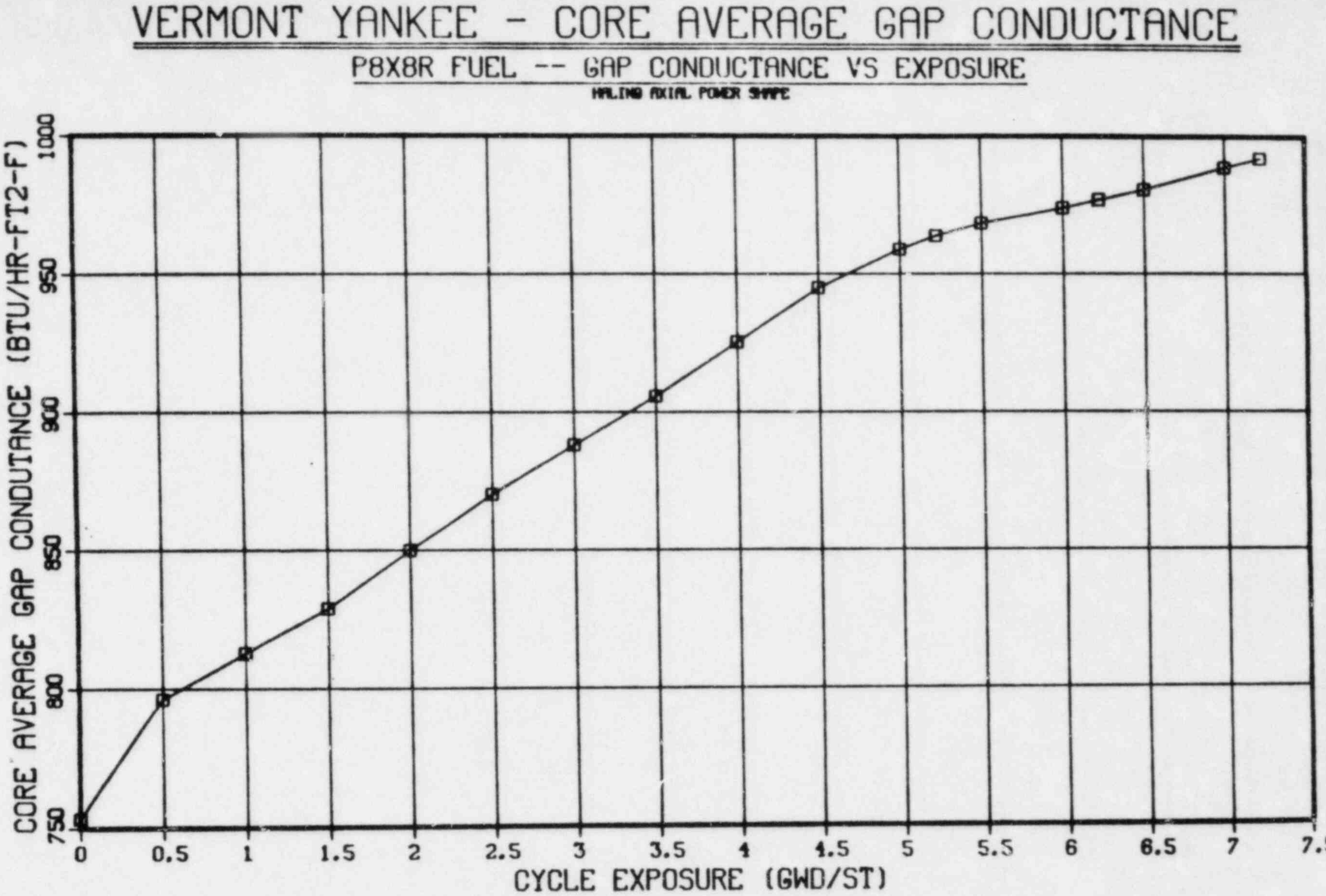

FIGURE 4.2.1

VY CYCLE 10 CORE AVERAGE GAP CONDUCTANCE VERSUS CYCLE BURNUP

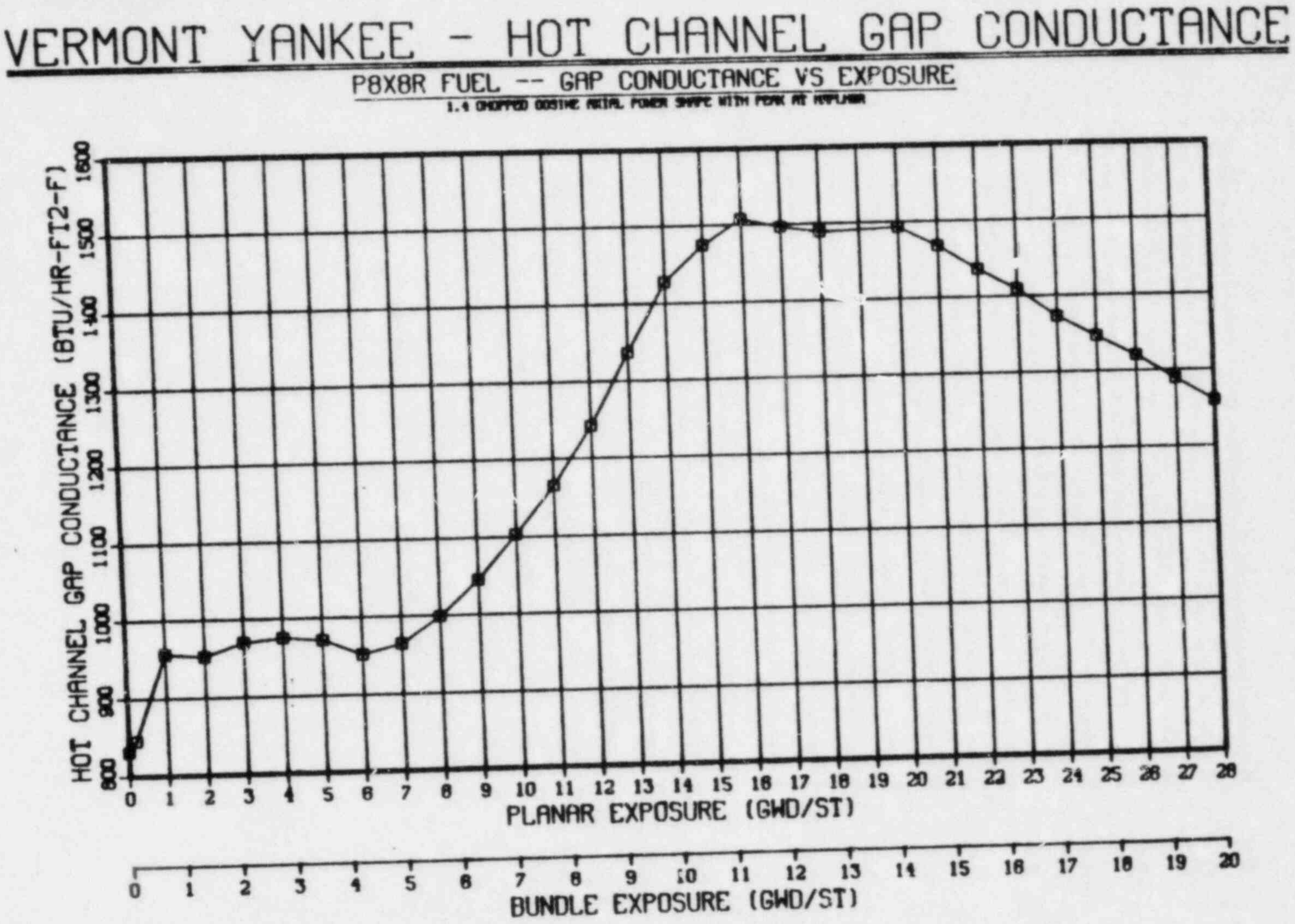

FIGURE 4.2.2

VERMONT YANKEE HOT CHANNEL GAP CONDUCTANCE FOR P8X8R VERSUS EXPOSURE

5.0 NUCLEAR DESIGN

5.1 Core Power Distributions

The cycle was depleted using SIMULATE [3] to give both a rodded depletion and an All-Rods-Out (ARO) Haling depletion. The Haling depletion serves as the basis for defining core reactivity characteristics for most transient and accident evaluations. This is primarily because its flat power shape has conservatively weak scram characteristics. The rodded depletion was used to evaluate the misloaded bundle error and the rod withdrawal error. This is because of the more realistic predictions it makes of initial CPR values. It was used in the calculation of rod drop worth because it burns the top of the core more realistically than the Haling.

5.1.1 Haling Power Distribution

The Haling power distribution is calculated in the All-Rods-Out condition. The Haling iteration converges on a self-consistent power and exposure shape for the exposure step to end of cycle. In principle, this should provide the overall minimum peaking power shape for the cycle. During the actual cycle, flatter power distributions might occasionally be achieved by shaping with control rods. However, such shaping would leave underburned regions in the core which would peak at another point in time. Figures 5.1.1 and 5.1.2 give the Haling radial and axial average power distributions.

5.1.2 Rodded Depletion Power Distribution

To generate the rodded depletion, control rod patterns were developed which gave critical eigenvalues at each point in the cycle and gave peaking similar to the Haling calculation. The resulting patterns were frequently more peaked than the Haling, but were not in excess of expected operating limits. However, as stated above, the underburned regions of the core can exhibit peaking in excess of the Haling peaking when pulling ARO at end of cycle. Figures 5.1.3 and 5.1.4 give the ARO end of cycle power distributions for the rodded depletion. Note in Figure 5.1.4 that the average axial power at ARO for the rodded depletion is more bottom peaked than the Haling (Figure 5.1.2). This would result in better scram characteristics.

5.2 Core Exposure Distributions

Cycle 10 was calculated to be capable of a cycle exposure of 7222 MWD/ST at EOFPL (no coastdown) Table 3.3.1 summarizes the resultant core average exposures. The projected BOC radial exposure distribution is given in Figure 3.2.1. The Haling calculation produced the EOFPL radial exposure distribution given in Figure 5.2.1. Since the Haling power shape is constant, it can be held fixed by SIMULATE to give the exposure distributions at various mid-cycle points. BOC, EOC-2000 MWD/ST, EOC-1000 MWD/ST, and EOC conditions were used to develop reactivity input for the core wide transient analyses.

The rodded depletion may differ from the Haling during the cycle due to the shaping of the power by the rods. However, rod sequences are swapped frequently and the overall exposure distribution at end of cycle is similar to the Haling. Figure 5.2.2 gives the EOFPL radial exposure distribution for the rodded depletion.

5.3 Cold Core Reactivity and Shutdown Margin

The cold K_{eff} with all rods withdrawn (ARO) and the cold K_{eff} with all rods inserted (ARI) at BOC were calculated using the SIMULATE code [3,4] and are shown in Table 5.3.1. K_{eff} with ARO minus the cold critical K_{eff} is the amount of excess core reactivity. K_{eff} with ARI minus the K_{eff} with ARO is the worth of all the control rods.

The cold critical eigenvalue K_{eff} was defined as the average calculated critical eigenvalue minus a 95% confidence level uncertainty. Then all cold results were normalized to make the critical K_{eff} equal to 1.000.

Technical Specifications [8] state that, for sufficient shutdown margin, the core must be subcritical by at least 0.25% +R (defined below) with the strongest worth control rod withdrawn. Again, using SIMULATE, a search was made for the strongest worth control rod at various exposures in the cycle. This is necessary because rod worths change with exposure. Then the cold K_{eff} with the strongest rod out was calculated at approximately 900 MWD/ST intervals through the cycle. Subtracting each cold K_{eff} with the strongest rod out from the cold critical K_{eff} defines the shutdown margin as a function of exposure. Figure 5.3.1 is the result. Because the local reactivity may increase with exposure, the shutdown margin may decrease. To account for this, the value R is calculated as the difference between the cold K_{eff} with the strongest rod out at BOC and the maximum cold K_{eff} with the strongest rod out in the cycle. The R for Cycle 10 is given in Table 5.3.1.

5.4 Standby Liquid Control System Shutdown Capability

The shutdown capability of the standby liquid control system (SLCS) is designed to bring the reactor from full power to cold, ARO, xenon free shutdown with at least 5% margin. Using the boron concentration search option in SIMULATE [3], the ppm of boron was adjusted until the K_{eff} reached the cold critical K_{eff} minus .05. This case assumed cold, xenon-free conditions, with All-Rods-Out at the most reactive time in the cycle. The criticality search found that the plant would be 5% subcritical at the worst point in time with 670 ppm of boron injected. VY Technical Specifications [8] require a minimum of 800 ppm of boron be available for injection. Table 5.4.1 lists the amount of boron concentration and the corresponding shutdown margin capability of the SLCS.

TABLE 5.3.1

VY CYCLE 10

K_{eff} VALUES AND SHUTDOWN MARGIN CALCULATION

BOC K_{eff} - Uncontrolled	1.1142
BOC K_{eff} - Controlled	.9676
Cold Critical K_{eff} Eigenvalue	1.0000
BOC K_{eff} - Controlled With Strongest Worth Rod Withdrawn	.9854
BOC Minimum Shutdown Margin With Strongest Worth Rod Withdrawn	1.46% ΔK
R, Maximum increase in Cold K_{eff} With Exposure	.28% ΔK
Cycle Minimum Shutdown Margin at 6000 MWD/ST With Strongest Worth Rod Withdrawn	1.18% ΔK

TABLE 5.4.1

VY CYCLE 10

STANDBY LIQUID CONTROL SYSTEM SHUTDOWN CAPABILITY

ppm of Boron	Shutdown Margin
670	.050 ΔK
800	.076 ΔK

VERMONT YANKEE
CYCLE 10 HALING DEPLETION
EOC BUNDLE AVERAGE RELATIVE POWERS

PLANT COORD	23	25	27	29	31	33	35	37	39	41	43
22	R6 1.002	R7 1.120	R9 1.358	R6 1.042	R8 1.211	R7 1.143	R9 1.348	R8 1.153	R9 1.169	R8 0.837	R6 0.444
20	R7 1.119	R9 1.361	R8 1.272	R9 1.367	R7 1.134	R9 1.364	R7 1.157	R9 1.270	R8 1.021	R8 0.792	R6 0.415
18	R9 1.358	R8 1.272	R7 1.141	R8 1.231	R9 1.359	R7 1.133	R9 1.312	R8 1.099	R9 1.063	R8 0.700	R6 0.360
16	R6 1.042	R9 1.367	R8 1.231	R9 1.361	R7 1.109	R9 1.308	R8 1.136	R8 1.145	R8 0.824	R6 0.501	
14	R8 1.212	R7 1.134	R9 1.359	R7 1.107	R8 1.168	R7 1.046	R9 1.167	R8 0.903	R7 0.624		
12	R7 1.146	R9 1.364	R7 1.133	R9 1.306	R7 1.045	R8 1.061	R7 0.899	R8 0.783	R6 0.451		
10	R9 1.348	R7 1.152	R9 1.312	R8 1.136	R9 1.167	R7 0.898	R9 0.929	R8 0.653	R6 0.357		
08	R8 1.153	R9 1.270	R8 1.098	R9 1.145	R8 0.903	R8 0.783	R8 0.650	R7 0.461			
06	R9 1.169	R8 1.020	R9 1.063	R8 0.824	R7 0.626	R6 0.452	R6 0.357				
04	R8 0.838	R8 0.793	R8 0.703	R6 0.500							
02	R6 0.444	R6 0.412	R6 0.361								

BUNDLE ID
RELATIVE POWERS

R6 - P8DPB289, RELOAD 6
R7 - P8DPB289, RELOAD 7
R8 - P8DPB289, RELOAD 8
R9 - P8DPB289, RELOAD 9

FIGURE 5.1.1

VY CYCLE 10 HALING DEPLETION EOC BUNDLE AVERAGE RELATIVE POWERS

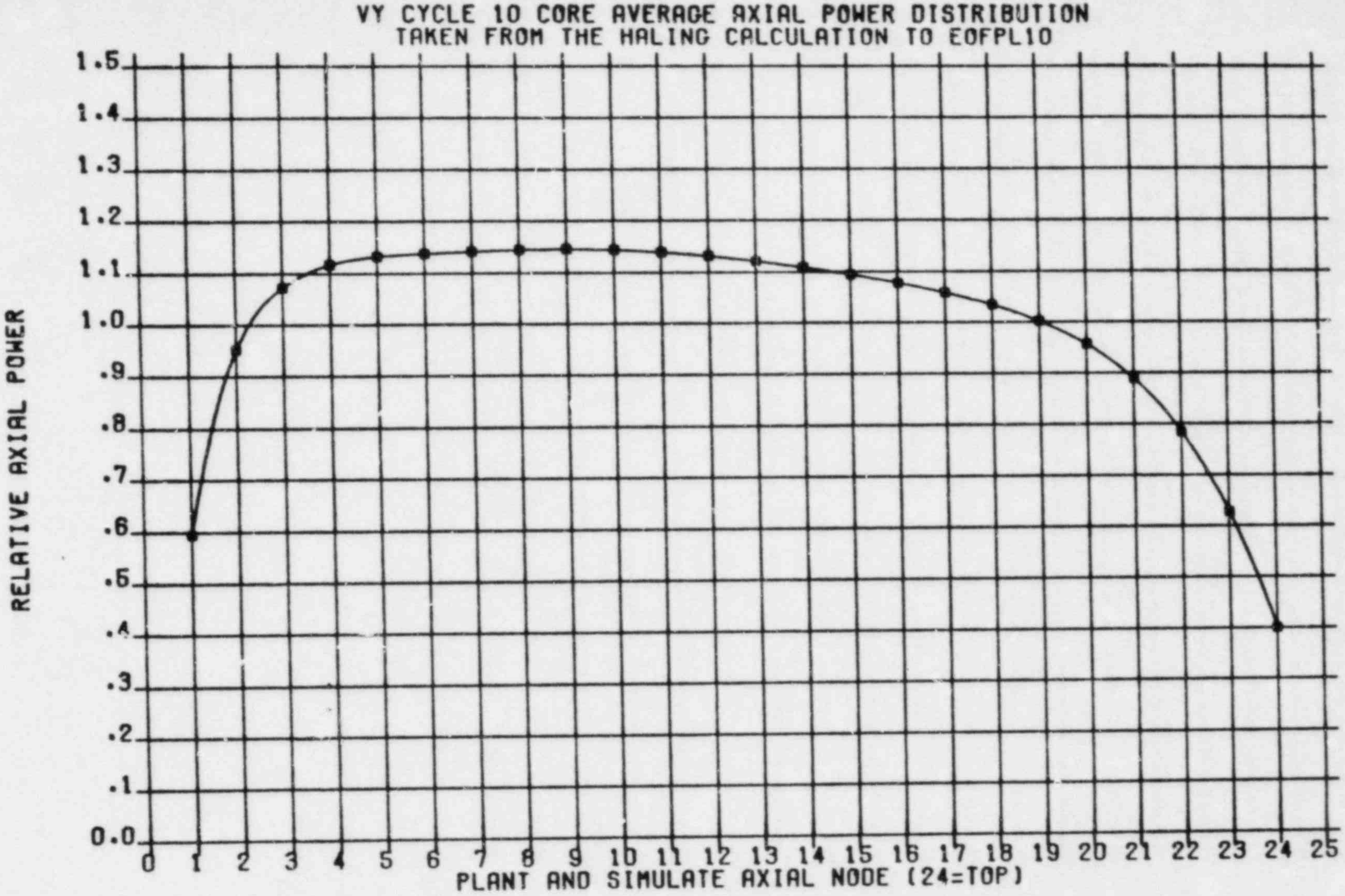

FIGURE 5.1.2

VY CYCLE 10 CORE AVERAGE AXIAL POWER DISTRIBUTION TAKEN FROM THE HALING CALCULATION TO EOFPL

VERMONT YANKEE CYCLE 10
RODDED DEPLETION -- ALL RODS OUT AT EOFPL10
BUNDLE AVERAGE RELATIVE POWERS

PLANT COORD	23	25	27	29	31	33	35	37	39	41	43
22	R6 1.053	R7 1.181	R9 1.428	R6 1.077	R8 1.229	R7 1.148	R9 1.338	R8 1.132	R9 1.140	R8 0.812	R6 0.426
20	R7 1.179	k9 1.433	R6 1.328	R9 1.408	R7 1.151	R9 1.353	R7 1.149	R9 1.246	R8 0.995	R8 0.767	R6 0.398
18	R9 1.431	R8 1.332	R7 1.180	R8 1.258	R9 1.372	R7 1.132	R9 1.298	R8 1.078	R9 1.034	R8 0.678	R6 0.343
16	R6 1.086	R9 1.421	R8 1.269	R9 1.383	R7 1.114	R9 1.293	R8 1.118	R9 1.117	R8 0.803	R6 0.477	
14	R8 1.246	R7 1.168	R9 1.389	R7 1.118	R8 1.159	R7 1.030	R9 1.141	R8 0.880	R7 0.598		
12	R7 1.163	R9 1.376	R7 1.149	R9 1.305	R7 1.034	R8 1.025	R7 0.875	R8 0.757	R6 0.433		
10	R9 1.357	R7 1.163	R9 1.316	R8 1.130	R9 1.150	R7 0.877	R9 0.902	R8 0.630	R6 0.340		
08	R8 1.148	R9 1.284	R6 1.091	R9 1.131	R8 0.887	R8 0.761	R8 0.630	R7 0.438			
06	R9 1.155	R8 1.008	R9 1.048	R8 0.812	R7 0.805	R6 0.437	R6 0.341				
04	R8 0.822	R8 0.777	R6 0.690	R6 0.482							
02	R6 0.431	R6 0.400	R6 0.349								

BUNDLE ID
RELATIVE POWERS

R6 - P8DPB289, RELOAD 6
R7 - P8DPB289, RELOAD 7
R8 - P8DPB289, RELOAD 8
R9 - P8DPB289, RELOAD 9

FIGURE 5.1.3

VY CYCLE 10 RODDED DEPLETION-ARO AT EOFPL BUNDLE AVERAGE RELATIVE POWERS

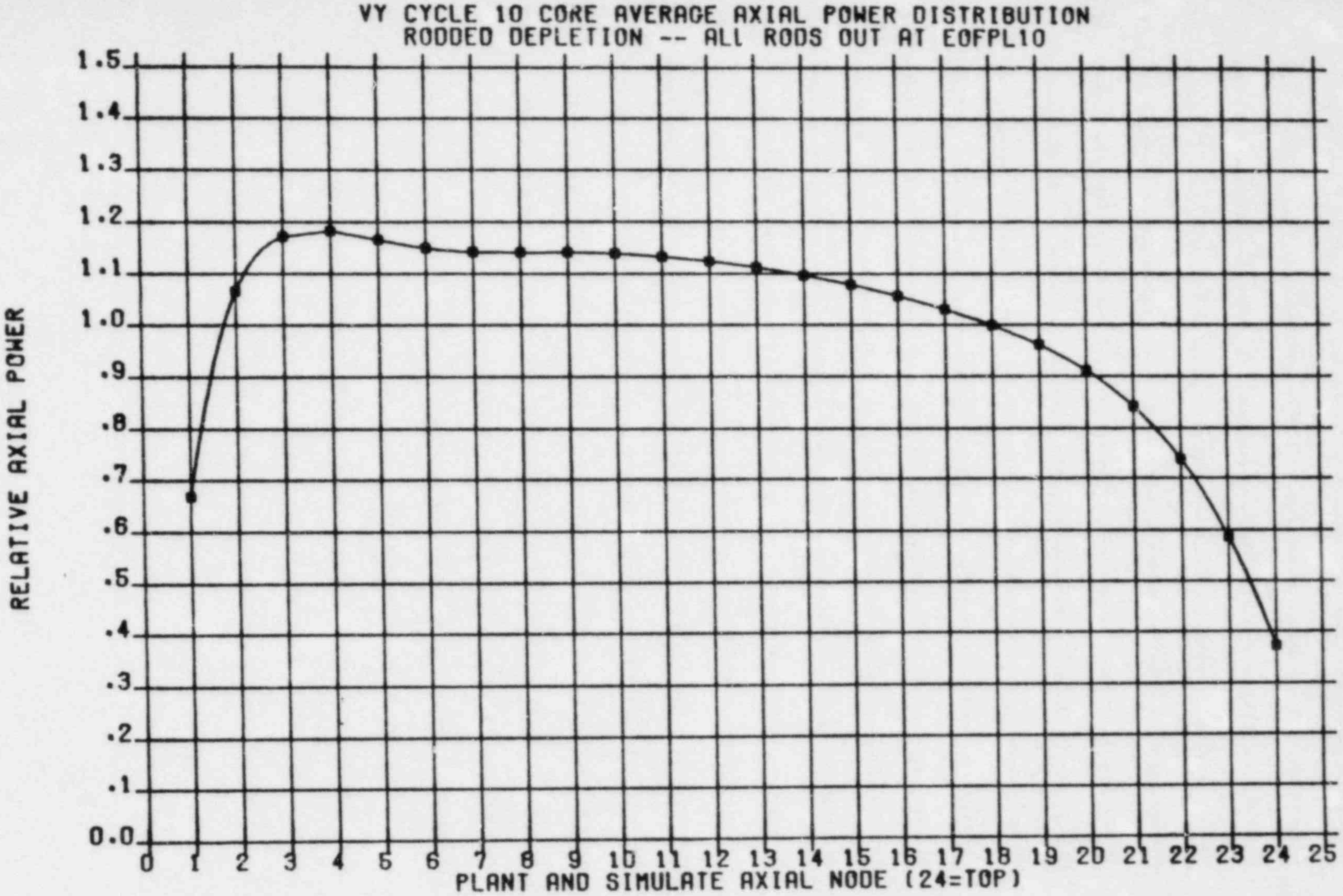

FIGURE 5.1.4

VY CYCLE 10 CORE AVERAGE AXIAL POWER DISTRIBUTION, RODDED DEPLETION-ARO AT EOFPL

VERMONT YANKEE
CYCLE 10 HALING DEPLETION
EOC BUNDLE AVERAGE EXPOSURES

PLANT COORD	23	25	27	29	31	33	35	37	39	41	43
22	R6 26.99	R7 23.43	R9 9.79	R8 30.18	R8 17.20	R7 23.09	R9 9.72	R8 19.66	R9 8.44	R8 15.76	R6 26.28
20	R7 23.49	R9 9.81	R8 16.15	R9 9.85	R7 24.94	R9 9.75	R7 21.85	R9 9.17	R8 18.01	R8 15.89	R6 25.75
18	R9 9.79	R8 16.16	R7 25.81	R8 19.53	R9 9.79	R7 23.78	R9 9.46	R8 19.03	R9 7.67	R8 16.66	R6 25.88
16	R6 30.24	R9 9.85	R8 19.52	R9 9.81	R7 25.09	R9 9.41	R8 17.88	R9 8.27	R8 17.13	R8 26.42	
14	R8 17.18	R7 24.89	R9 9.79	R7 25.20	R8 16.68	R7 22.39	R9 8.42	R8 18.18	R7 21.86		
12	R7 22.95	R9 9.75	R7 23.74	R9 9.41	R7 23.05	R8 15.84	R7 21.53	R8 16.35	R6 26.15		
10	R9 9.72	R7 22.11	R9 9.46	R8 17.86	R9 8.42	R7 21.62	R9 6.71	R8 15.70	R6 25.73		
08	R8 19.62	R9 9.16	R8 19.10	R9 8.27	R8 18.16	R8 16.28	R8 15.87	R7 20.81			
06	R9 8.44	R8 18.02	R9 7.67	R8 17.19	R7 21.73	R6 26.05	R6 25.78				
04	R8 15.73	R8 15.89	R8 16.48	R6 26.36							
02	R6 26.19	R6 26.24	R6 25.73								

BUNDLE ID
EXPOSURE (GWD/ST)

R6 - P8DPB289, RELOAD 6
R7 - P8DPB289, RELOAD 7
R8 - P8DPB289, RELOAD 8
R9 - P8DPB289, RELOAD 9

FIGURE 5.2.1

VY CYCLE 10 HALING DEPLETION, EOC BUNDLE AVERAGE EXPOSURES

VERMONT YANKEE
CYCLE 10 RODDED DEPLETION
EOC BUNDLE AVERAGE EXPOSURES

PLANT COORD	23	25	27	29	31	33	35	37	39	41	43
22	R6 26.63	R7 22.79	R9 8.52	R6 29.84	R8 17.10	R7 23.22	R9 9.46	R8 20.02	R9 8.43	R8 16.20	R6 26.56
20	R7 22.94	R9 8.65	R8 15.59	R9 9.12	R7 24.91	R9 9.44	R7 22.04	R9 9.12	R8 18.39	R8 16.34	R6 26.03
18	R9 8.60	R8 15.57	R7 25.48	R8 19.41	R9 9.35	R7 23.93	R9 9.28	R8 19.36	R9 7.64	R8 17.02	R6 26.11
16	R6 29.78	R9 8.87	R8 19.20	R9 9.30	R7 25.23	R9 9.30	R8 18.22	R9 8.28	R8 17.49	R6 26.67	
14	R8 16.88	R7 24.59	R9 9.04	R7 25.26	R8 17.01	R7 23.44	R9 8.47	R8 18.65	R7 22.21		
12	R7 22.94	R9 9.11	R7 23.62	R9 9.15	R7 23.45	R8 16.43	R7 22.02	R8 16.87	R6 26.47		
10	R9 9.32	R7 22.05	R9 8.99	R8 18.06	R9 8.38	R7 22.08	R9 6.79	R8 16.12	R6 26.00		
08	R8 19.86	R9 8.95	R8 19.28	R9 8.16	R8 18.55	R8 15.77	R8 16.28	R7 21.13			
06	R9 8.32	R8 18.30	R9 7.53	R8 17.47	R7 22.03	R6 26.35	R6 26.03				
04	R8 16.10	R8 16.27	R8 16.78	R6 26.56							
02	R6 26.43	R6 26.48	R8 25.92								

BUNDLE ID
EXPOSURE (GWD/ST)

R6 - P8DPB289, RELOAD 6
R7 - P8DPB289, RELOAD 7
R8 - P8DPB289, RELOAD 8
R9 - P8DPB289, RELOAD 9

FIGURE 5.2.2

VY CYCLE 10 RODDED DEPLETION, EOC BUNDLE AVERAGE EXPOSURES

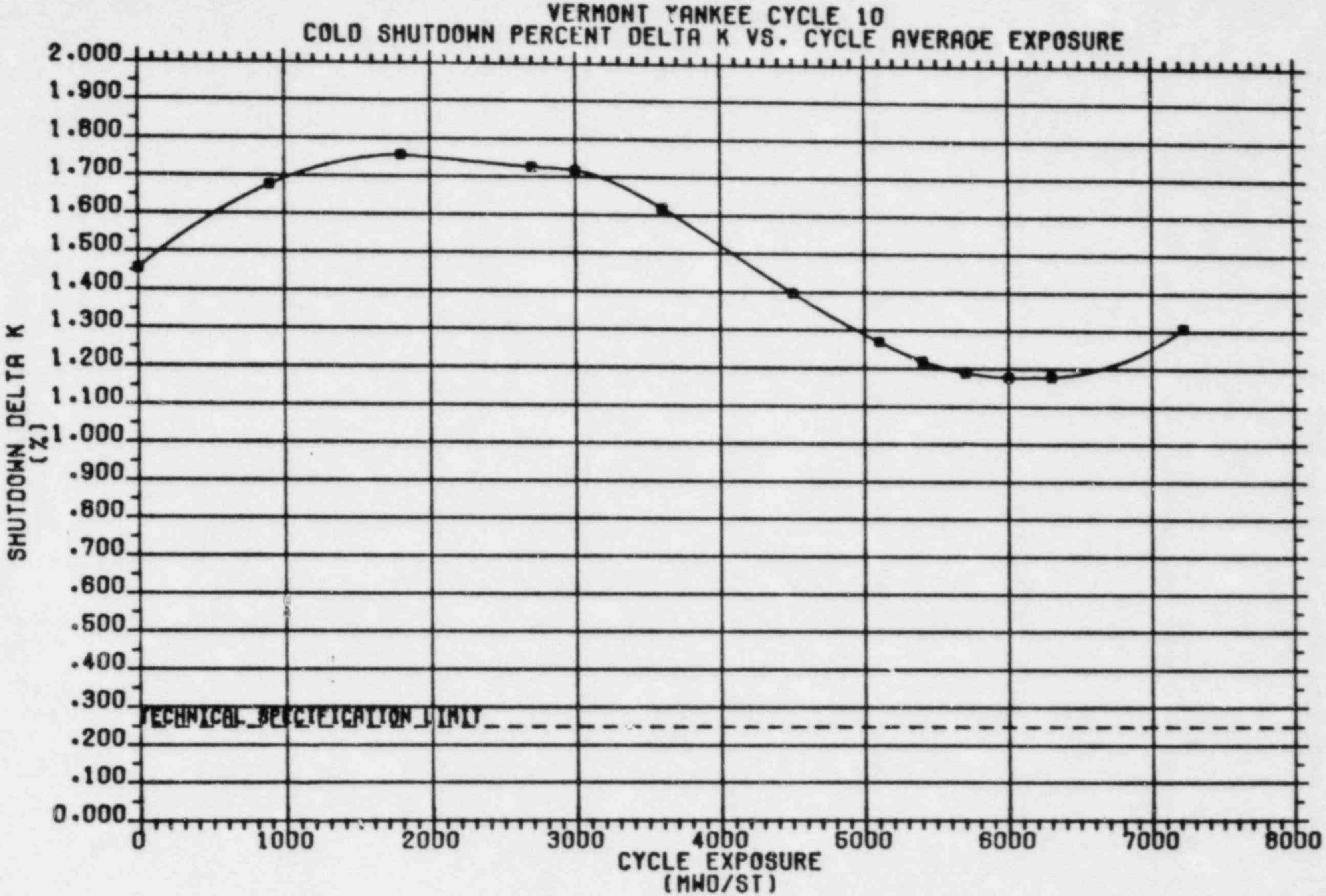

FIGURE 5.3.1

VY CYCLE 10 COLD SHUTDOWN DELTA K IN PERCENT VERSUS CYCLE EXPOSURE

6.0 THERMAL-HYDRAULIC DESIGN

The thermal-hydraulic evaluation of the reload cycle was performed using the methods described in the following section.

6.1 Steady-State Thermal Hydraulics

Core steady-state thermal-hydraulic analyses were performed using the FIBWR [9,10] computer code. The FIBWR code incorporates a detailed geometrical representation of the complex flow paths in a BWR core, and explicitly models the leakage flow to the bypass region. FIBWR calculates the core pressure drop and total bypass flow for a given total core flow. The power distribution, inlet enthalpy, and geometry are presumed known and are supplied to FIBWR. The power distribution is derived by the 3-D neutronic simulator SIMULATE [3]. Core pressure drop and total leakage flow predicted by the FIBWR code were used in setting the initial conditions for the system's transient analysis model.

6.2 Reactor Limits Determination

The objective for normal operation and anticipated transient events is to maintain nucleate boiling and thus avoid a transition to film boiling, thereby protecting the fuel cladding integrity. Based on Reference 11, the fuel cladding integrity safety limit for Vermont Yankee is a lowest allowable minimum critical power ratio (LAMCPR) of 1.07 for P8X8R reload fuel. Operating limits are specified to maintain adequate margin to onset of the boiling transition. The figure of merit utilized for plant operation is the critical power ratio (CPR). This is defined as the ratio of the critical power (bundle power at which some point within the assembly experiences onset of boiling transition) to the operating bundle power. Thermal margin is stated in terms of the minimum value of the critical power ratio MCPR, which corresponds to the most limiting fuel assembly in the core. Both the transient (safety) and normal operating thermal limits in terms of MCPR are derived based on the GEXL correlation as described in Reference 11.

Vermont Yankee Technical Specifications [8] limit the operation of P8X8R fuel to a maximum linear heat generation rate (MLHGR) of 13.4 KW/ft. The basis for a MLHGR of 13.4 KW/ft can be found in Reference 2.

7.0 ACCIDENT ANALYSIS

7.1 Core Wide Transient Analysis

Core wide transient simulations are performed to assess the impact of the particular transient on the heat transfer characteristics of the fuel. The figure of merit used is the critical power ratio (CPR). It is the purpose of the analysis to determine the minimum critical power ratio such that the safety limit critical power ratio (LAMCPR) is not violated for the transients considered.

7.1.1 Methodology

The analysis requires two types of simulations. A system level simulation is performed to determine the overall plant response. Transient core inlet and exit conditions and normalized power from the system level calculation are used to perform detailed thermal-hydraulic simulations of the fuel (referred to as "hot channel calculations"). The result of each of these latter simulations is the bundle transient Δ CPR (the initial bundle CPR minus the minimum CPR experienced during the transient).

The system level simulations are performed with the model documented in Reference 12.

The hot channel calculations are performed with the RETRAN [13] and TCPYA01 [14] computer codes. The GEXL correlation [11] is used in TCPYA01 to evaluate critical power ratio. The calculational procedure is outlined below.

The hot channel transient Δ CPR calculations are performed via a series of "inner" and "outer" iterations, as illustrated by the flow chart in Figure 7.1.1. The outer loop represents iterations on the hot channel initial power level. These iterations are necessary, because the Δ CPR for a given transient varies with Initial Critical Power Ratio (ICPR), yet only the Δ CPR corresponding to a transient MCPR equal to the safety limit (i.e., 1.07 + Δ CPR = ICPR) is appropriate. The approximate constancy of the Δ CPR/ICPR ratio is useful in these iterations. Each outer iteration requires a RETRAN hot channel run to calculate the transient enthalpies, flows, pressure and saturation properties at each time step. These are required for input to the TCPYA01 code. TCYPA01 is then used to calculate a CPR at each time step during the transient, from which a transient ΔCPR is derived. The hot channel is modeled using a chopped cosine axial power shape with a peak/average ratio of 1.4.

The inner loop represents iterations on the hot channel inlet flow. These iterations are necessary, because the RETRAN hot channel model calculates the entrance loss coefficient when given the initial power level, flow, and pressure drop as input. The pressure drop is assumed equal to the core average pressure drop, and the flow is varied for a given power level until the calculated entrance loss coefficient is correct. FIBWR [9] is utilized to estimate the correct inlet flow for a particular power level and pressure drop.

7.1.2 Initial Conditions and Assumptions

The initial conditions for the system simulations are based on 105% rated steam flow (maximum turbine capacity) and 100% core flow. The core axial power distribution for each of the exposure points is based on Haling-mode 3-D SIMULATE predictions associated with the generation of the reactivity data (Section 7.1.3). The core inlet enthalpy is set so that the amount of carryunder from the steam separators and the quality in the liquid region outside the separators is as close to zero as possible. For fast pressurization transients, this maximizes the initial pressurization rate and predicts a more severe neutron power spike. A summary of the initial operating state used for the system simulations is provided in Table 7.1.1.

Assumptions specific to a particular transient are discussed in the section describing the transient. In general, the following assumptions are made for all transients:

1. Scram setpoints are at Technical Specification limits.

2. Protective system logic delays are at equipment specification limits.

3. Safety/relief valve and safety valve capacities are based on Technical Specification rated values.

4. Safety/relief valve and safety valve setpoints are modeled as being 1% above the Technical Specification upper limit. Valve responses are based on slowest specified response values.

5. Control rod drive scram speed is based on the Technical Specification limits. The analysis addresses a dual set of scram speeds as given in the Technical Specifications. These are referred to as the "measured" and "67B" scram time sets.

7.1.3 Reactivity Functions

The methods used to generate the fuel temperature, moderator density, and scram reactivity functions are described in Reference 15 and are outlined in Figures 2.1 through 2.3 of that document. A complete set of reactivity functions, the axial power distribution, and the kinetics parameters are generated from base states established for EOC, EOC-1000 MWD/ST, EOC-2000 MWD/ST, and BOC exposure conditions. These states are characterized by exposure and void history distributions, control rod pattern, and core thermal-hydraulic conditions. The latter core conditions are consistent with the assumed system transient conditions provided in Table 7.1.1.

The BOC base state is established from the previously defined Cycle 9 endpoint, the Cycle 10 reload pattern, and an estimate of the BOC10 critical rod pattern. The EOC and intermediate core exposure and void history distributions were calculated via a Haling depletion as described in Section 5.2. The EOC state is unrodded and, as such, is defined sufficiently. However, EOC-1000 MWD/ST and EOC-2000 MWD/ST exposure points require base control rod patterns. These are developed to be as "black and white" as possible. That is, beginning with the rodded depletion configuration, all control rods which are more than half inserted are fully inserted, and all control rods which are less than half inserted are fully withdrawn. If the SIMULATE-calculated parameters are within operating limits, then this configuration becomes the base case. If the limits are exceeded, a minimum number of control rods are adjusted a minimum number of notches until the parameters fall within limits. Using this method, the control rod patterns and resultant power distributions are established so as to minimize the scram reactivity function and to maximize the core average moderator density reactivity coefficient. For the transients analyzed, this tends to maximize the power response.

In generating the fuel reactivity function data for RETRAN, twelve unique volume-specific table sets are produced which are analogous to those shown in Figure 3.7 of Reference 15. The moderator and relative moderator density functions also are twelve unique volume-specific tables, analogous to Figures 3.10 and 3.11 in Reference 15. A moderator density set is generated specifically for each transient type. The density reactivity functions for the subcooling transient are generated by quasi-statically varying the inlet subcooling only. The moderator enthalpy source distribution is in equilibrium with the calculated nuclear power. The density reactivity functions of the pressurization transients are generated by quasi-statically varying the core pressure. A series of the calculations are performed for various inlet moderator temperatures. The moderator enthalpy source distribution is that of the base state case.

In order to qualitatively compare the core reactivity characteristics between different base configurations, core average reactivity coefficients are calculated and provided in Table 7.1.2. Calculated point kinetics parameters for RETRAN are also provided in the table.

The reactivities versus scram insertion are calculated at constant, pre-transient moderator conditions. These calculated data are fit and evaluated to yield highly detailed scram reactivity curves. These are then combined with the appropriate rod position versus time curves to establish the final RETRAN scram reactivity functions. Figures 7.1.2 through 7.1.4 display the inserted rod worths and rod positions as functions of scram time for the "measured" scram time analysis. Figures 7.1.5 through 7.1.7 display similar curves for the "67B" scram time analysis.

7.1.4 Transients Analyzed

Past licensing experience has shown that the core wide transients which result in the minimum core thermal margins are:

1. Generator load rejection with complete failure of the turbine bypass system.

2. Turbine trip with complete failure of the turbine bypass system.

3. Loss of feedwater heating.

The "feedwater controller failure" (maximum demand) transient is not a severe transient for Vermont Yankee, because of the plant's 110% steam flow bypass system. Past analyses have shown this transient to be considerably less severe than any of the above for all exposure points. Brief descriptions and the results of the core wide transients analyzed are provided in the following section.

7.2 Core Wide Transient Analysis Results

The transients selected for consideration were analyzed at exposure points of end of cycle (EOC), EOC-1000 MWD/ST, and EOC-2000 MWD/ST; the loss of feedwater heating was also evaluated at beginning of cycle (BOC) conditions. A summary of the results of the analyses is provided in Table 7.2.1.

7.2.1 Turbine Trip Without Bypass Transient (TTWOB)

The transient is initiated by a rapid closure (0.1 second closing time) of the turbine stop valves. It is assumed that the steam bypass valves, which normally open to relieve pressure, remain closed. A reactor protection system signal is generated by the turbine stop valve closure switches. Control rod drive motion is conservatively assumed to occur 0.27 seconds after the start of turbine stop valve motion. The ATWS recirculation pump trip is assumed to occur at a setpoint of 1150 psig dome pressure. A pump trip time delay of 1.0 second is assumed to account for logic delay and M-G set generator field collapse. In simulating the transient, the bypass piping volume up to the valve chest is lumped into the control volume upstream of the turbine stop valves. As an example, predictions of the salient system parameters are shown in Figures 7.2.1 through 7.2.3 for the three exposure points for the "measured" scram time analysis.

7.2.2 Generator Load Rejection Without Bypass Transient (GLRWOB)

The transient is initiated by a rapid closure (0.3 seconds closing time) of the turbine control valves. As in the case of the turbine trip transient, the bypass valves are assumed to fail. A reactor protection system signal is generated by the hydraulic fluid pressure switches in the acceleration relay of the turbine control system. Control rod drive motion is conservatively assumed to occur 0.28 seconds after the start of turbine control valve motion. The same modeling regarding the ATWS pump trip and bypass piping is used as in the turbine trip simulation. The influence of the accelerating main turbine generator on the recirculation system is simulated by specifying the main turbine generator electrical frequency as a function of time for the M-G set drive motors. The main turbine generator frequency curve is based on a 100% power plant startup test and is considered representative for the simulation. As an example, the system model predictions for the three exposure points are shown in Figures 7.2.4 through 7.2.6 for the "measured" scram time analysis.

7.2.3 Loss of Feedwater Heating Transient (LOFWH)

A feedwater heater can be lost in such a way that the steam extraction line to the heater is shut off or the feedwater flow bypasses one of the heaters. In either case, the reactor will receive cooler feedwater, which will produce an increase in the core inlet subcooling, resulting in a reactor power increase.

The response of the system due to the loss of $100^{o}F$ of the feedwater heating capability was analyzed. This represents the current licensing assumption for the maximum expected single heater or group of heaters that can be tripped or bypassed by a single event.

Vermont Yankee has a scram setpoint of 120% of rated power as part of the Reactor Protection System (RPS) on high neutron flux. In this analysis, no credit was taken for scram on high neutron flux, thereby allowing the reactor power to reach its peak without scram. This approach was selected to provide a bounding and conservative analysis.

The transient response of the system was evaluated at several exposures during the cycle. Transient evaluation at EOC-2000 MWD/ST was found to be the limiting case between BOC to EOC. The results of the system response to a loss of 100°F feedwater heating capability evaluated at EOC-2000 MWD/ST as predicted by the RETRAN code are presented in Figure 7.2.7.

7.3 Overpressurization Analysis Results

Compliance with ASME vessel code limits is demonstrated by an analysis of the main steam isolation valves (MSIV) closing with failure of the MSIV position switch scram. End of cycle conditions were analyzed. The system model used is the same as that used for the core wide transient analysis (Section 7.1.1). The initial conditions and modeling assumptions discussed in Section 7.1.2 are applicable to this simulation. The maximum pressure at the bottom of the reactor vessel is calculated to be 1266 psig for the "measured" scram time analysis and 1291 psig for the "67B" scram time analysis. These results are within the allowable code limit of 10% above vessel design pressure for upset conditions, or 1375 psig.

The transient is initiated by a simultaneous closure of all four MSIV's. A 3.0 second closing time, which is the Technical Specification minimum, is assumed. A reactor scram signal is generated on APRM high flux. Control rod drive motion is conservatively assumed to occur 0.28 seconds after reaching the high flux setpoint. The system response is shown in Figure 7.3.1 for the "measured" scram time analysis.

7.4 Local Rod Withdrawal Error Transient Results

The rod withdrawal error is a local core transient caused by an operator erroneously withdrawing a control rod in the continuous withdrawal mode. If the core is operating at its operating limits for MCPR and LHGR at the time of the error, then withdrawal of a control rod could increase both local and core power levels with the potential for overheating the fuel.

There is a broad spectrum of core conditions and control rod patterns which could be present at the time of such an error. For many situations it would be possible to fully withdraw a control rod without exceeding 1% clad plastic strain or violating the CPR based fuel cladding integrity safety limit.

To bound the most severe of postulated rod withdrawal error events, a portion of the core MCPR operating limit envelope is specifically defined such that the cladding limits are not violated. The consequences of the error depend on the local power increase, the initial MCPR of the neighboring locations and the ability of the Rod Block Monitor System to stop the withdrawing rod before MCPR reaches 1.07.

The most severe postulated transient begins with the core operating according to normal procedures and within normal operating limits. The operator makes a procedural error and attempts to fully withdraw the maximum worth control rod at maximum withdrawal speed. The core limiting locations are close to the error rod and therefore experience the spatial power shape transient as well as the overall core power increase.

The core conditions and control rod pattern for the bounding case are specified using the following set of concurrent worst case assumptions:

1. The rod should have high reactivity worth. This is provided for by analysis of the core at the exposure corresponding to maximum control inventory with the xenon-free condition superimposed. The xenon-free condition and the additional control rod inventory needed to maintain criticality exaggerates the worth of control rods substantially when compared to normal operation with normal xenon levels. A fully inserted high worth rod is selected as the error rod.

2. The core is initially at 105% power and rated flow.

3. The core power distribution is adjusted with the available control rods to place the locations within the four by four array of bundles around the error rod as nearly on the operating limits as practical.

The Rod Block Monitor System's ability to terminate the bounding case is evaluated on the following bases:

1. Technical Specifications allow each of the separate RBM channels to remain operable if at least half of the LPRM inputs at every level are operable. For the interior RBM channels tested in this analysis, there are a maximum of four LPRM inputs per level. One RBM channel averages the inputs from the A and C levels; the other channel averages the inputs from the B and D levels. Considering the inputs for a single channel, there are eleven failure combinations of none, one and two failed LPRM strings. The RBM channel responses are evaluated separately at these eleven input failure conditions. Then, for each channel taken separately, the lowest response as a function of error rod position is chosen for comparison to the RBM setpoint.

2. The event is analyzed separately in each of the four quadrants of the core due to the differing LPRM string physical locations relative to the error rod.

Technical Specifications require that both RBM channels be operable during normal operation. Thus, the first channel calculated to intercept the RBM setpoint is assumed to stop the rod. To allow for control system delay times, the rod is assumed to move two inches after the intercept and stop at the following notch.

The analysis is performed using the three dimensional steady state SIMULATE core model demonstrated in Reference 3. Necessary properties of that model for use in this analysis are:

1. Accurate bundle power calculation as shown by the PDQ and gamma scan comparisons.

2. Accurate LPRM signal calculation as shown by the detailed TIP trace comparisons.

3. Accurate control rod worths and core power coefficient as shown by the consistent core eigenvalues.

Two separate cases are presented from numerous explicit SIMULATE analyses. The reactor conditions and case descriptions are shown in Figures 7.4.1 and 7.4.2. Case 1 analyzes the bounding event with the concurrent abnormal xenon condition and rod pattern configuration necessary to increase the worth of the error rod. The initial conditions for Case 2 approximate the "normal" 105% power conditions at the most reactive point in the cycle; the control rod density is at its maximum at the normal equilibrium xenon condition. The ΔCPR and MLHGR values for both cases are shown in Table 7.4.1. The ΔCPR values are evaluated such that the implied operating limit MCPR equals 1.07 + ΔCPR, conserving the figure of merit (ΔCPR/Initial CPR) shown by the SIMULATE calculations. The use of this method provides valid ΔCPR values in the analysis of normal operating states where locations near the assumed error rod are not initially near the MCPR operating limit. Case 2 is the worst of thirteen rod withdrawal transients analyzed from normal initial 105% power, full flow and rod pattern conditions at various exposure points throughout the cycle. Case 2 is bounded by Case 1 with substantial MCPR margin.

For Case 1: Figures 7.4.3 and 7.4.4 show the end of transient control rod position. This is determined from the point where the weakest RBM channel response first intercepts the RBM setpoint. For this same bounding case, the operating limit ΔCPR envelope component versus Rod Block Monitor setpoint is taken from the Table 7.4.1. The same table demonstrates margin to the 1% plastic strain limit. The MLHGR values include the 2.2% power spiking penalty.

7.5 Misloaded Bundle Error Analysis Results

7.5.1 Rotated Bundle Error

The primary result of an assembly rotation is a large increase in local pin peaking and R-factor as higher enrichment pins are placed adjacent to the surrounding wide water gaps. In addition, there may be a small increase in reactivity, depending on the exposure and void fraction states. The R-factor increase results in a CPR reduction, while the local pin peaking factor increase results in a higher pin linear heat generation rate. The objective of the analysis is to insure that in the worst possible rotation, the safety limit linear heat generation rate and CPR are not violated with the most limiting monitored bundles on their operating limits.

To analyze the CPR response, rotated bundle R-factors as a function of exposure are developed by adding the largest possible ΔR-factor increase resulting from a rotation to the exposure dependent R-factors of the properly oriented bundles [11]. Using these rotated bundle R-factors, the minimum CPR values resulting from a bundle rotation are determined using SIMULATE. This is done for each control rod sequence throughout the cycle. These minimum CPR values are, in addition, modified slightly to account for the change in reactivity resulting from the rotation. For each sequence, the MCPR for the properly oriented assemblies is adjusted by a ratio necessary to place the corresponding rotated CPR on its 1.07 safety limit. The maximum of these adjusted MCPR's is the rotated bundle operating limit.

To determine the maximum linear heat generation rate (MLHGR) resulting from a rotation, the ratios of the maximum rotated local peaking factor to the maximum unrotated local peaking are determined for the expected range of exposure and void conditions. The maximum of this ratio is applied to the operating limit LHGR of 13.4 kw/ft. This maximum rotated bundle LHGR is in addition modified to account for the possible reactivity increase resulting from the rotation. It is also increased by the 2.2% power spiking penalty.

The results of the rotated bundle analysis are as given in Table 7.5.1.

7.5.2 Mislocated Bundle Error

Misloading a high reactivity assembly into a region of high neutron importance results in a location of high relative assembly average power. Since the assembly is assumed to be properly oriented (not rotated), R-factors used for the misloaded bundle are the standard values for the fuel type.

The analysis for Cycle 10 consists of an iterative procedure which successively eliminates potential misloading locations from any MCPR safety limit violations. The first step is to use SIMULATE to determine the largest possible ΔCPR which could result, at any location, as the result of misloading a high reactivity assembly into the location. This maximum ΔCPR is then subtracted from all the other bundle CPR's in the core. This is done at the various cycle exposures. Even with this maximum ΔCPR applied, some locations will never exceed the MCPR safety limit of 1.07. These locations are eliminated from further investigation.

The next iteration consists of applying the same procedure to the locations which appeared to violate the safety limit when the maximum ΔCPR from the first iteration was applied. Since these locations are of higher reactivity than those eliminated in the first iteration, they will result in a smaller ΔCPR when misloaded. Using this smaller ΔCPR, some of the remaining locations will be eliminated from potential CPR safety limit violations. This procedure is continued until all locations are shown to be above the MCPR safety limit due to a misloading, or until a limiting location is identified.

Using the above procedure, it has been demonstrated that for Cycle 10 all possible mislocations resulted in calculated MCPR's above the 1.07 safety limit, assuming an initial operating CPR limit of 1.22. This makes the mislocated bundle analysis less limiting than the rotated bundle analysis.

7.6 Control Rod Drop Accident Results

The control rod sequences are a series of rod withdrawal and banked withdrawal instructions specifically designed to minimize the worths of individual control rods. The sequences are examined so that, in the event of the uncoupling and subsequent free fall of the rod, the incremental rod worth is acceptable. Incremental worth refers to the fact that rods beyond Group 2 are banked out of the core and can only fall the increment from all in to the rod drive withdrawal position. Acceptable worth is one which produces a maximum fuel enthalpy less than 280 calories/gram.

Some out-of-sequence control rods could accrue potentially high worths. However, the Rod Worth Minimizer (RWM) will prevent withdrawing an out-of-sequence rod if accidentally selected. The RWM is functionally tested before each startup.

The sequence entered into the RWM will take the plant from All-Rods-In (ARI) to well above 20% core thermal power. Above 20% power even multiple operator errors will not create a potential rod drop situation above 280 calories per gram. [16, 17] Below 20% power, however, the sequences must be examined for incremental rod worth. This is done using the full core, xenon free SIMULATE model at the projected most reactive point in the cycle. This assures that the maximum amount of reactivity is held in the rods.

Both the A and B sequences were examined. It was found that the highest worth occurred in the first rod pull of the second group. Any of the first four rod arrays shown in Figures 7.6.1 and 7.6.2 may be designated as the first group pulled. But, then a specific second group must follow as Table 7.6.1 illustrates. For added conservatism, the highest worth rod in the second group was deliberately assigned to be the first rod pulled. This assures that in any sequence followed at the plant, the worths will always be less than those calculated here. The results of the calculations are presented in Table 7.6.2.

Beyond Group 2, procedures [18] apply which severely reduce the rod incremental worths. This makes the xenon free, hot standby worths much less than the cold xenon free worths. [1]

7.7 Stability Analysis Results

The analysis of reactor stability has been performed by General Electric as described in Section S.2.4 of Reference 2. The 105% power rod line was analyzed and the resultant decay ratio as a function of reactor power level is provided in Figure 7.7.1.

The reactor core stability decay ratio at natural circulation conditions and a power level corresponding to the 105% power rod line, is calculated to be 0.87. The channel hydrodynamic performance decay ratio associated with this condition is 0.30.

TABLE 7.1.1

VY CYCLE 10 SUMMARY OF SYSTEM TRANSIENT MODEL
INITIAL CONDITIONS FOR CORE WIDE TRANSIENT ANALYSES

Core Thermal Power (MWth)	1664.0
Turbine Steam Flow (% NBR)	105
Total Core Flow (10^6lbm/hr)	48.0
Core Bypass Flow (10^6lbm/hr)	5.3
Core Inlet Enthalpy (BTU/lbm)	520.9
Steam Dome Pressure (psia)	1034.7
Turbine Inlet Pressure (psia)	986.0
Total Recirculation Flow (10^6lbm/hr)	23.4
Core Plate Differential Pressure (psi)	18.5
Narrow Range Water Level (in.)	35
Average Fuel Gap Conductance	(See Section 4.2)

TABLE 7.1.2

VY CYCLE 10 TRANSIENT ANALYSIS REACTIVITY COEFFICIENTS

Calculated Parameter	Cycle Exposure Point (MWD/ST)			
	EOC	(EOC-1000)	(EOC-2000)	BOC
Axial Shape Index(1)	-0.0824	-0.1802	-0.2137	-0.2463
Moderator Density Coefficient (Subcooling), ¢/Δu(2) Pressure = 1050 psia Subcooling = 30 BTU/lbm	20.8	22.0	24.4	19.7
Moderator Density Coefficient (Pressurization), ¢/Δu Pressure = 1050 psia Inlet Enthalpy = 520 BTU/lbm	23.3	24.3	26.3	(3)
Fuel Temperature Coefficient at 1130°F, ¢/°F	-0.282	-0.283	-0.283	-0.261
Effective Delayed Neutron Fraction	0.005390	0.005473	0.005557	0.006028
Prompt Neutron Generation Time in Microseconds	42.67	42.49	41.81	40.07

Notes: (1) Axial Shape Index (ASI) = $\frac{P_T - P_B}{P_T + P_B}$

(2) Δu = change in density, in percent

(3) Pressurization transients are not calculated at BOC

TABLE 7.2.1

VY CYCLE 10 CORE WIDE TRANSIENT ANALYSIS RESULTS

Transient	Exposure	Peak Prompt Power (Fraction of Initial Value)	Peak Avg. Heat Flux (Fraction of Initial Value)	ΔCPR P8X8R
Turbine Trip Without Bypass, "Measured" Scram Time	EOC	2.931	1.183	.19
	EOC-1000	2.189	1.102	.10
	EOC-2000	1.208	1.000	.00
Turbine Trip Without Bypass, "67B" Scram Time	EOC	3.433	1.234	.25
	EOC-1000	2.694	1.168	.17
	EOC-2000	1.634	1.031	.03
Generator Load Rejection Without Bypass, "Measured" Scram Time	EOC	2.793	1.164	.18
	EOC-1000	2.076	1.078	.09
	EOC-2000	1.086	1.000	.00
Generator Load Rejection Without Bypass, "67B" Scram Time	EOC	3.381	1.225	.26
	EOC-1000	2.658	1.155	.18
	EOC-2000	1.522	1.012	.02
Loss of 100°F Feedwater Heating	EOC	1.198	1.190	.15
	EOC-1000	1.210	1.203	.16
	EOC-2000	1.215	1.207	.17
	BOC	1.201	1.193	.15

TABLE 7.4.1

VY CYCLE 10 ROD WITHDRAWAL ERROR TRANSIENT SUMMARY
(WITH LIMITING INSTRUMENT FAILURE)

Case 1
Conditions in Figure 7.4.1

RBM Setpoint	Rod Position	ΔCPR P8X8R	MLHGR (kw/ft) P8X8R
104	10	.09	13.7
105	12	.12	13.9
106	14	.17	15.8
107	14	.17	15.8
108	16	.21	17.7

Case 2
Conditions in Figure 7.4.2

RBM Setpoint	Rod Position	ΔCPR P8X8R	MLHGR (kw/ft)* P8X8R
104	22	.06	12.7
105	24	.07	12.7
106	26	.09	12.7
107	30	.11	12.7
108	34	.15	13.4

* Not initially on limits

TABLE 7.5.1

ROTATED BUNDLE ANALYSIS RESULTS

Initial MCPR	Resulting MCPR	Resulting LHGR (kw/ft)
1.24	1.07	17.47

TABLE 7.6.1

CONTROL ROD DROP ANALYSIS - ROD ARRAY PULL ORDER

The order in which rod arrays are pulled is specific once the choice of first group is made.

First Group Pulled is:	Second Group Pulled Must Be:	Successive Group Is Banked Out
Array 1	Array 2	Array 3 or 4
Array 2	Array 1	Array 3 or 4
Array 3	Array 4	Array 1 or 2
Array 4	Array 3	Array 1 or 2

TABLE 7.6.2

VY CYCLE 10 CONTROL ROD DROP ANALYSIS RESULTS

Maximum Incremental Rod Worth Calculated Cold Xenon Free	.84% ΔK
Bounding Analysis Worth for Enthalpy Less than 280 Calories per Gram (References 16, 17 and 19)	1.30% ΔK

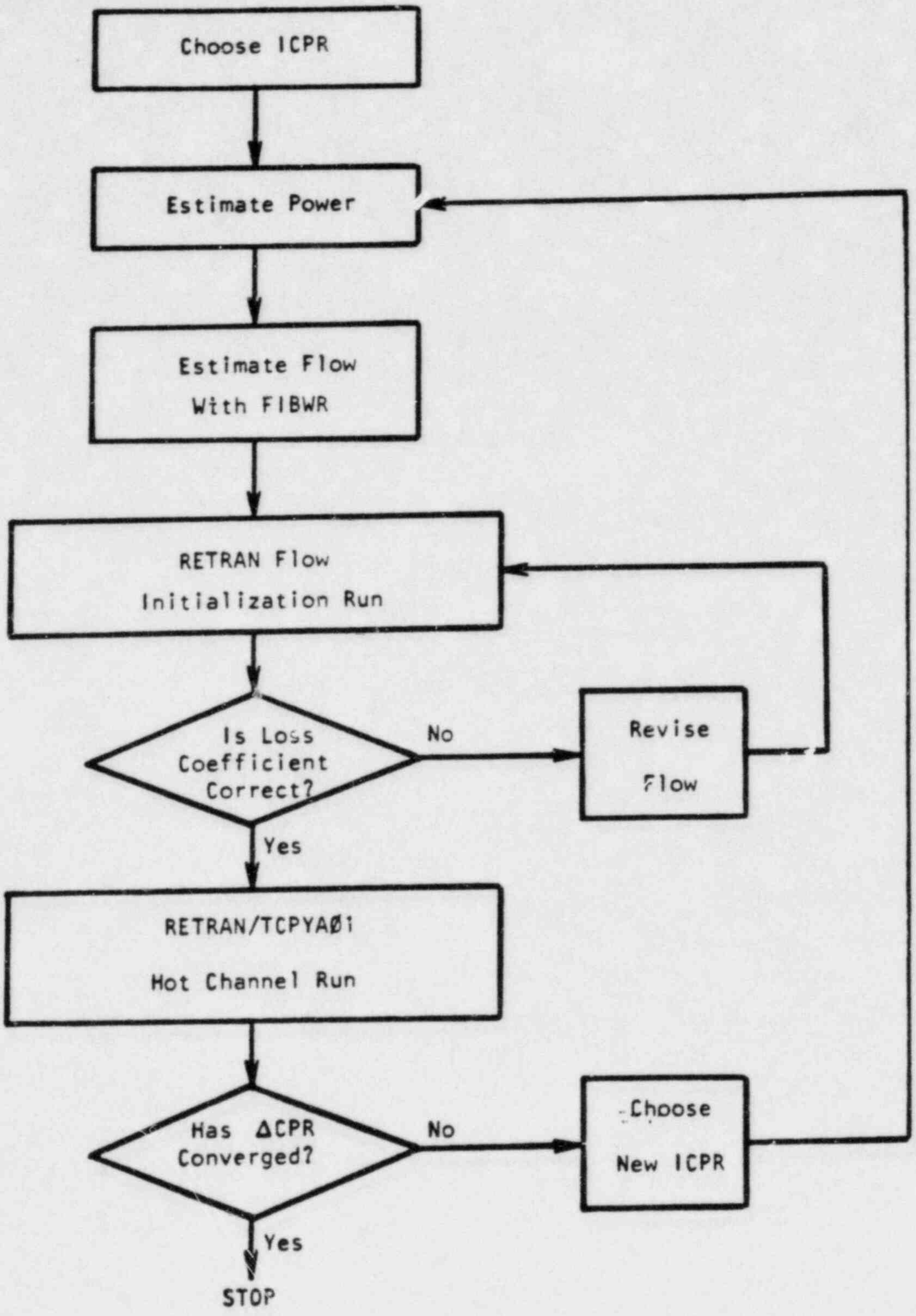

FIGURE 7.1.1

FLOW CHART FOR THE CALCULATION OF ΔCPR USING THE RETRAN/TCPYA01 CODES

VY CYCLE 10 - MST, EOC

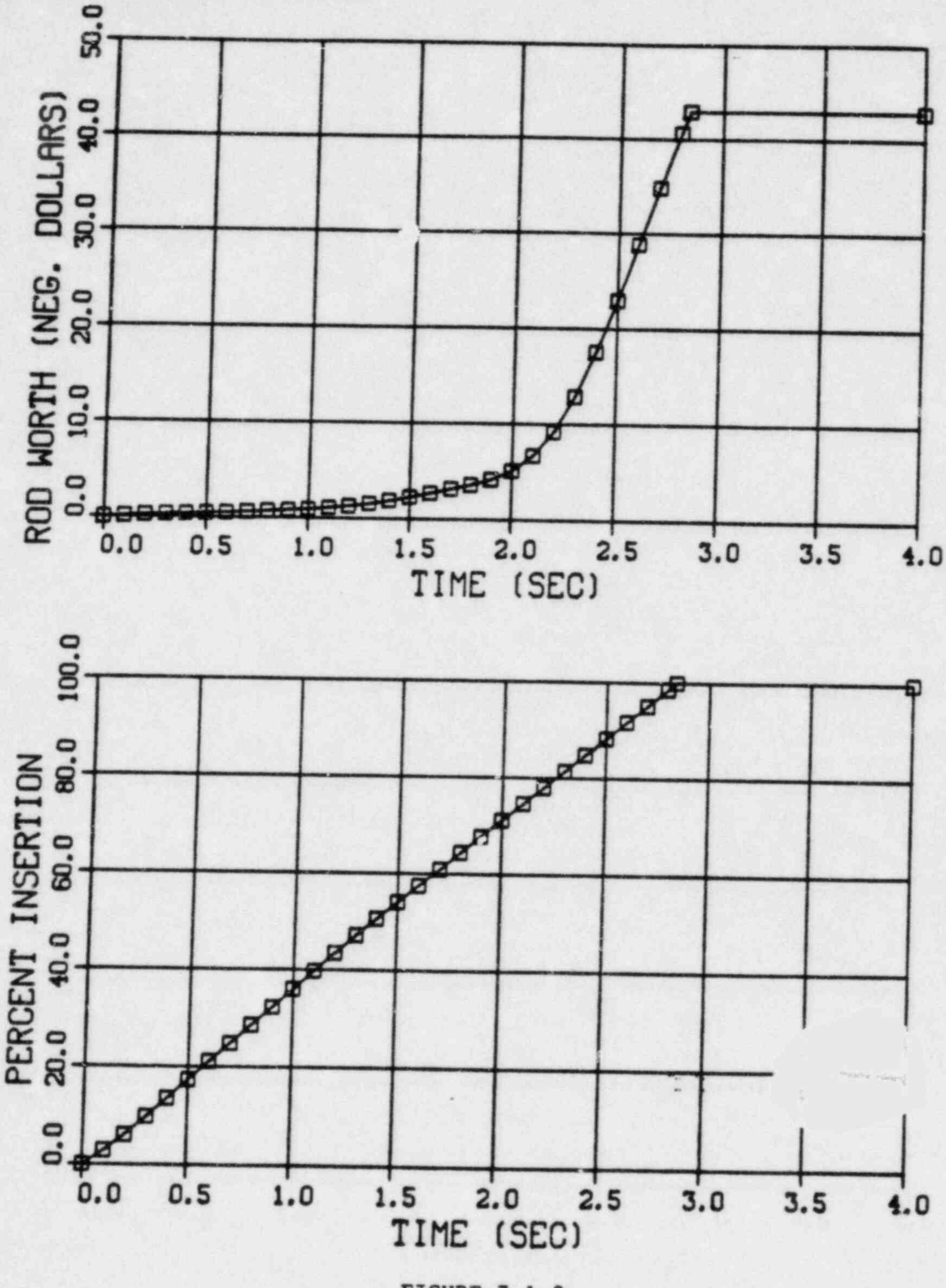

FIGURE 7.1.2

INSERTED ROD WORTH AND ROD POSITION VERSUS TIME FROM INITIAL ROD MOVEMENT AT EOC10, "MEASURED" SCRAM TIME

VY CYCLE 10 - MST, EOC-1

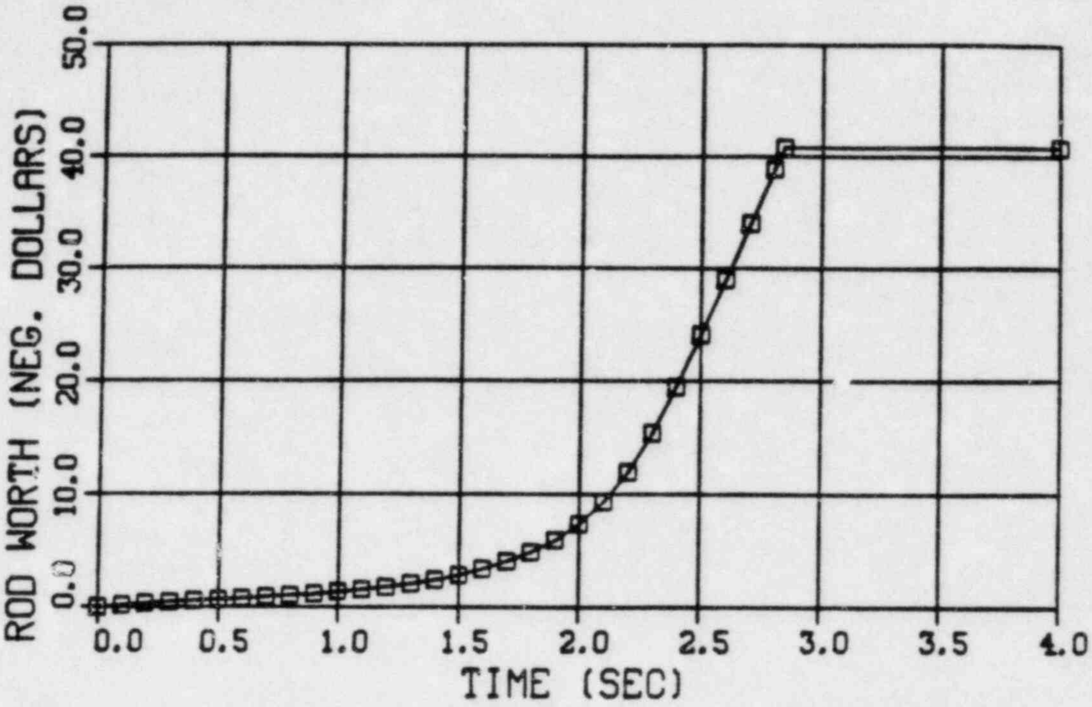

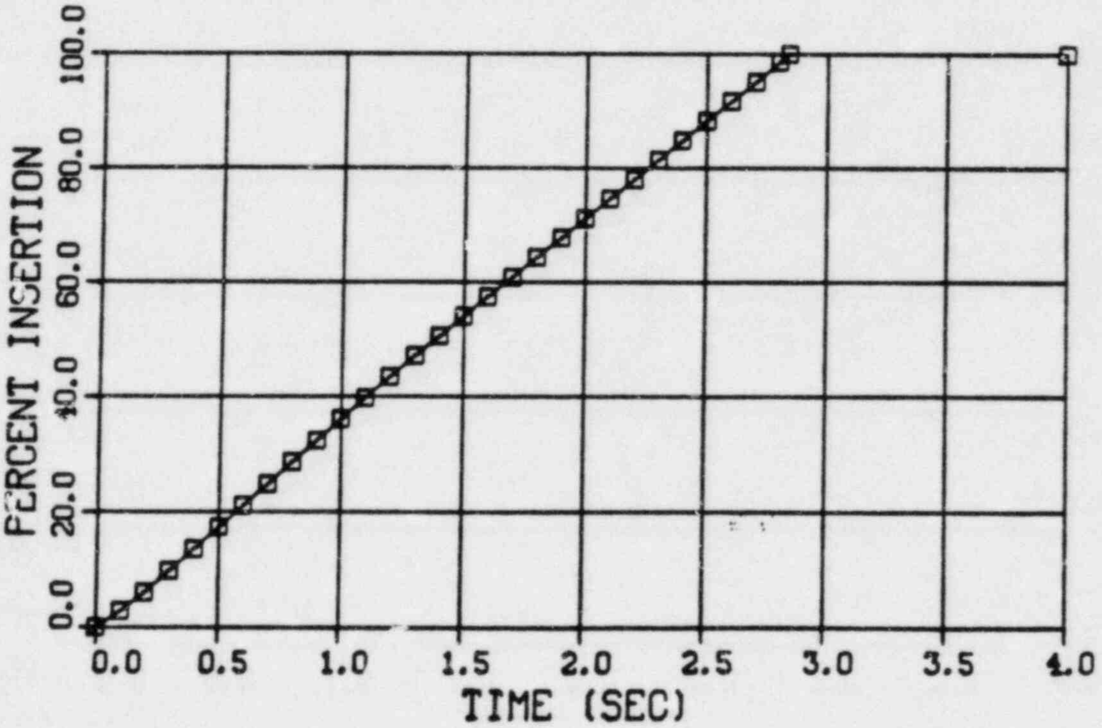

FIGURE 7.1.3

INSERTED ROD WORTH AND ROD POSITION VERSUS TIME FROM INITIAL ROD MOVEMENT AT EOC10-1000 MWD/ST, "MEASURED" SCRAM TIME

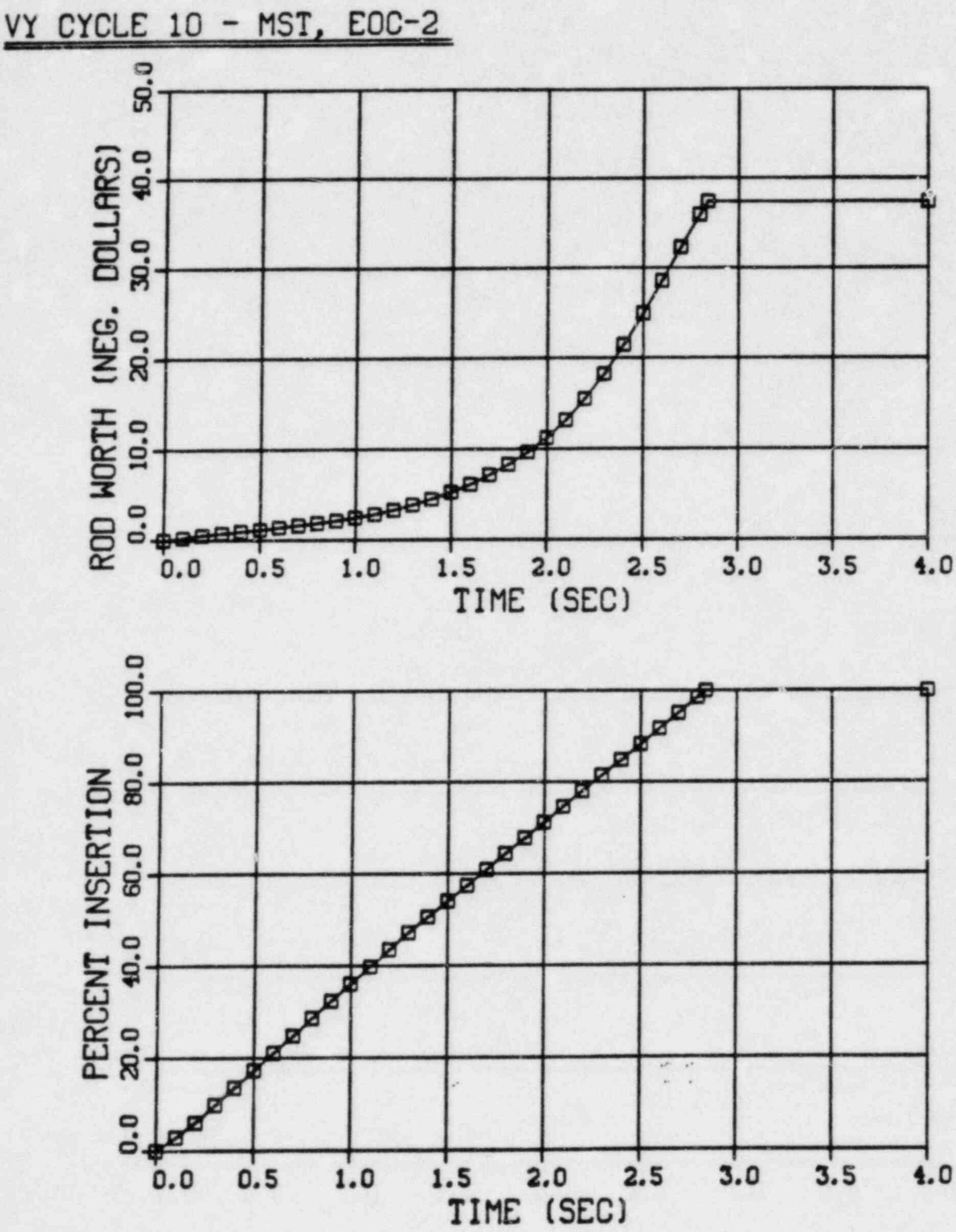

FIGURE 7.1.4

INSERTED ROD WORTH AND ROD POSITION VERSUS TIME FROM INITIAL ROD MOVEMENT AT EOC10-2000 MWD/ST, "MEASURED" SCRAM TIME

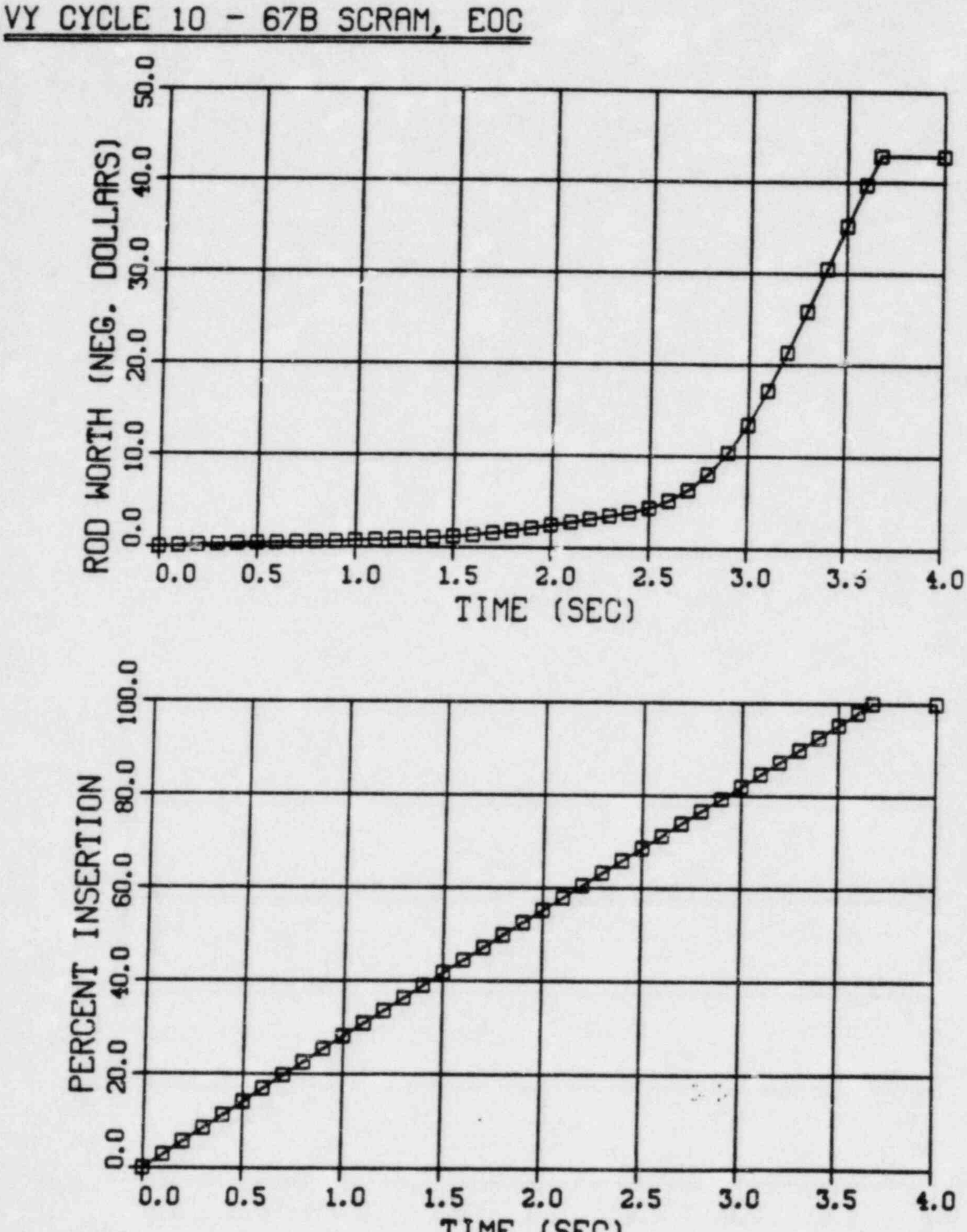

FIGURE 7.1.5

INSERTED ROD WORTH AND ROD POSITION VERSUS TIME FROM INITIAL ROD MOVEMENT AT EOC10, "67B" SCRAM TIME

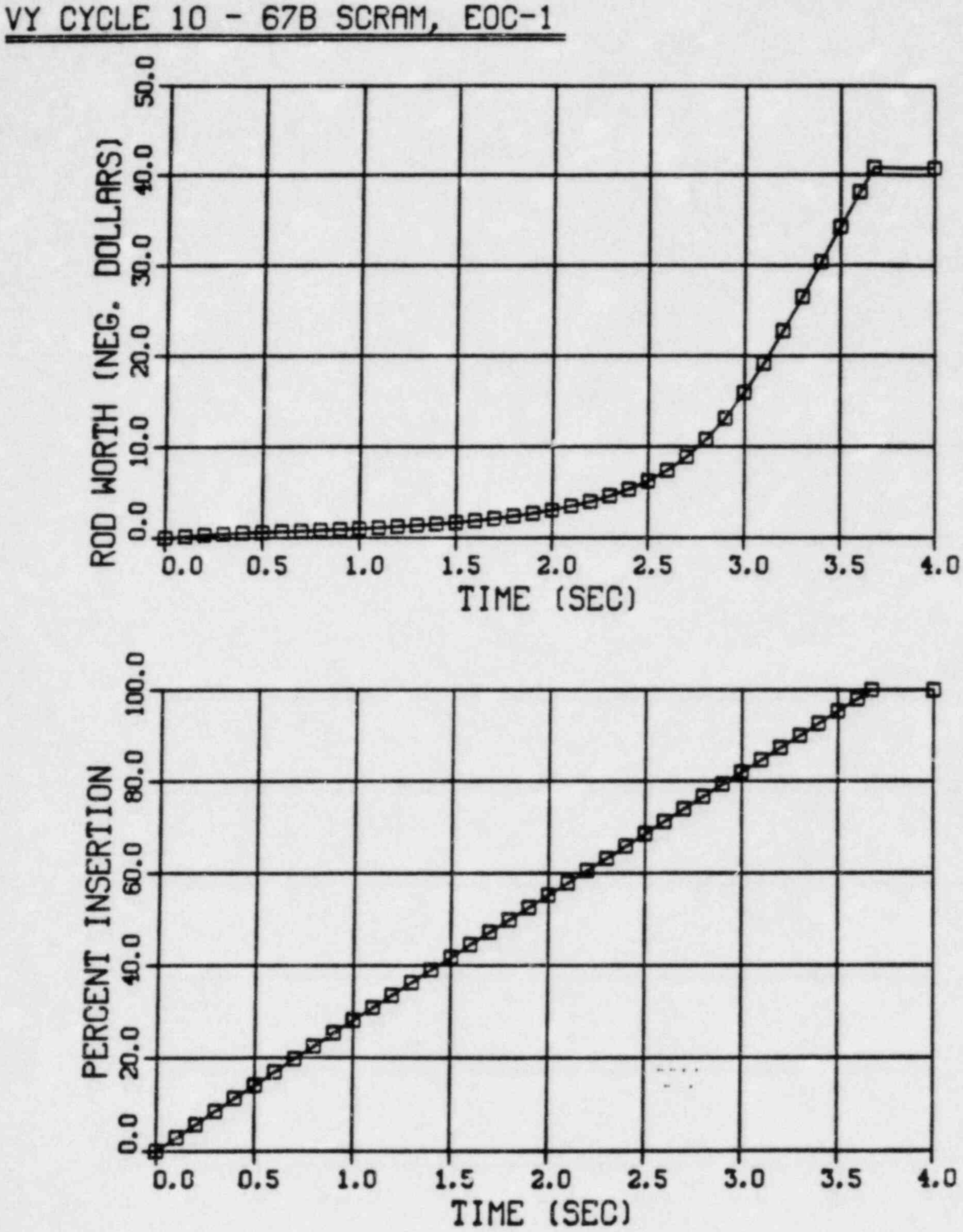

FIGURE 7.1.6

INSERTED ROD WORTH AND ROD POSITION VERSUS TIME FROM INITIAL ROD MOVEMENT AT EOC10-1000 MWD/ST, "67B" SCRAM TIME

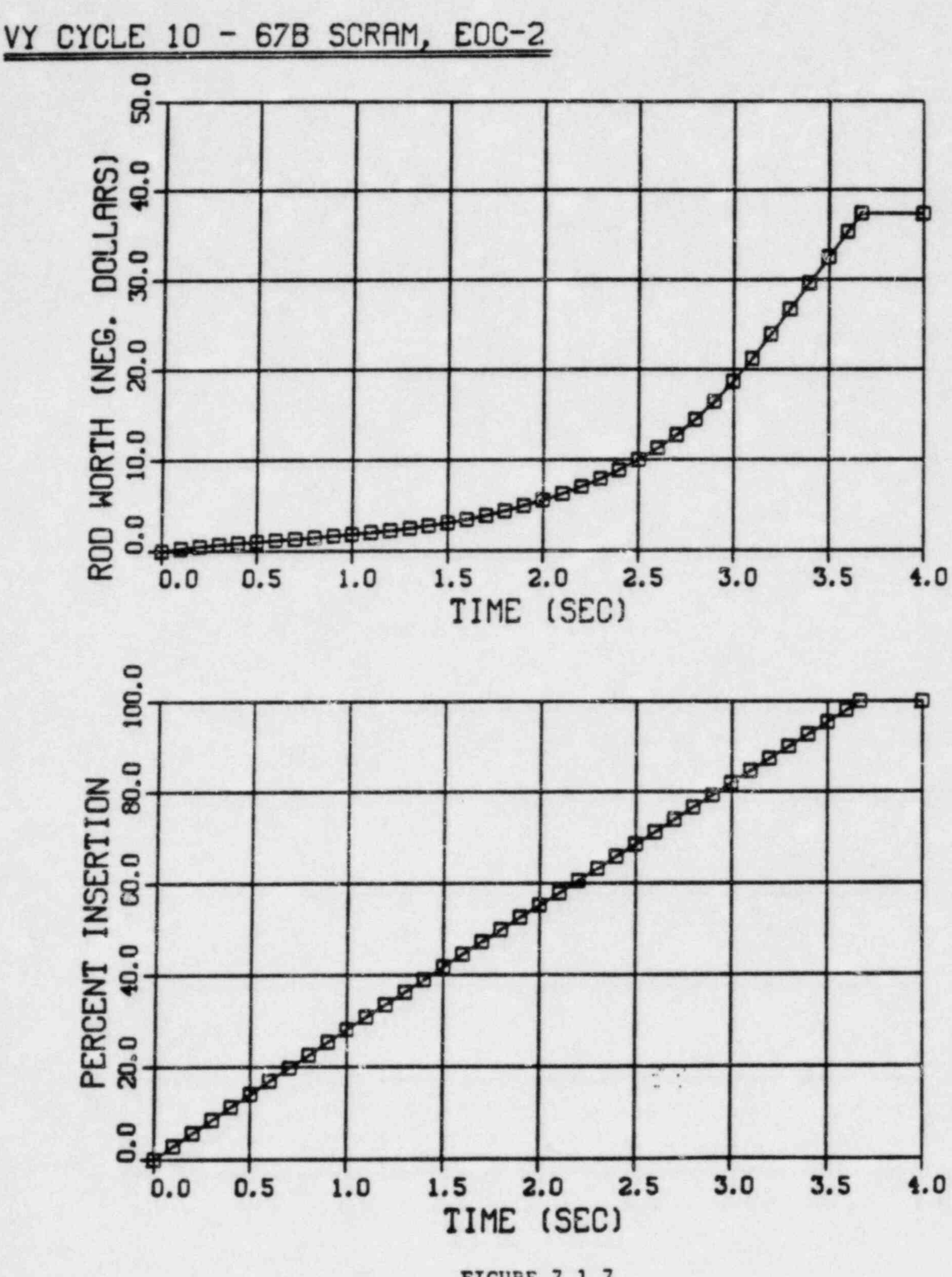

FIGURE 7.1.7

INSERTED ROD WORTH AND ROD POSITION VERSUS TIME FROM INITIAL ROD MOVEMENT AT EOC10-2000 MWD/ST, "67B" SCRAM TIME

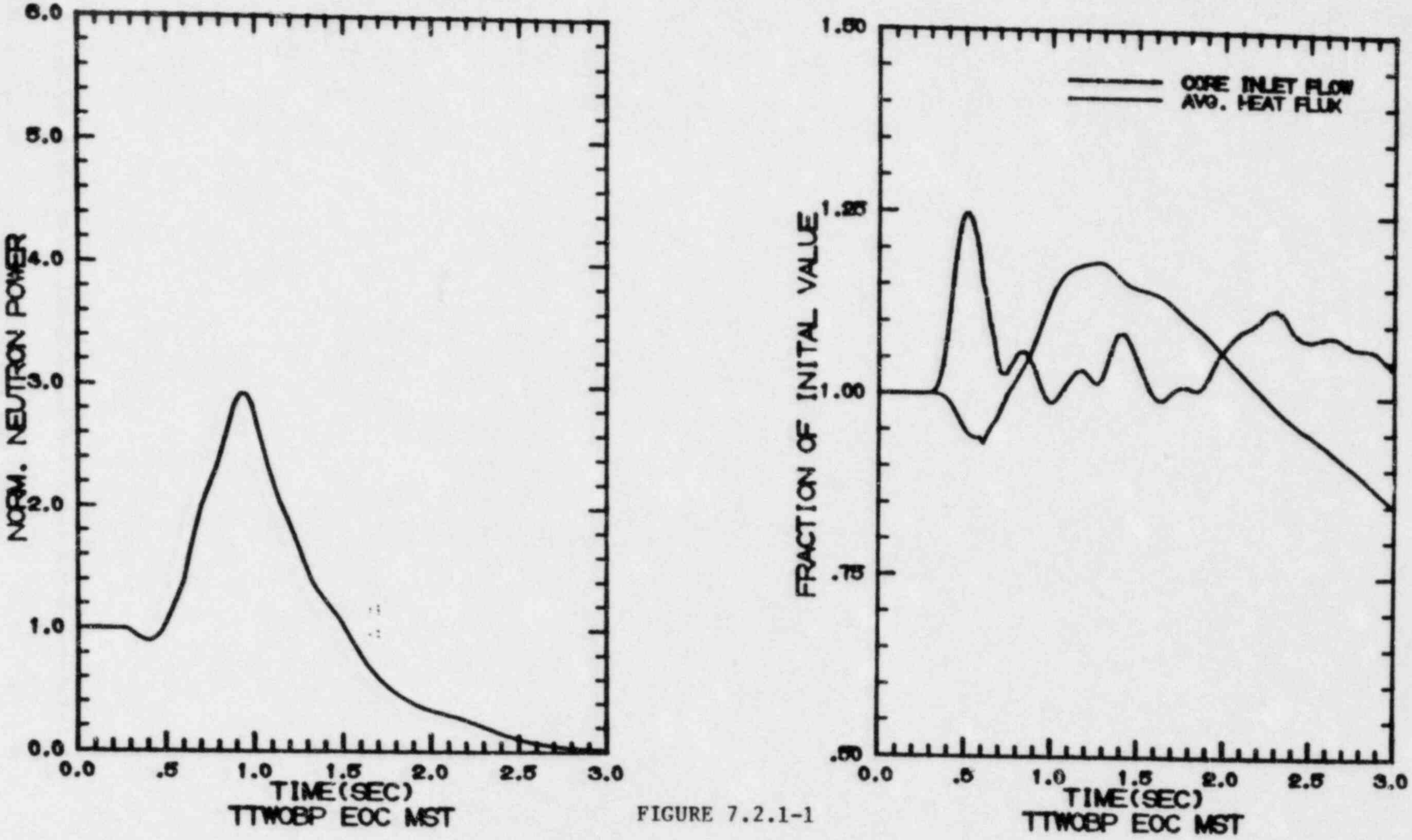

FIGURE 7.2.1-1

TURBINE TRIP WITHOUT BYPASS, EOC10

TRANSIENT RESPONSE VERSUS TIME, "MEASURED" SCRAM TIME

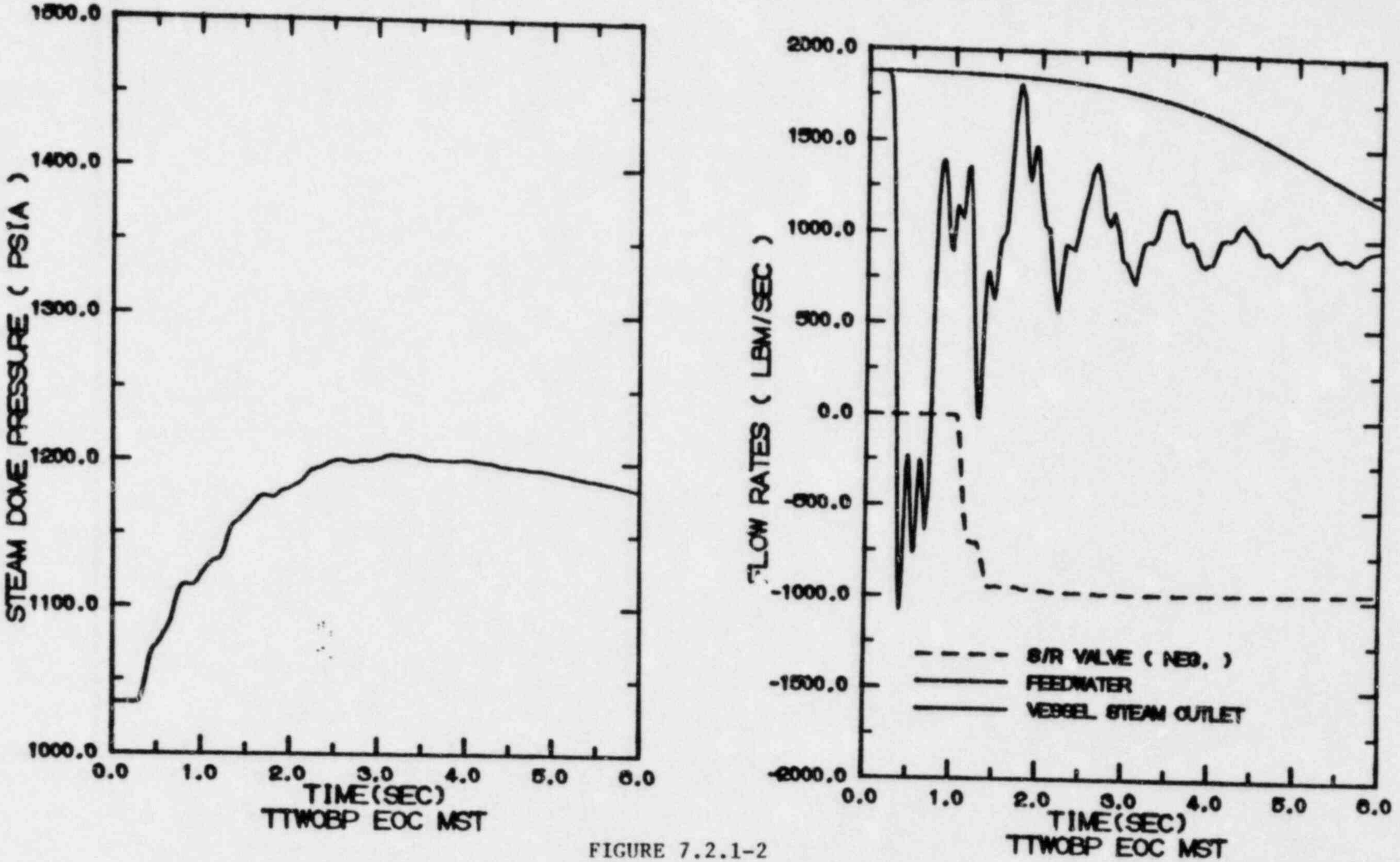

FIGURE 7.2.1-2

TURBINE TRIP WITHOUT BYPASS, EOC10

TRANSIENT RESPONSE VERSUS TIME, "MEASURED" SCRAM TIME

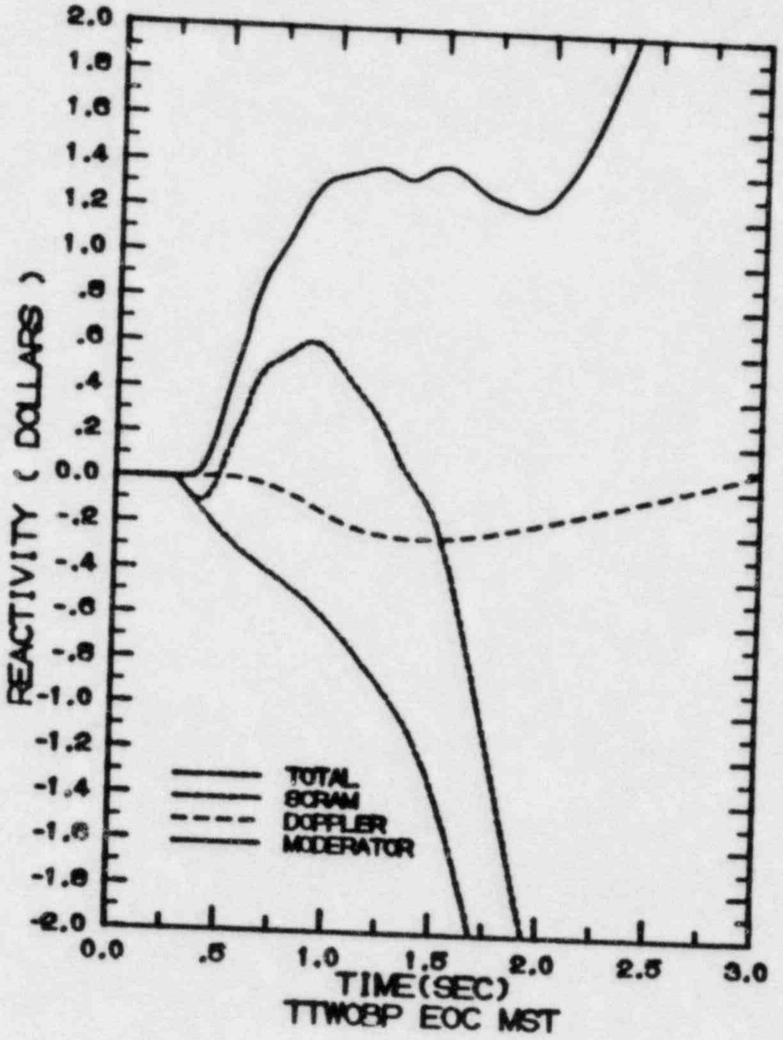

FIGURE 7.2.1-3

TURBINE TRIP WITHOUT BYPASS, EOC10

TRANSIENT RESPONSE VERSUS TIME, "MEASURED" SCRAM TIME

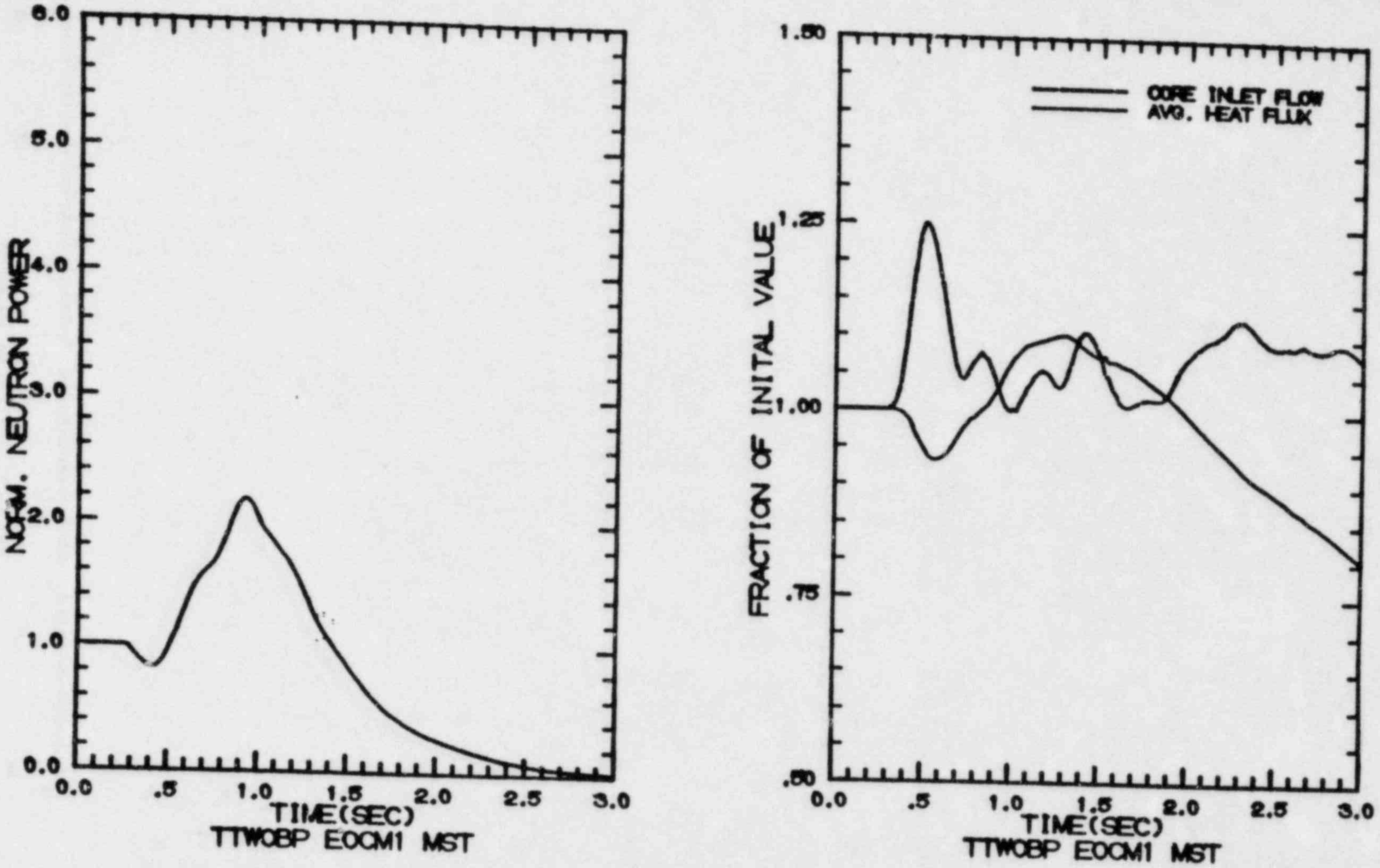

FIGURE 7.2.2-1

TURBINE TRIP WITHOUT BYPASS, EOC10-1000 MWD/ST

TRANSIENT RESPONSE VERSUS TIME, "MEASURED" SCRAM TIME

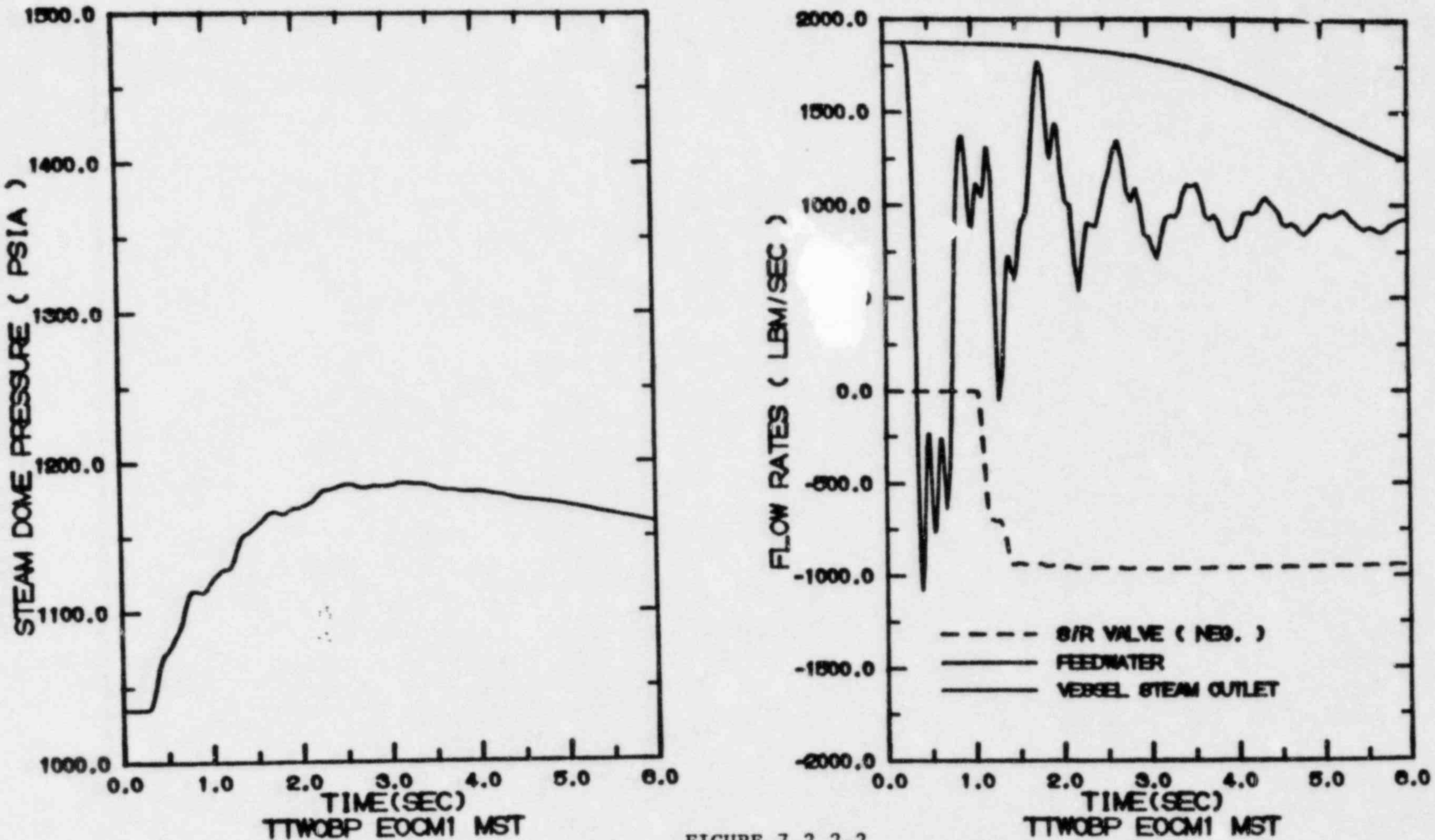

FIGURE 7.2.2-2

TURBINE TRIP WITHOUT BYPASS, EOC10-1000 MWD/ST

TRANSIENT RESPONSE VERSUS TIME, "MEASURED" SCRAM TIME

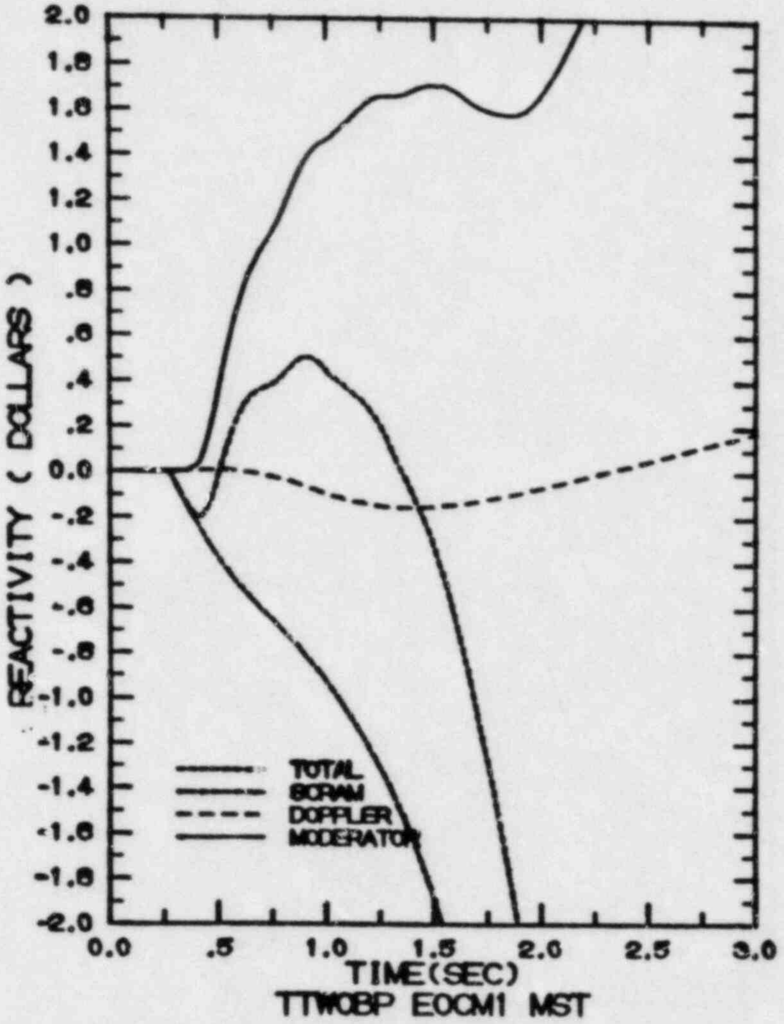

FIGURE 7.2.2-3

TURBINE TRIP WITHOUT BYPASS, EOC10-1000 MWD/ST

TRANSIENT RESPONSE VERSUS TIME, "MEASURED" SCRAM TIME

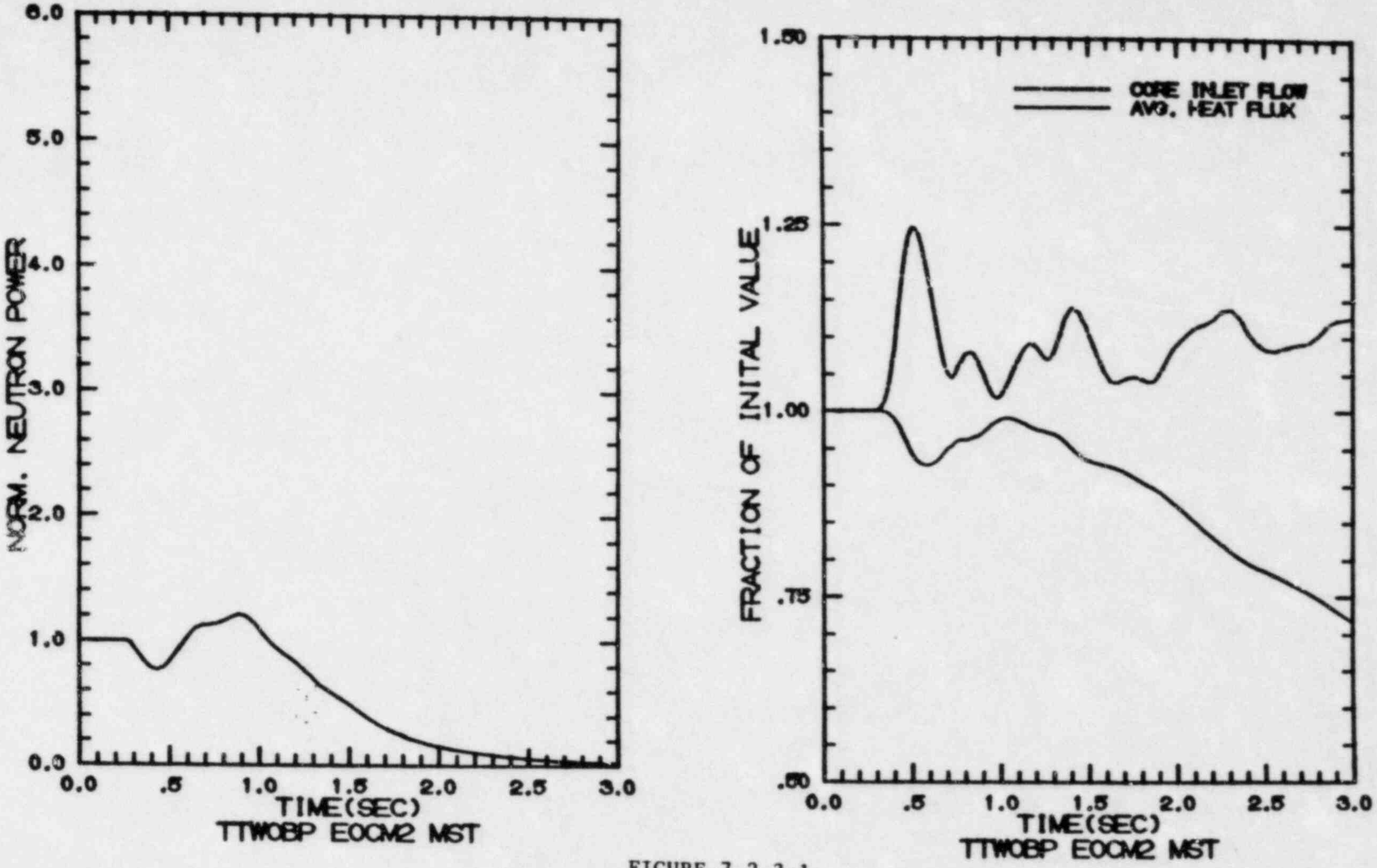

FIGURE 7.2.3-1

TURBINE TRIP WITHOUT BYPASS, EOC10-2000 MWD/ST

TRANSIENT RESPONSE VERSUS TIME, "MEASURED" SCRAM TIME

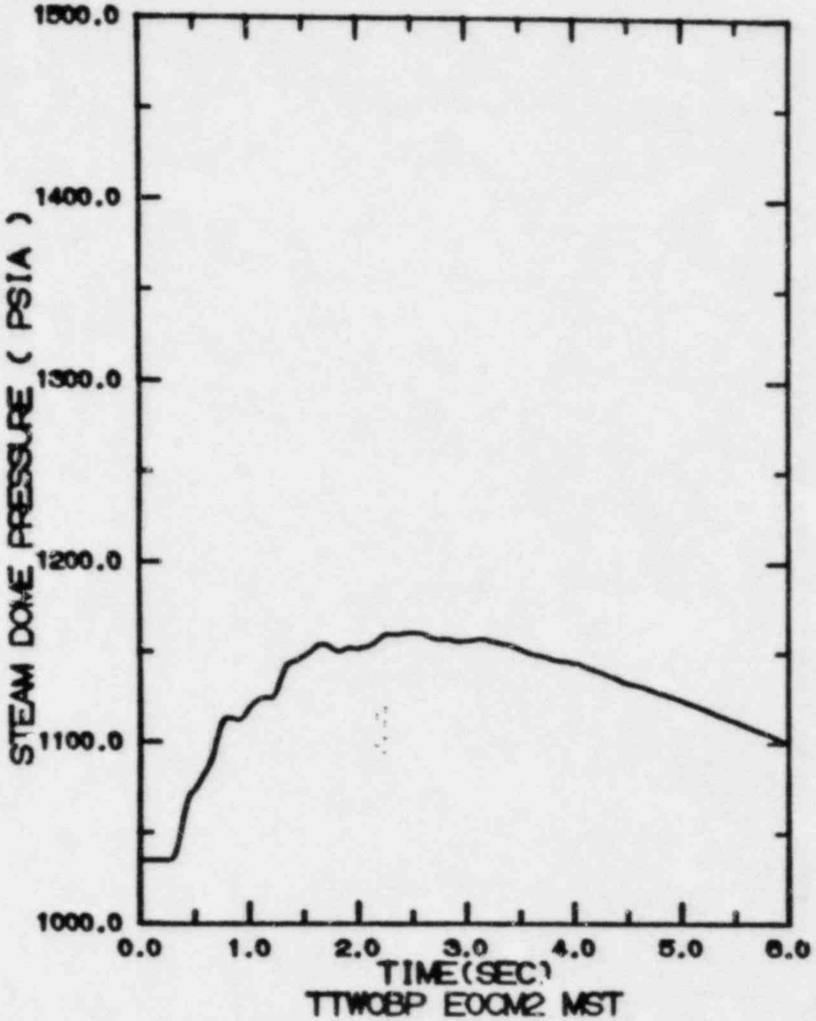

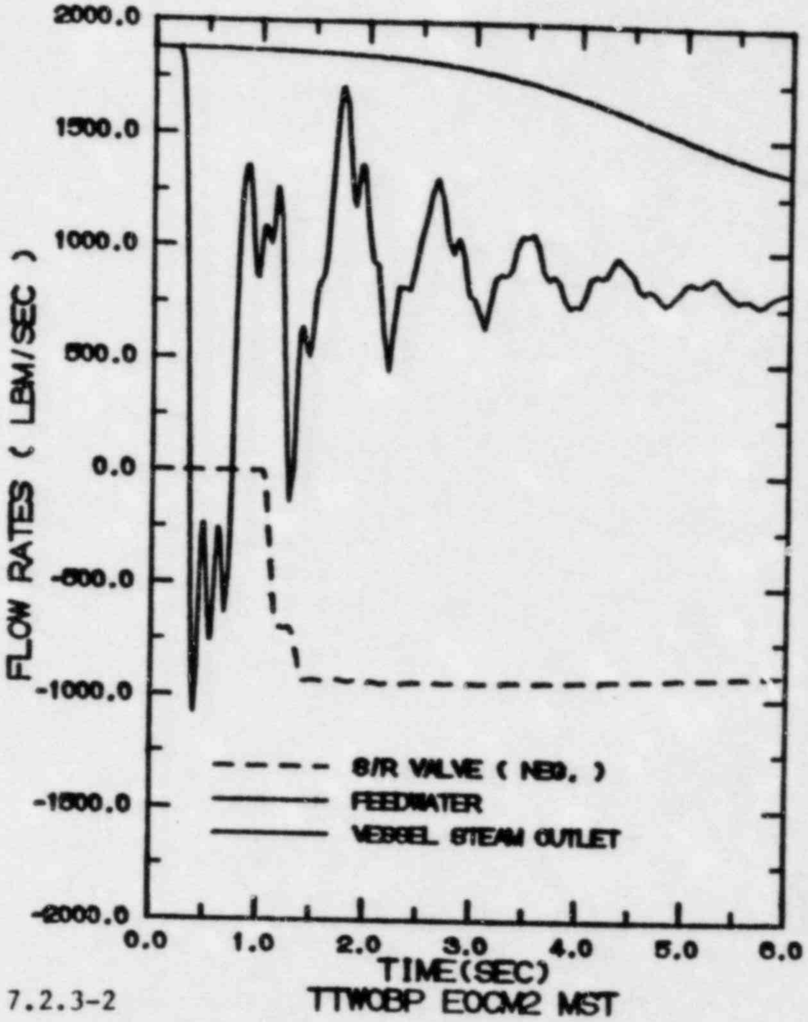

FIGURE 7.2.3-2

TURBINE TRIP WITHOUT BYPASS, EOC10-2000 MWD/ST

TRANSIENT RESPONSE VERSUS TIME, "MEASURED" SCRAM TIME

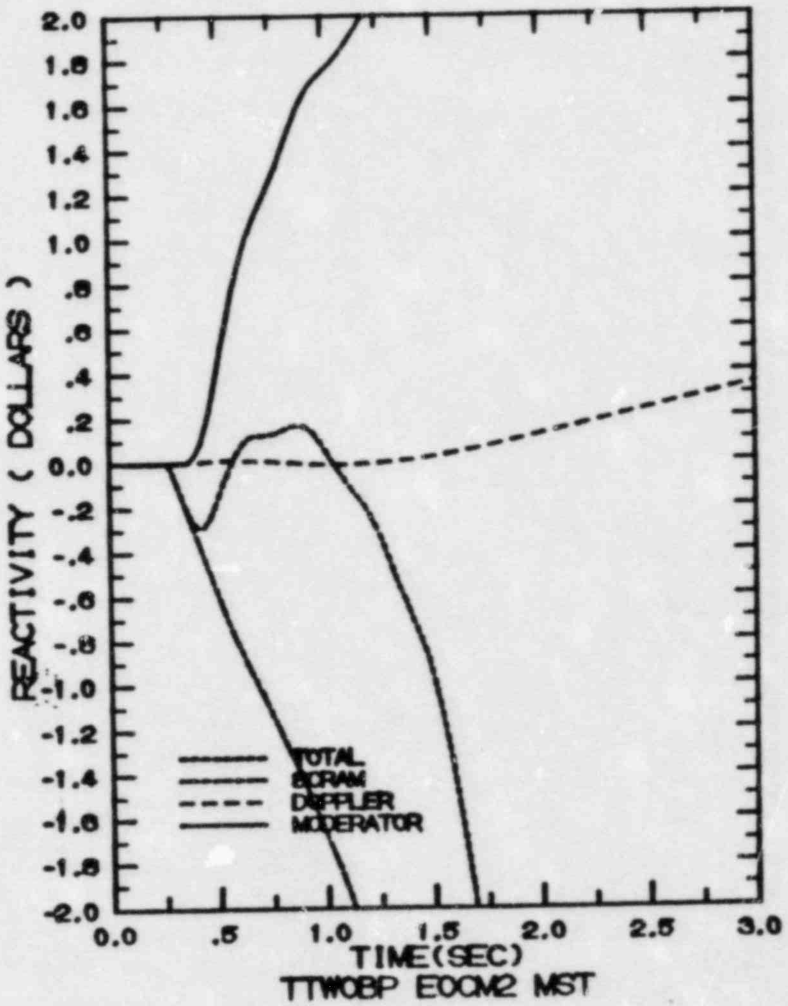

FIGURE 7.2.3-3

TURBINE TRIP WITHOUT BYPASS, EOC10-2000 MWD/ST

TRANSIENT RESPONSE VERSUS TIME, "MEASURED" SCRAM TIME

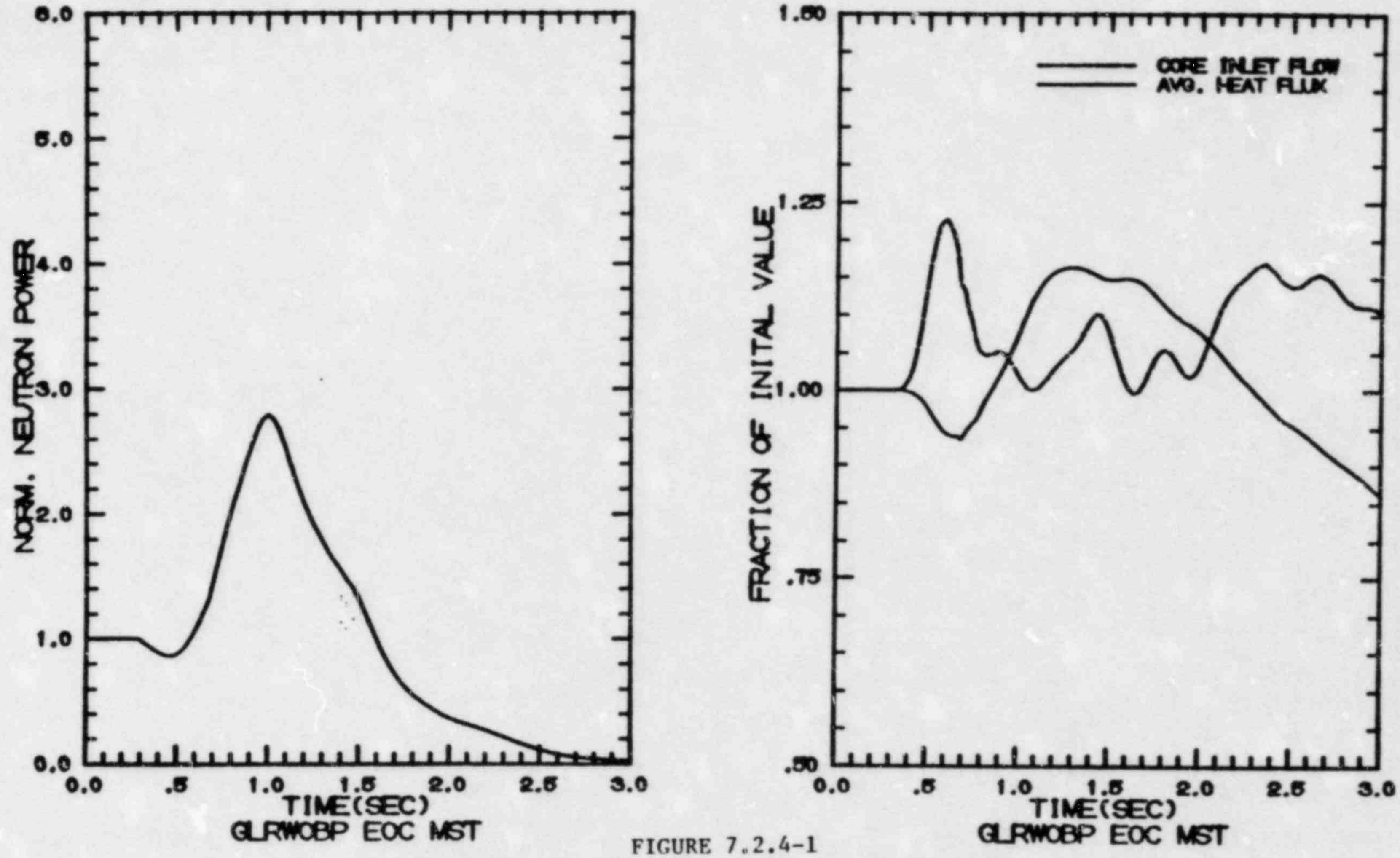

FIGURE 7.2.4-1

GENERATOR LOAD REJECTION WITHOUT BYPASS, EOC10

TRANSIENT RESPONSE VERSUS TIME, "MEASURED" SCRAM TIME

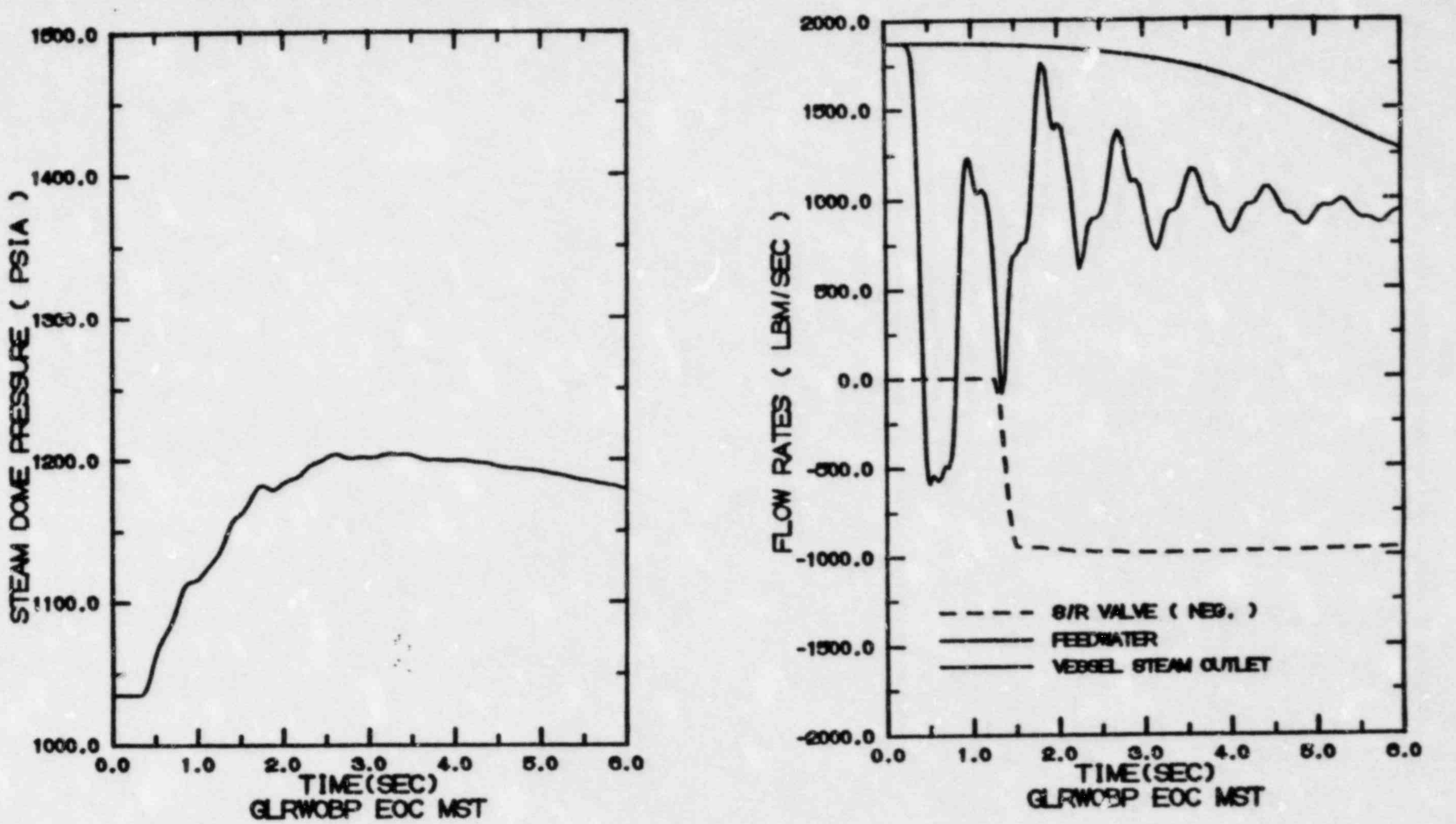

FIGURE 7.2.4-2

GENERATOR LOAD REJECTION WITHOUT BYPASS, EOC10
TRANSIENT RESPONSE VERSUS TIME, "MEASURED" SCRAM TIME

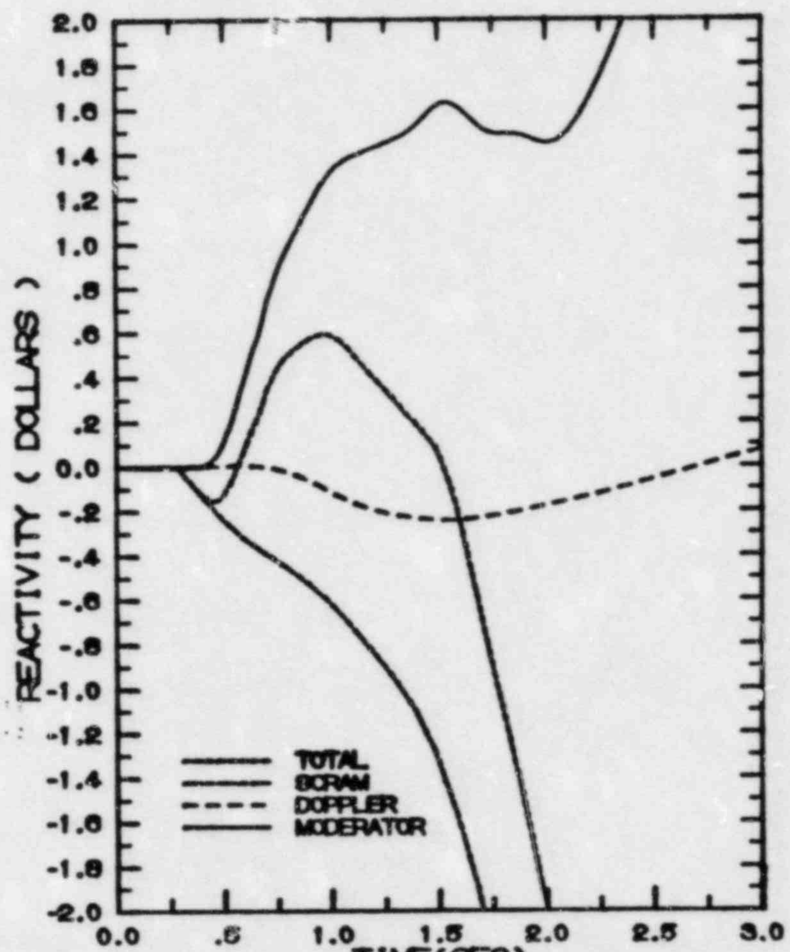

GLRWOBP EOC MST

FIGURE 7.2.4-3

GENERATOR LOAD REJECTION WITHOUT BYPASS, EOC10

TRANSIENT RESPONSE VERSUS TIME, "MEASURED" SCRAM TIME

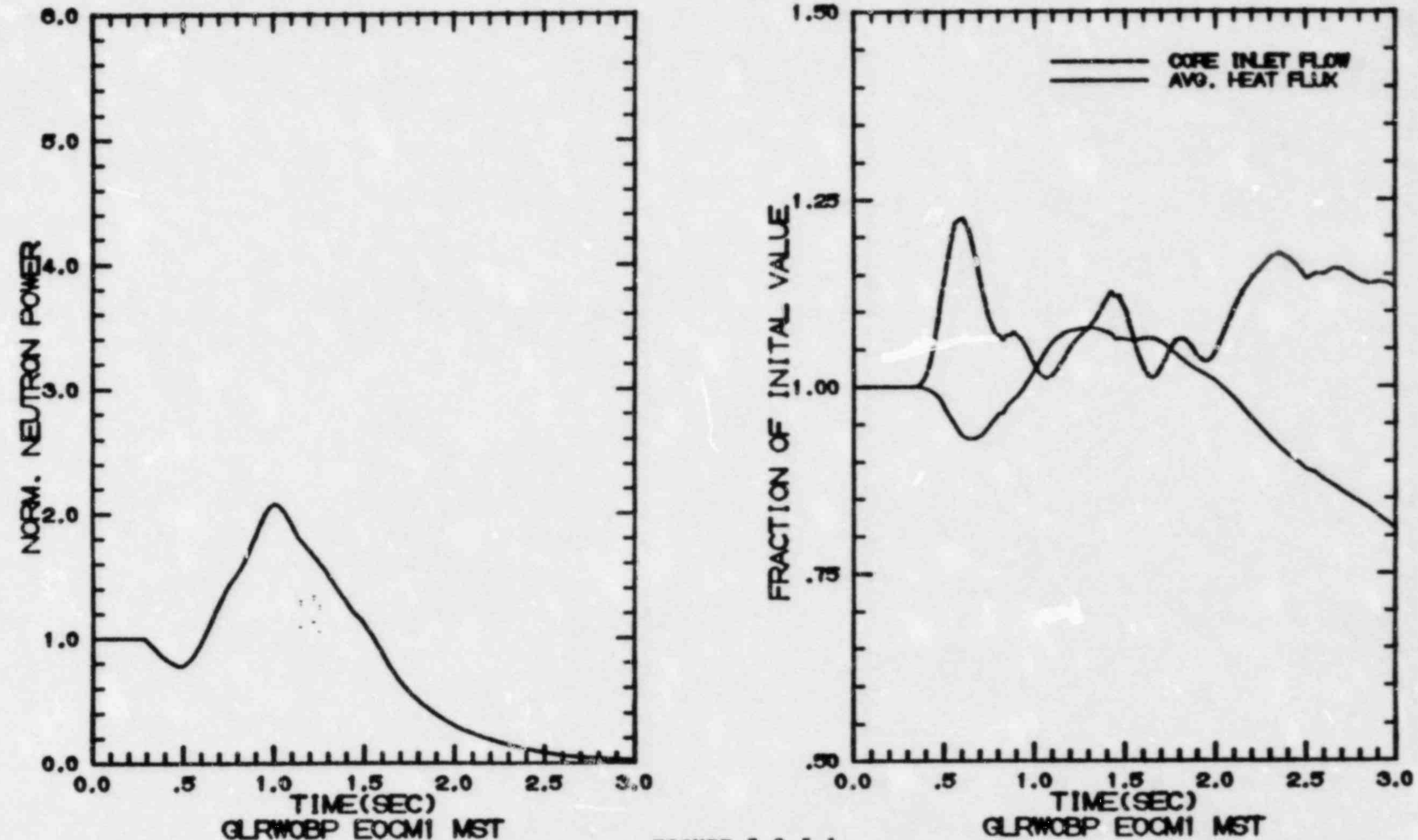

FIGURE 7.2.5-1

GENERATOR LOAD REJECTION WITHOUT BYPASS, EOC10-1000 MWD/ST

TRANSIENT RESPONSE VERSUS TIME, "MEASURED" SCRAM TIME

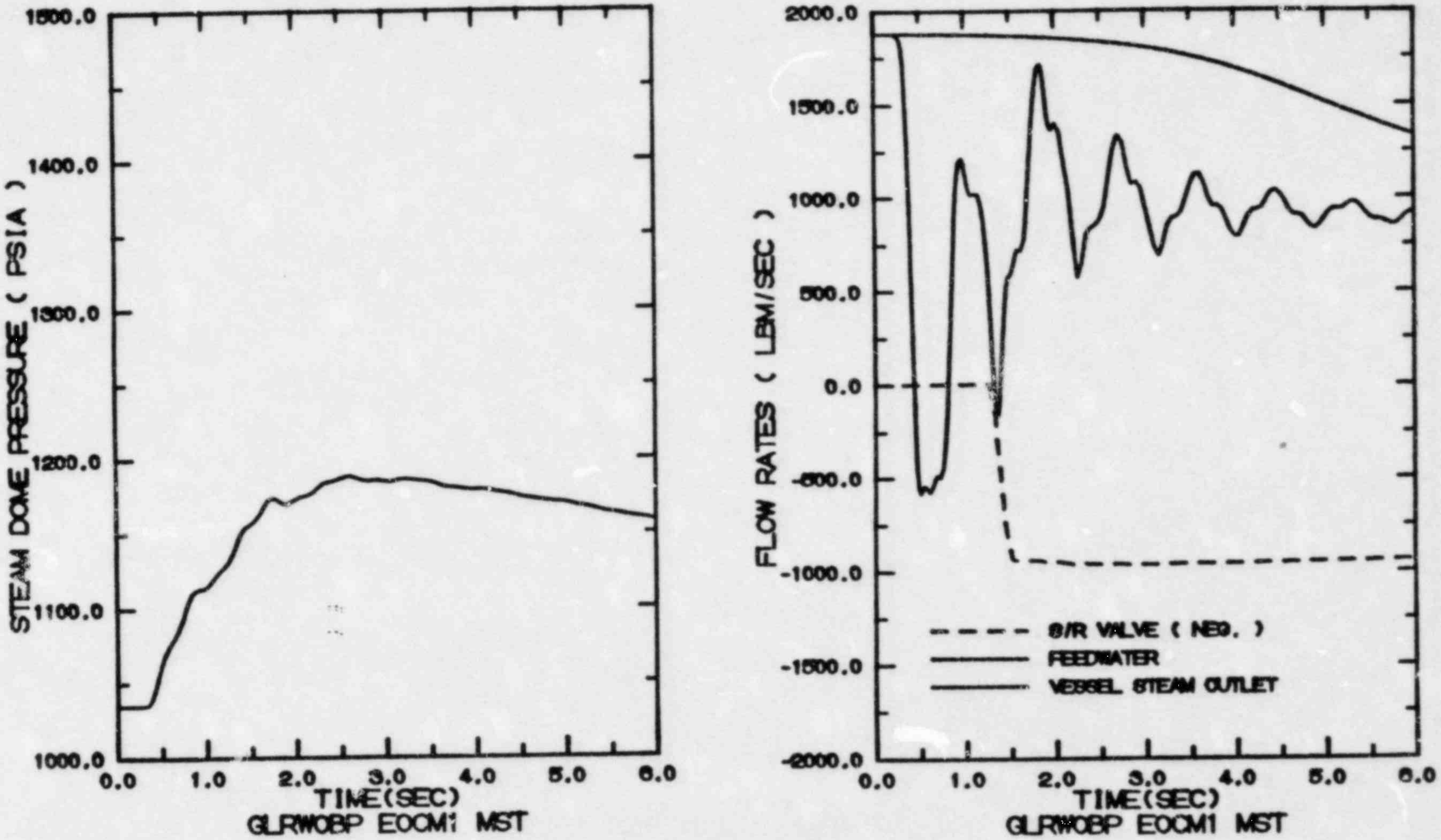

FIGURE 7.2.5-2

GENERATOR LOAD REJECTION WITHOUT BYPASS, EOC10-1000 MWD/ST
TRANSIENT RESPONSE VERSUS TIME, "MEASURED" SCRAM TIME

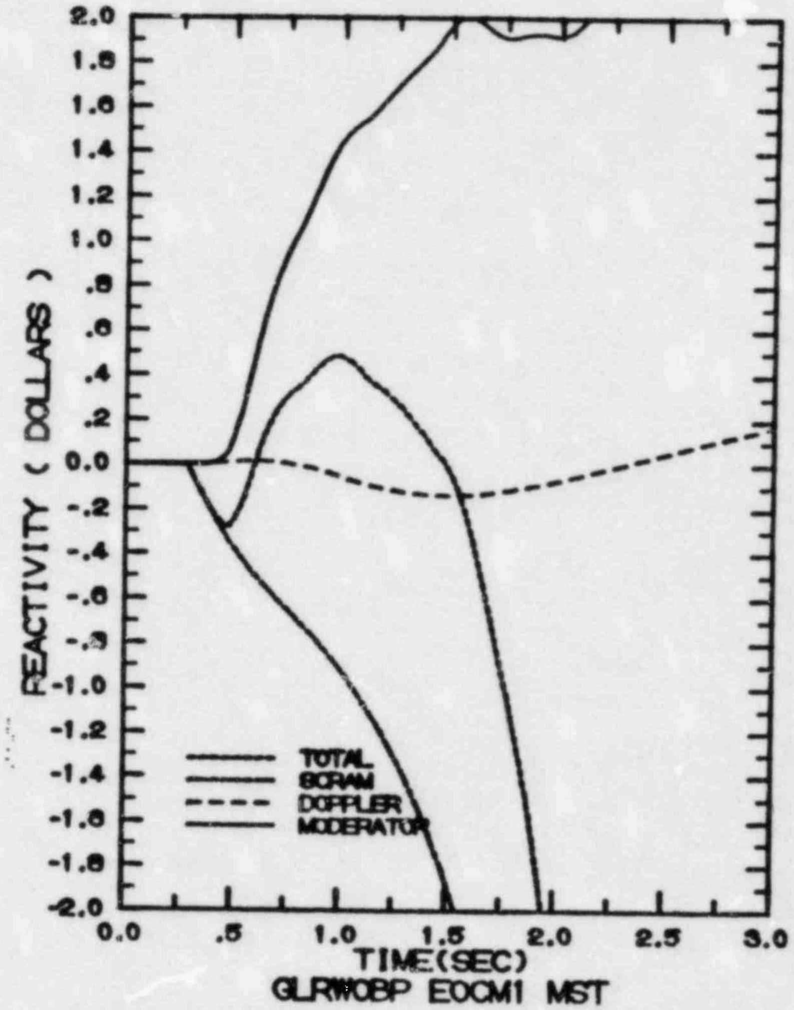

FIGURE 7.2.5-3

GENERATOR LOAD REJECTION WITHOUT BYPASS, EOC10-1000 MWD/ST

TRANSIENT RESPONSE VERSUS TIME, "MEASURED" SCRAM TIME

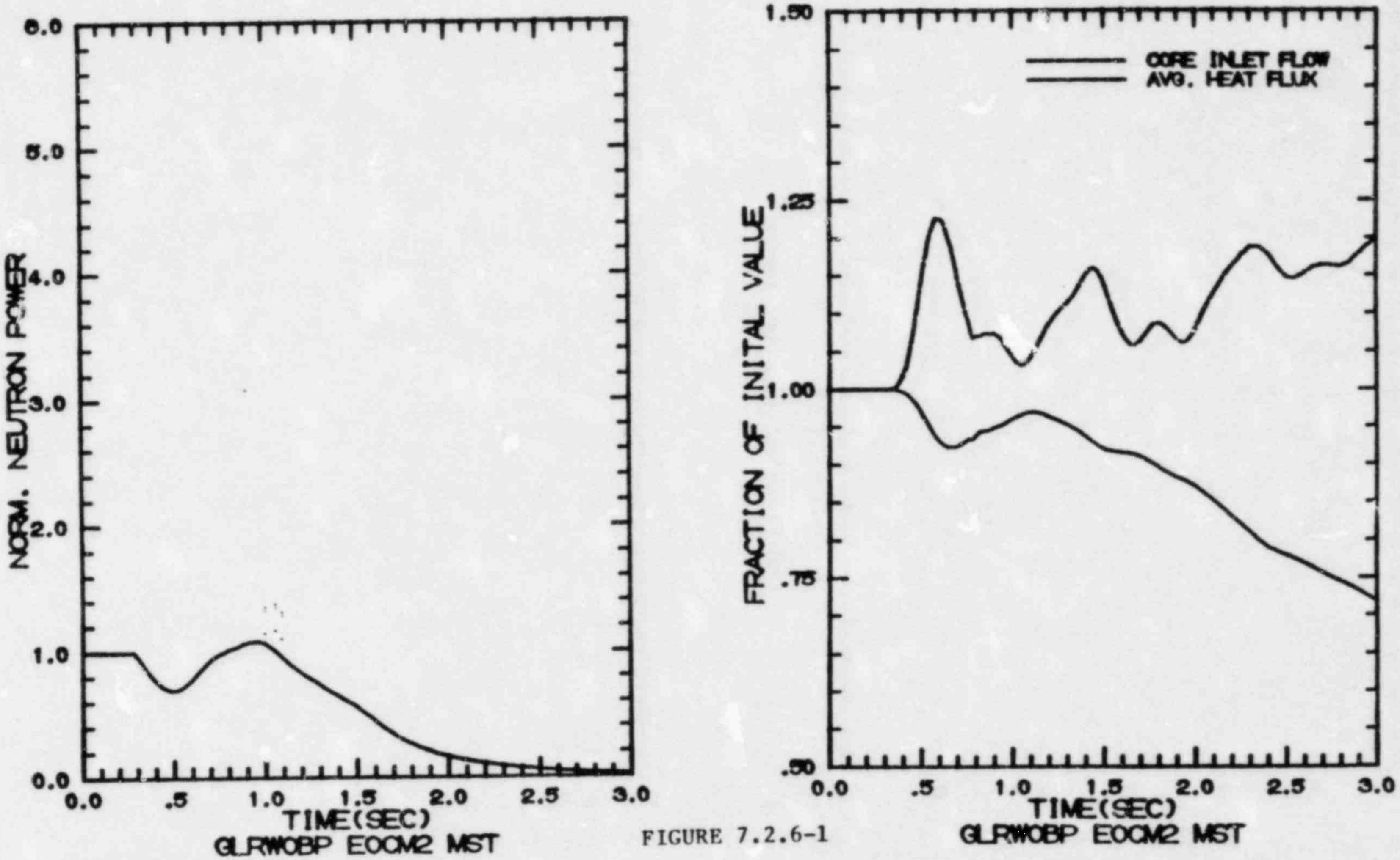

FIGURE 7.2.6-1

GENERATOR LOAD REJECTION WITHOUT BYPASS, EOC10-2000 MWD/ST

TRANSIENT RESPONSE VERSUS TIME, "MEASURED" SCRAM TIME

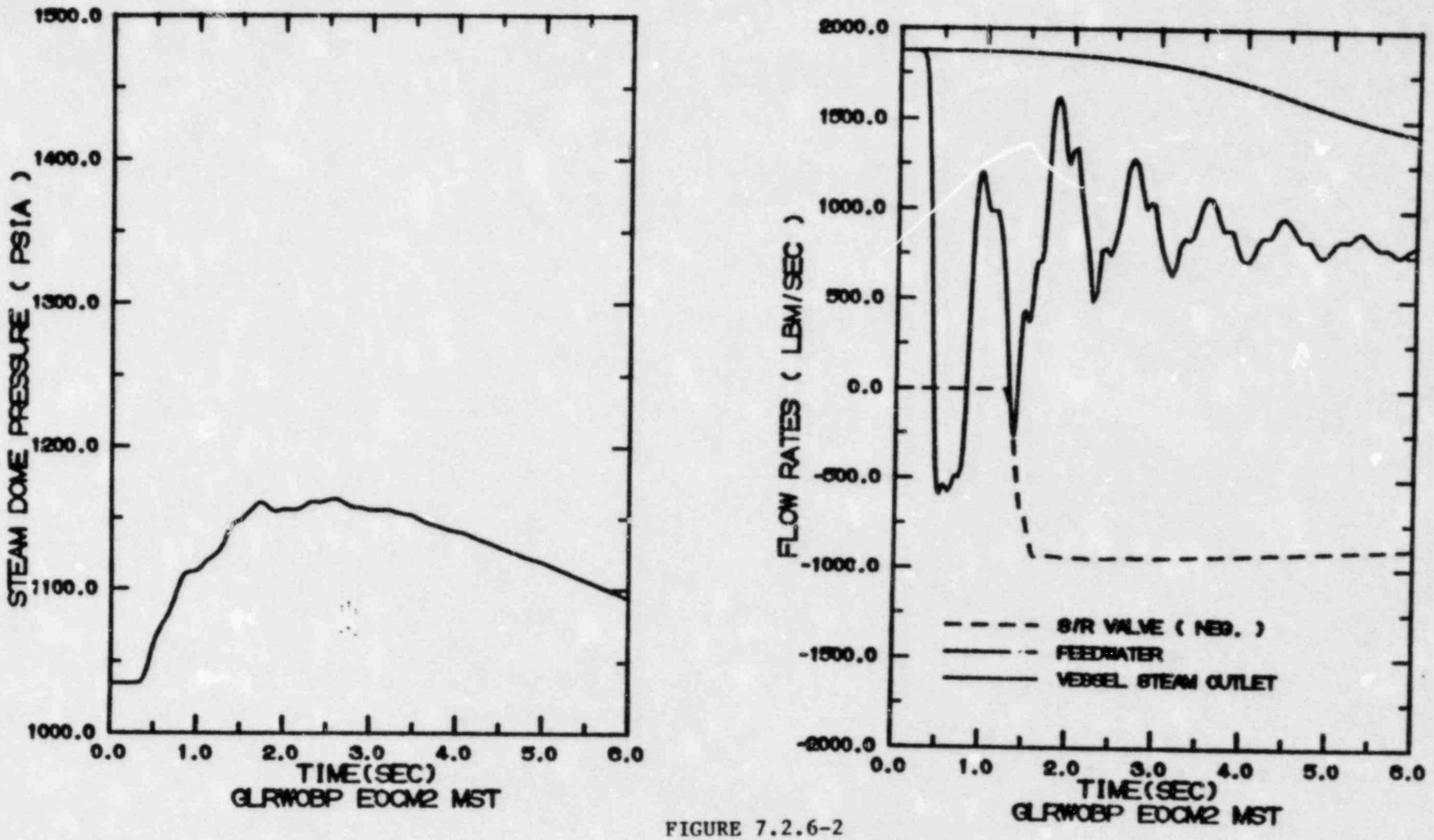

FIGURE 7.2.6-2

GENERATOR LOAD REJECTION WITHOUT BYPASS, EOC10-2000 MWD/ST
TRANSIENT RESPONSE VERSUS TIME, "MEASURED" SCRAM TIME

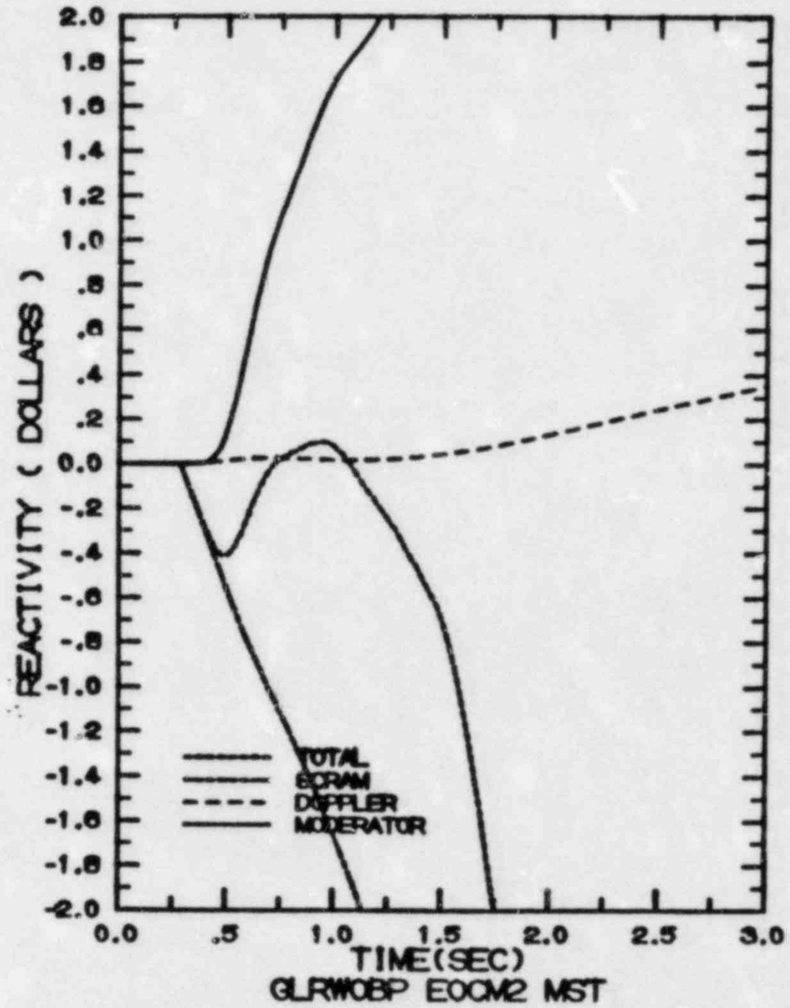

FIGURE 7.2.6-3

GENERATOR LOAD REJECTION WITHOUT BYPASS, EOC10-2000 MWD/ST
TRANSIENT RESPONSE VERSUS TIME, "MEASURED" SCRAM TIME

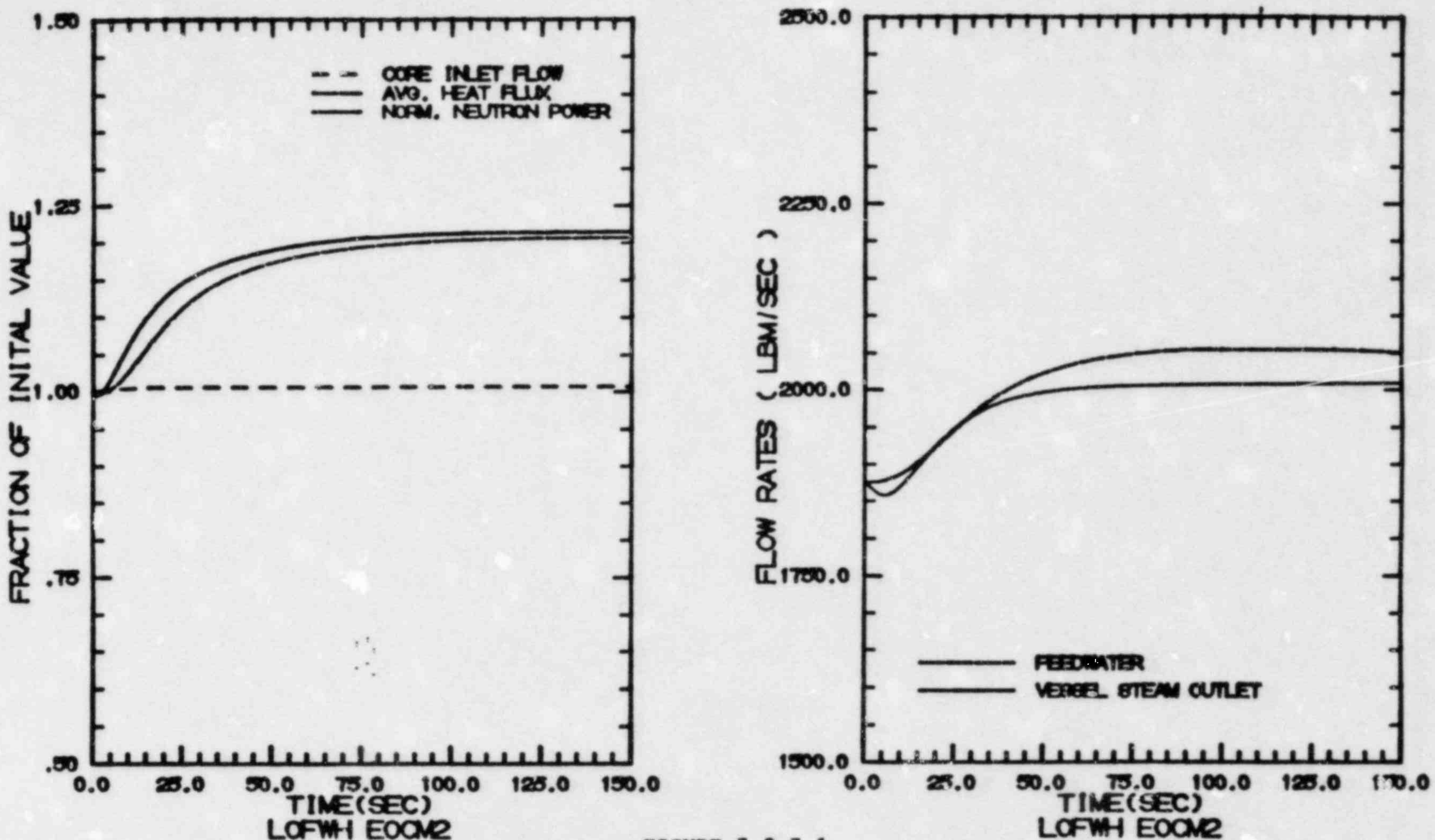

FIGURE 7.2.7-1

LOSS OF 100^{o}F FEEDWATER HEATING, EOC10-2000 MWD/ST (LIMITING CASE)
TRANSIENT RESPONSE VERSUS TIME

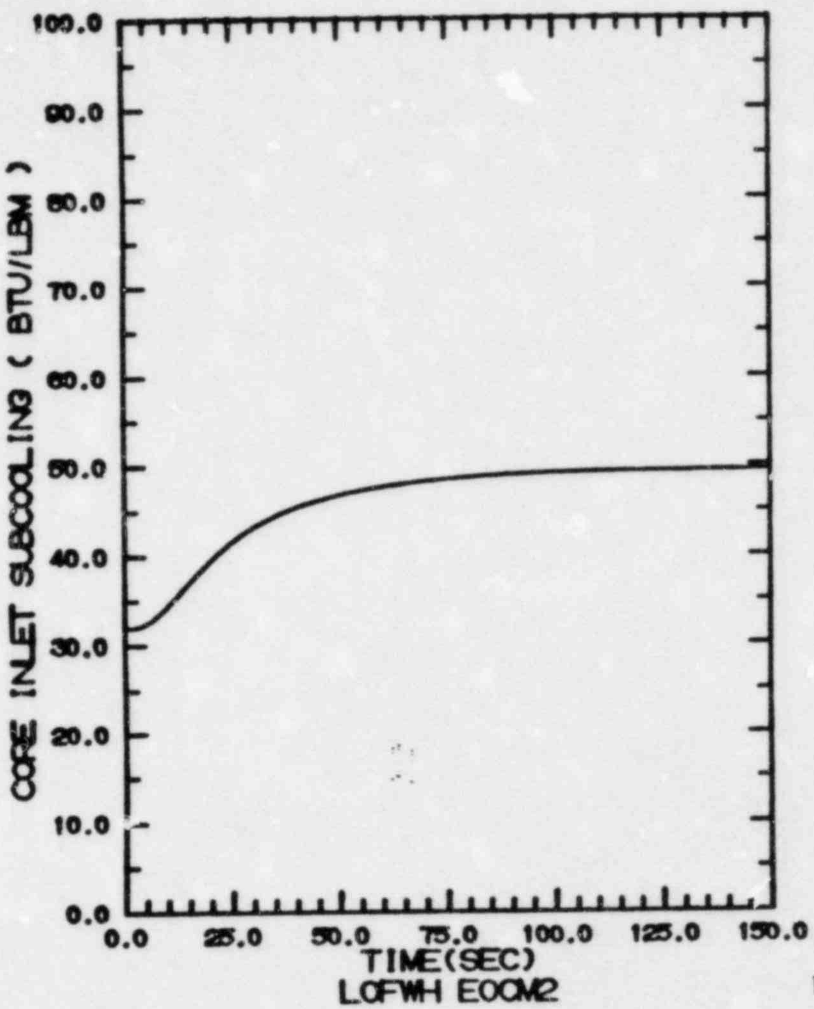

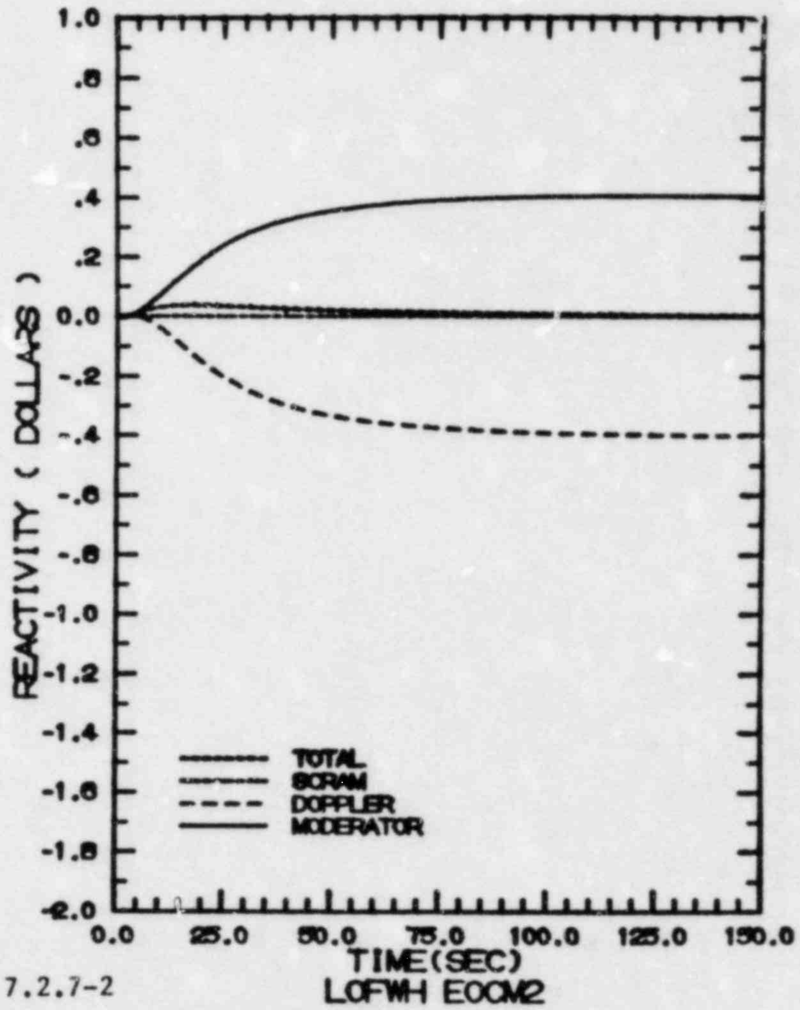

FIGURE 7.2.7-2

LOSS OF 100°F FEEDWATER HEATING, EOC10-2000 MWD/ST (LIMITING CASE)
TRANSIENT RESPONSE VERSUS TIME

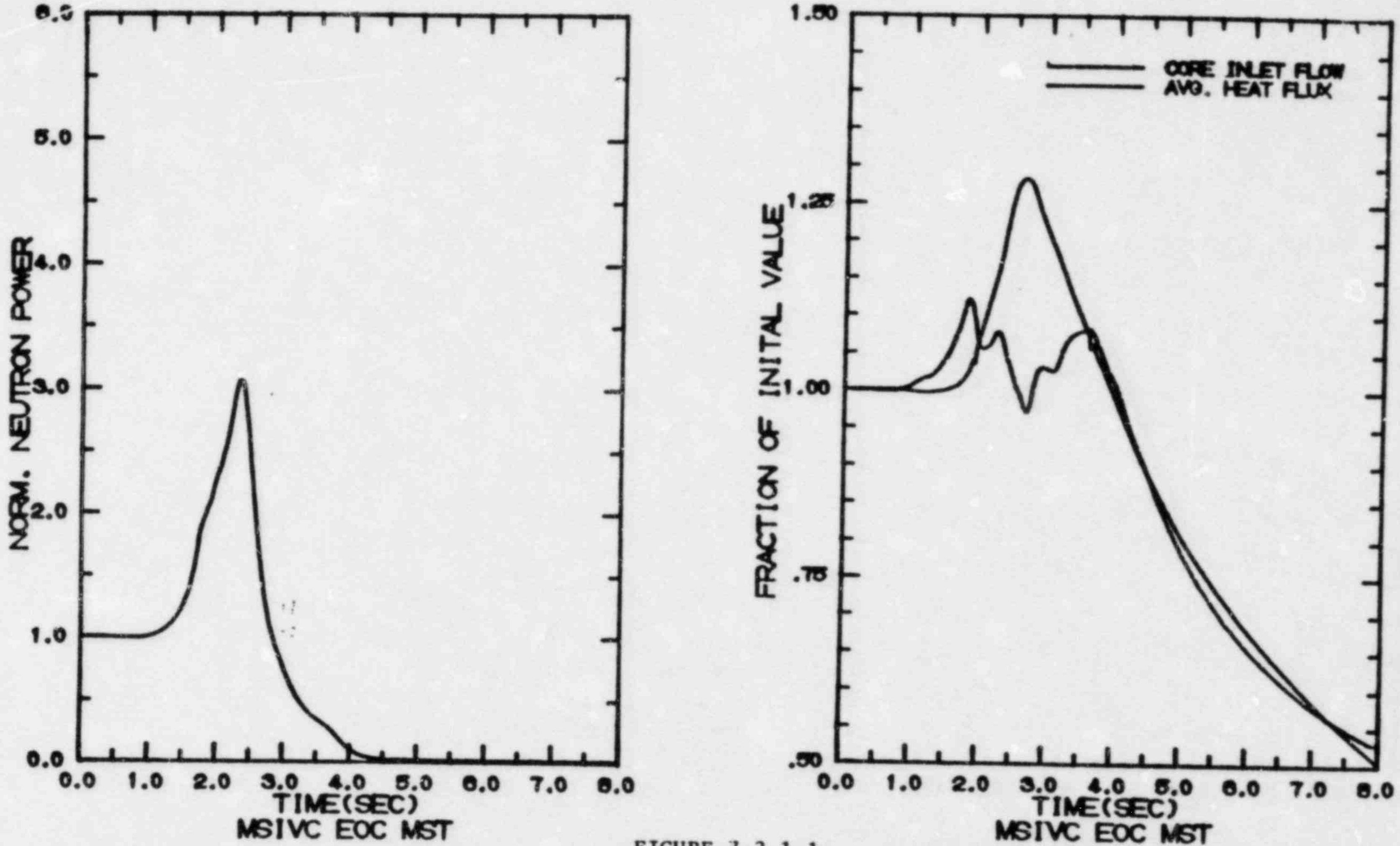

FIGURE 7.3.1-1

MSIV CLOSURE, FLUX SCRAM, EOC10
TRANSIENT RESPONSE VERSUS TIME, "MEASURED" SCRAM TIME

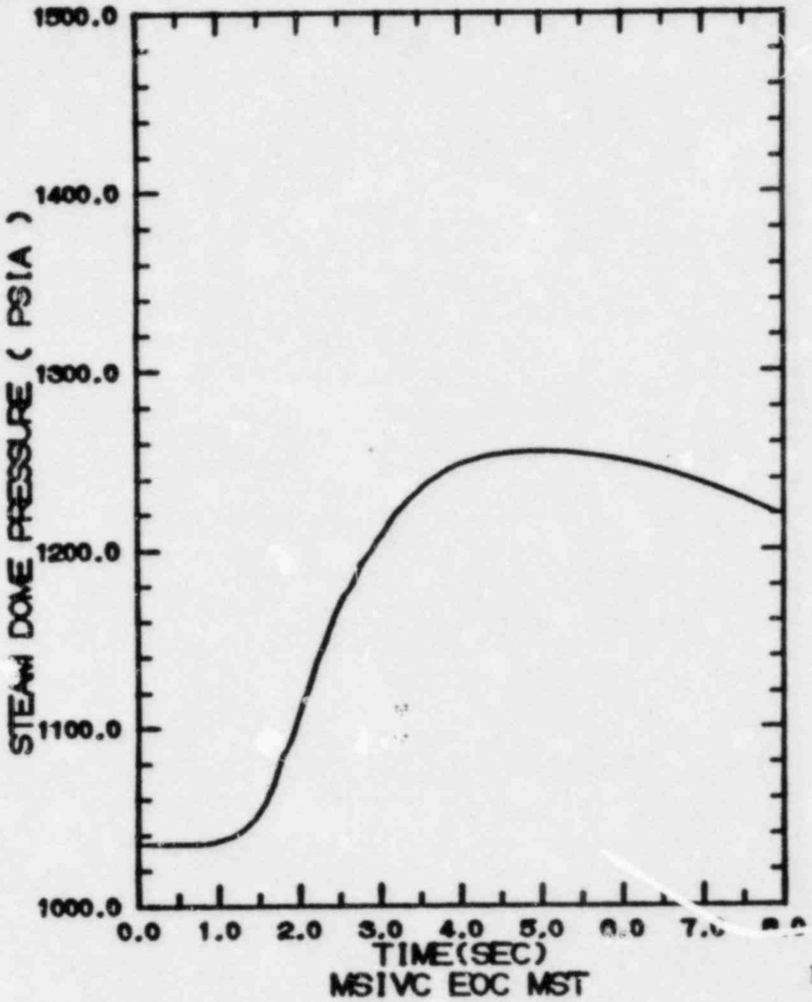

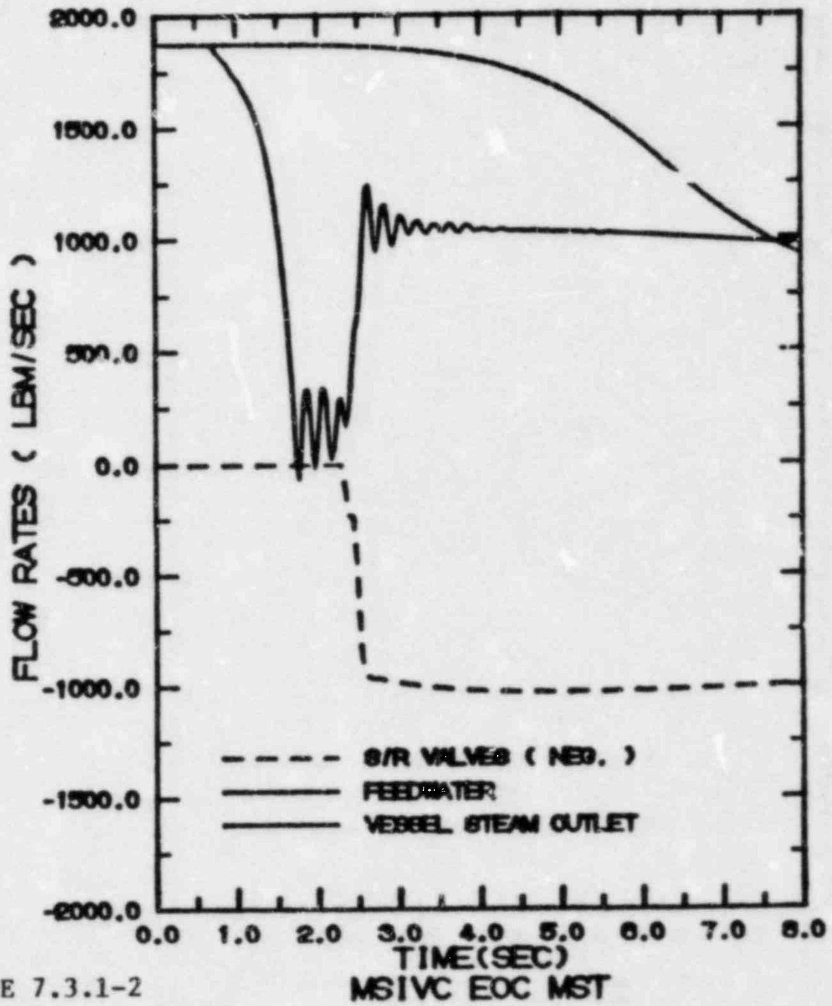

FIGURE 7.3.1-2

MSIV CLOSURE, FLUX SCRAM, EOC10

TRANSIENT RESPONSE VERSUS TIME, "MEASURED" SCRAM TIME

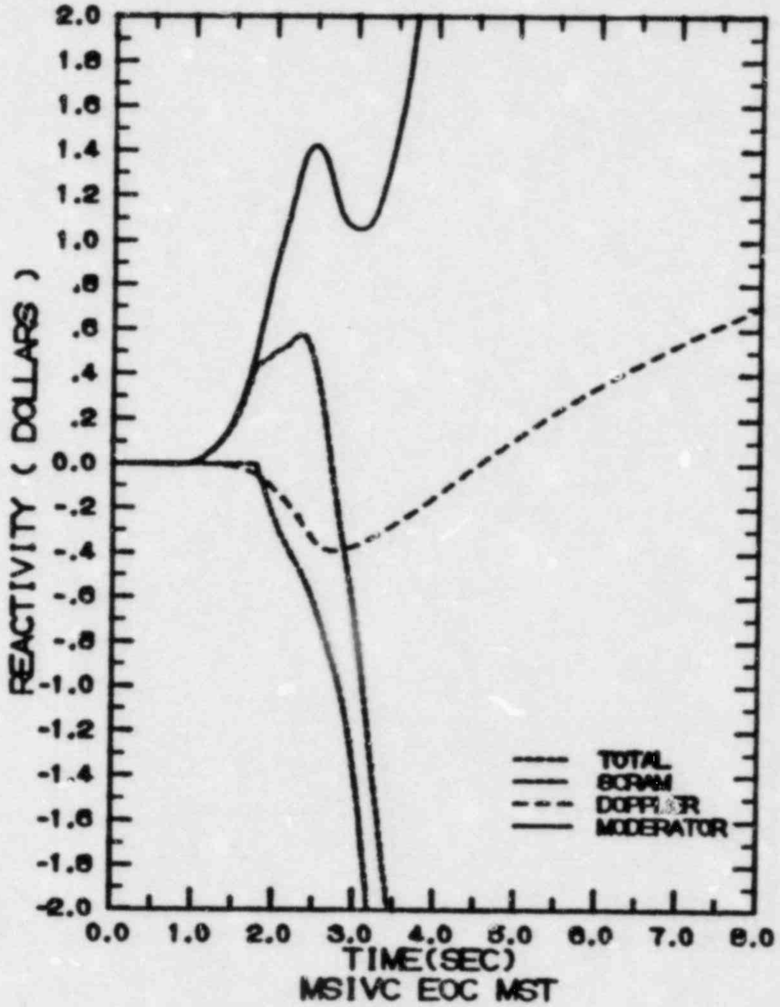

FIGURE 7.3.1-3

MSIV CLOSURE, FLUX SCRAM, EOC10
TRANSIENT RESPONSE VERSUS TIME, "MEASURED" SCRAM TIME

CONTROL ROD PATTERN

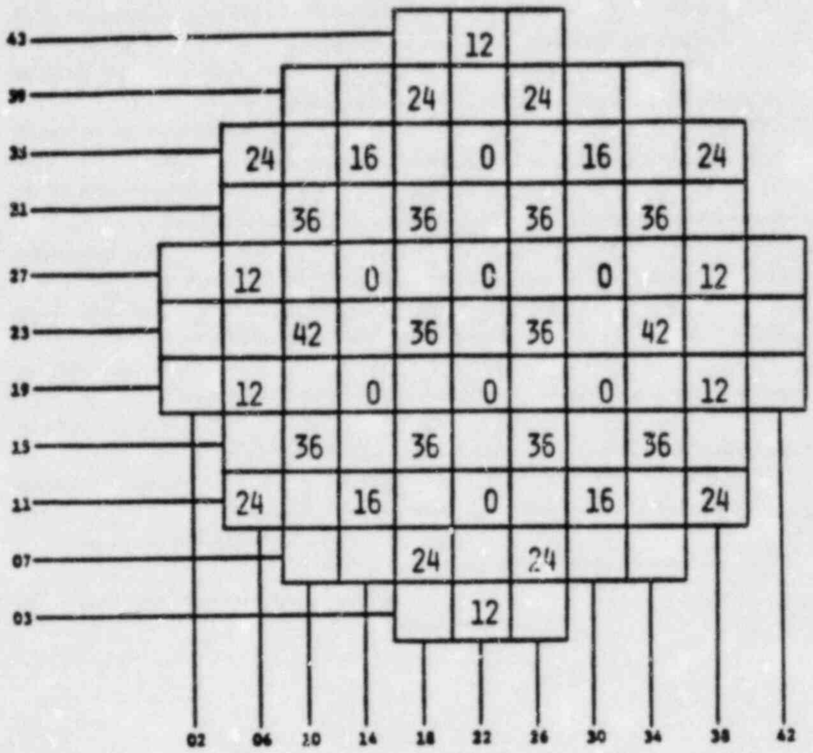

Reactor Conditions:

Core Thermal Power	= 1664 Mwt
Core Flow	= 48 Mlb/hr
Cycle Exposure	= 3600 MWD/T
Xenon Free	
Initial MCPR	= 1.310
Initial LHGR	= 13.4 kw/ft

Case Description

- Operator attempts full withdrawal of the fully inserted rod at coordinates (22, 35).
- Bounding Case.

FIGURE 7.4.1

REACTOR INITIAL CONDITIONS FOR THE VY CYCLE 10 RWE CASE 1

CONTROL ROD PATTERN

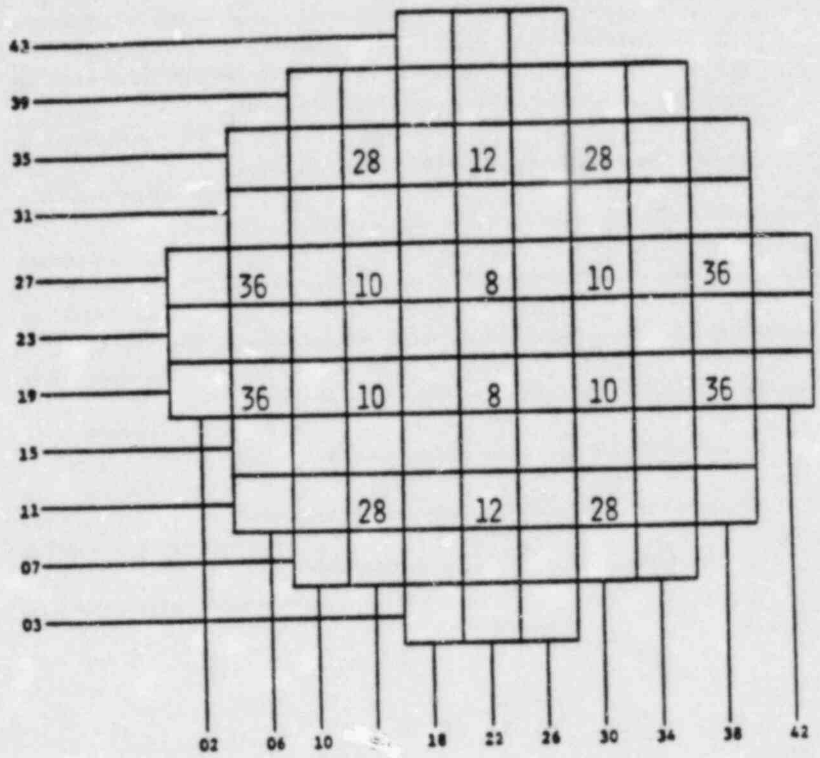

Reactor Conditions:

Core Thermal Power	= 1664 Mwt
Core Flow	= 48 Mlb/hr
Cycle Exposure	= 3600 MWD/T
Equilibrium Xenon	
Initial MCPR	= 1.435
Initial LHGR	= 12.7 kw/ft

Case Description

- Operator attempts full withdrawal of the partially inserted rod at coordinates (22,35).
- Normal Xenon condition and control rod pattern.

FIGURE 7.4.2

REACTOR INITIAL CONDITIONS FOR THE VY CYCLE 10 RWE CASE 2

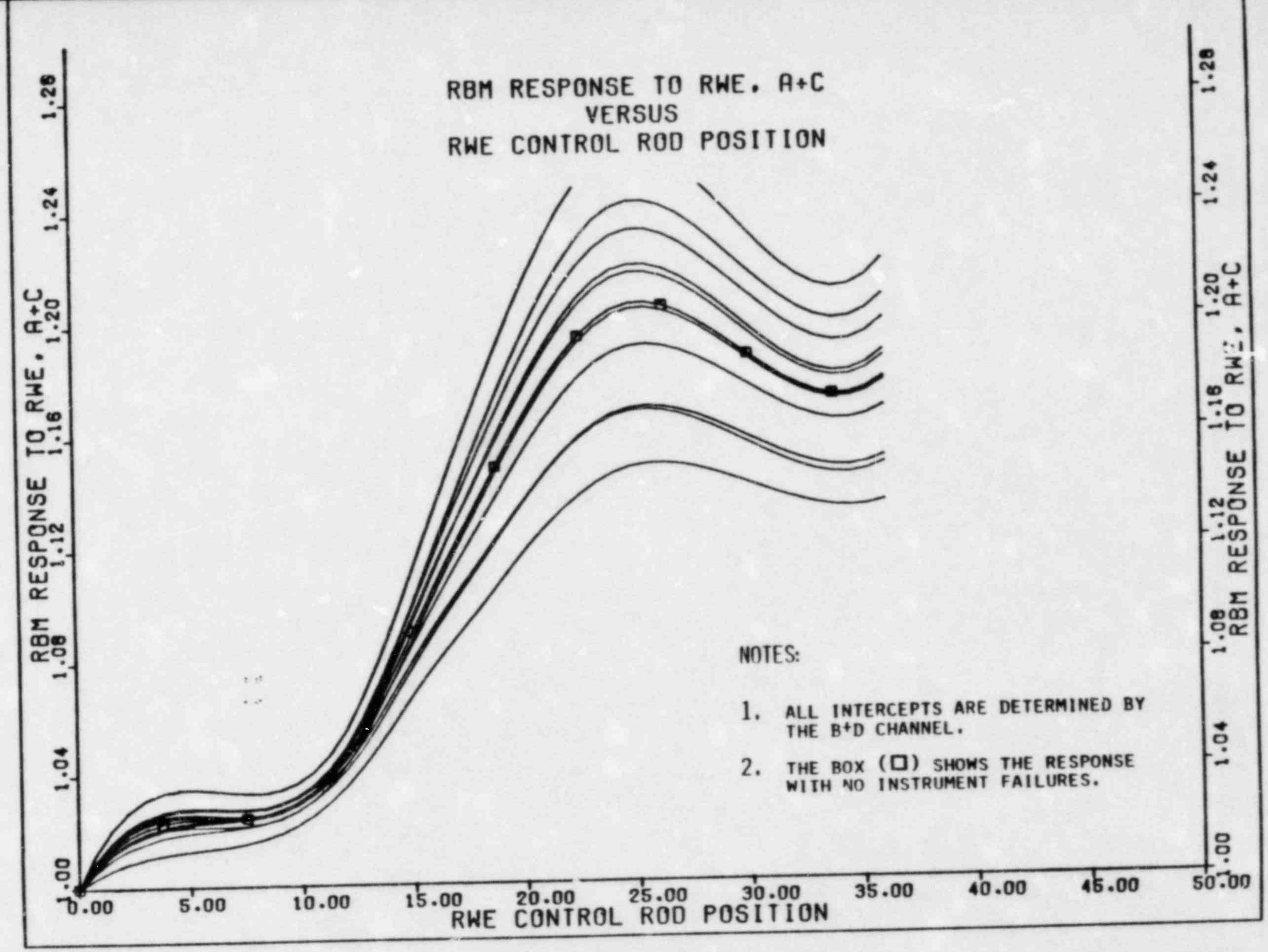

FIGURE 7.4.3

VY CYCLE 10 RWE CASE 1 SETPOINT INTERCEPTS DETERMINED BY THE A+C CHANNEL

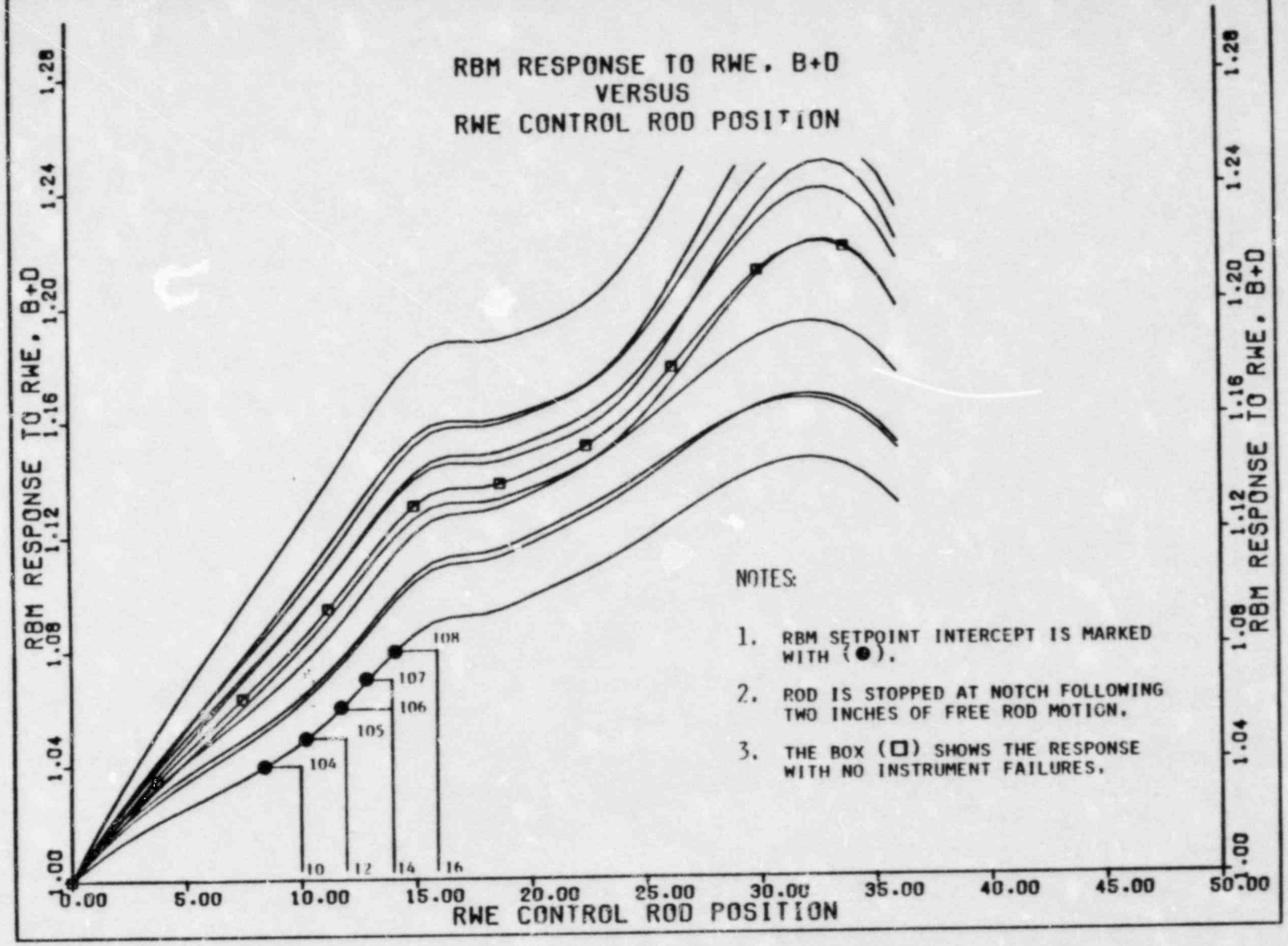

FIGURE 7.4.4

VY CYCLE 10 RWE CASE 1 SETPOINT INTERCEPTS DETERMINED BY THE B+D CHANNEL

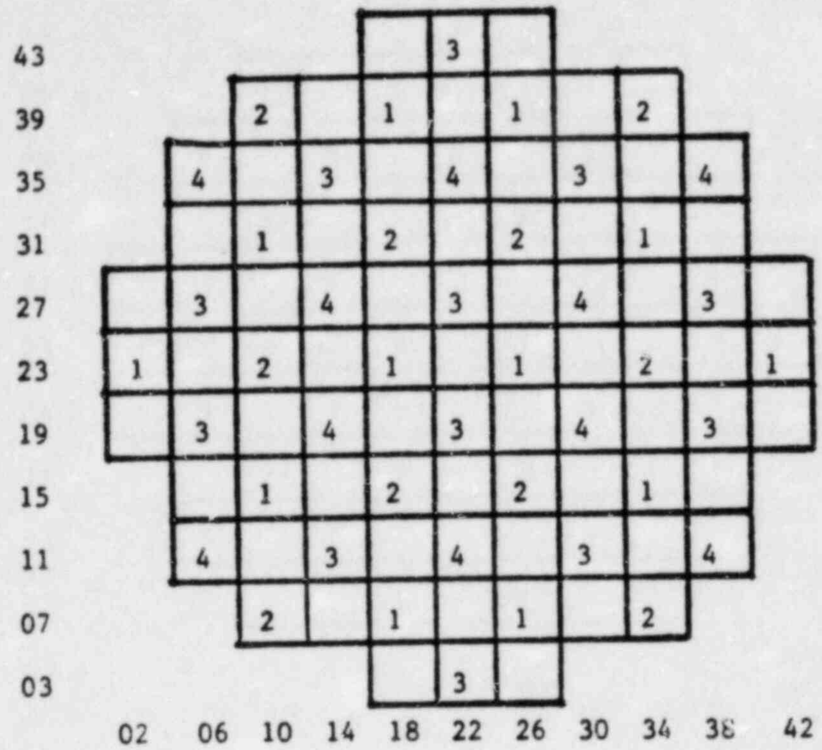

FIGURE 7.6.1 FIRST FOUR ROD ARRAYS PULLED IN THE A SEQUENCES

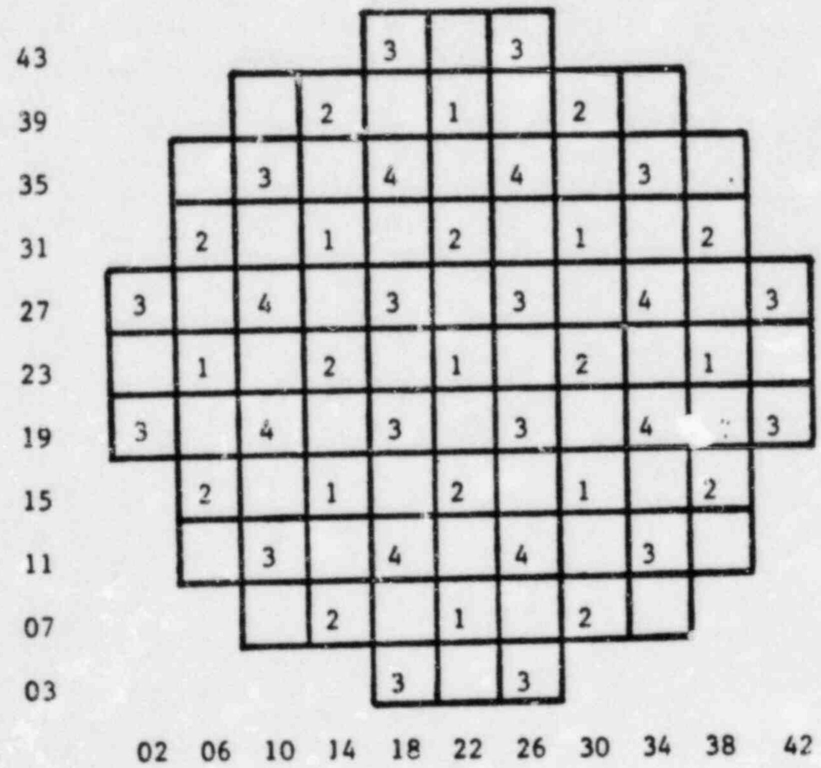

FIGURE 7.6.2 FIRST FOUR ROD ARRAYS PULLED IN THE B SEQUENCES

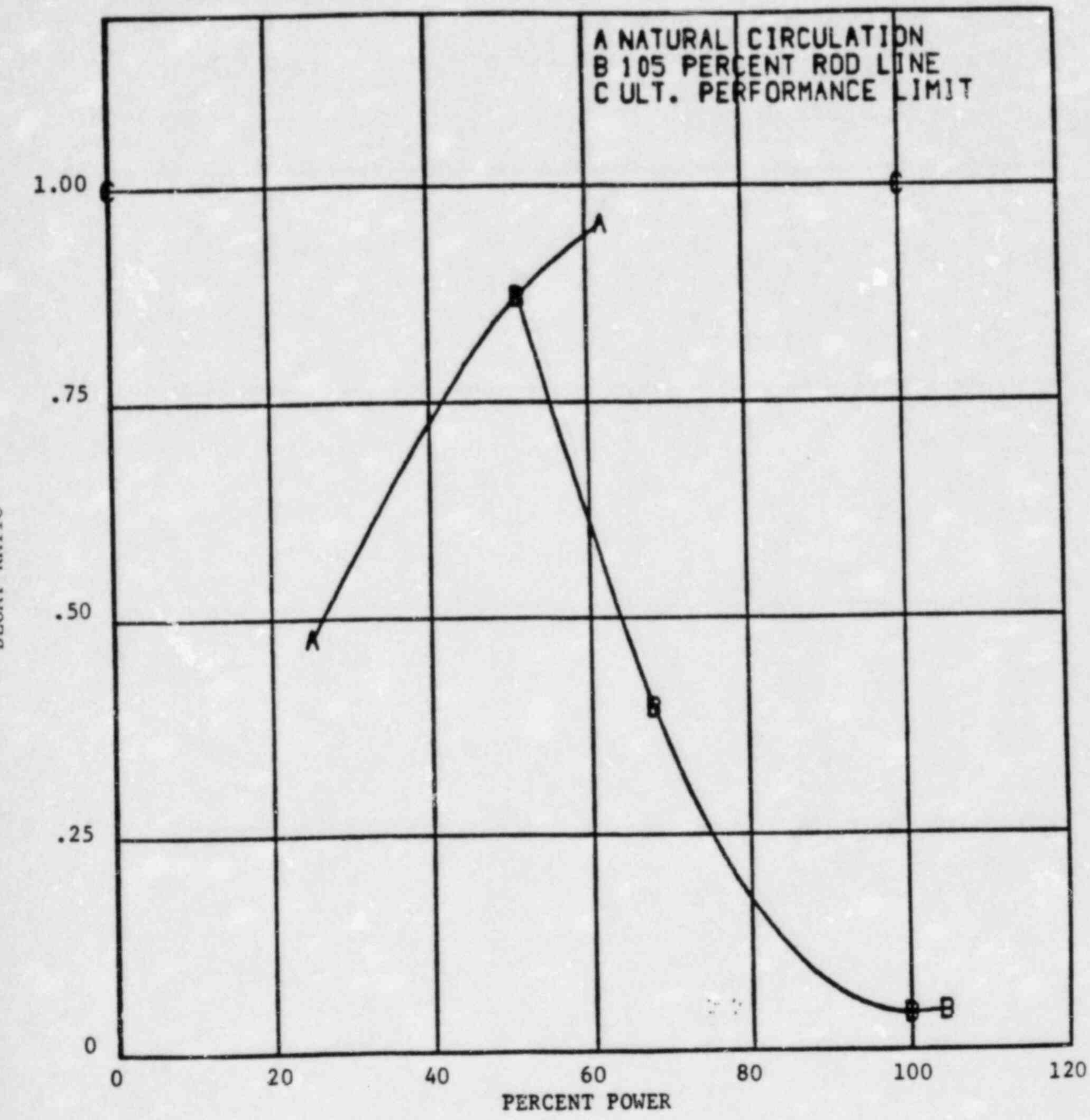

FIGURE 7.7.1

REACTOR CORE DECAY RATIO VERSUS POWER

8.0 STARTUP PROGRAM

Following refueling and prior to vessel reassembly, fuel assembly position and orientation will be verified and videotaped by underwater television.

The Vermont Yankee Startup Program will include process computer data checks, shutdown margin demonstration, in-sequence critical measurement, rod scram tests, power distribution comparisons, TIP reproducibility, and TIP symmetry checks. The content of the Startup Test Report will be similar to that sent to the Office of Inspection and Enforcement subsequent to the start of Cycle 9 [20].

9.0 LOSS-OF-COOLANT ACCIDENT ANALYSIS

The results of the complete evaluation of the loss-of-coolant accident for Vermont Yankee as documented in Reference 21 provide required support for the operation of Vermont Yankee Cycle 10. No new fuel types have been introduced in this reload, therefore, the MAPLHGR limits as a function of average planar exposure remain the same as in the previous cycle. [1,8]

APPENDIX A

CALCULATED CYCLE DEPENDENT LIMITS

The MCPR limits appropriate for Cycle 10 are calculated by adding the calculated ΔCPR to the safety limit LAMCPR of 1.07. This is done for each of the analyses in Section 7 at each of the exposure statepoints. For an exposure interval between statepoints, the highest MCPR limit at either end is assumed to apply to the whole interval.

Table A.1 provides the highest calculated MCPR limits for Cycle 10 for each of the exposure intervals for the various scram speeds and for the various rod block lines.

With regard to MAPLHGR, no new fuel types have been introduced. The MAPLHGR limits given in Reference 8 for the P8X8R fuel type apply to Cycle 10. The MCPR limits presently employed in Cycle 9 are also bounding for Cycle 10. These are given in Reference 8 and are reproduced here as Table A.2.

TABLE A.1

VERMONT YANKEE NUCLEAR POWER STATION
CALCULATED CYCLE 10 MCPR LIMITS

Value of "N" in RBM Equation(1)	Average Control Rod Scram Time	Cycle Exposure Range	MCPR Limit for P8X8R Fuel
42%	"MEASURED"	BOC to EOC-2 GWD/T	1.28
		EOC-2 GWD/T to EOC-1 GWD/T	1.28
		EOC-1 GWD/T to EOC	1.28
	"67B"	BOC to EOC-2 GWD/T	1.28
		EOC-2 GWD/T to EOC-1 GWD/T	1.28
		EOC-1 GWD/T to EOC	1.33
41%	"MEASURED"	BOC to EOC-2 GWD/T	1.24
		EOC-2 GWD/T to EOC-1 GWD/T	1.24
		EOC-1 GWD/T to EOC	1.26
	"67B"	BOC to EOC-2 GWD/T	1.24
		EOC-2 GWD/T to EOC-1 GWD/T	1.25
		EOC-1 GWD/T to EOC	1.33
$\leq$ 40%	"MEASURED"	BOC to EOC-2 GWD/T	1.24
		EOC-2 GWD/T to EOC-1 GWD/T	1.24
		EOC-1 GWD/T to EOC	1.26
	"67B"	BOC to EOC-2 GWD/T	1.24
		EOC-2 GWD/T to EOC-1 GWD/T	1.25
		EOC-1 GWD/T to EOC	1.33

NOTES:

(1) The Rod Block Monitor (RBM) trip setpoints are determined by the equation shown in Table 3.2.5 of the Technical Specifications [Reference 8].

TABLE A.2

THE MCPR OPERATING LIMITS FOR CYCLE 9
ARE BOUNDING FOR CYCLE 10. THESE ARE
FOUND IN REFERENCE 8 AS TABLE 3.11-2

Value of "N" in RBM Equation(1)	Average Control Rod Scram Time	Cycle Exposure Range	MCPR Operating Limit for Fuel Type (2) 8X8	8X8R	P8X8R
42%	Equal or better	BOC to EOC-2 GWD/T	1.29	1.29	1.29
	than L.C.O.	EOC-2 GWD/T to EOC-1 GWD/T	1.29	1.29	1.29
	3.3 C.1.1	EOC-1 GWD/T to EOC	1.30	1.30	1.30
	Equal or better	BOC to EOC-2 GWD/T	1.29	1.29	1.29
	than L.C.O.	EOC-2 GWD/T to EOC-1 GWD/T	1.33	1.31	1.31
	3.3 C.1.2	EOC-1 GWD/T to EOC	1.36	1.35	1.35
41%	Equal or better	BOC to EOC-2 GWD/T	1.25	1.25	1.25
	than L.C.O.	EOC-2 GWD/T to EOC-1 GWD/T	1.26	1.25	1.25
	3.3 C.1.1	EOC-1 GWD/T to EOC	1.30	1.30	1.30
	Equal or better	BOC to EOC-2 GWD/T	1.25	1.25	1.25
	than L.C.O.	EOC-2 GWD/T to EOC-1 GWD/T	1.33	1.31	1.31
	3.3 C.1.2	EOC-1 GWD/T to EOC	1.36	1.35	1.35
$\leq$ 40%	Equal or better	BOC to EOC-2 GWD/T	1.25	1.25	1.25
	than L.C.O.	EOC-2 GWD/T to EOC-1 GWD/T	1.26	1.25	1.25
	3.3 C.1.1	EOC-1 GWD/T to EOC	1.30	1.30	1.30
	Equal or better	BOC to EOC-2 GWD/T	1.25	1.25	1.25
	than L.C.O.	EOC-2 GWD/T to EOC-1 GWD/T	1.33	1.31	1.31
	3.3 C.1.2	EOC-1 GWD/T to EOC	1.36	1.35	1.35
75%	Special Testing at Natural Circulation (Note 3, 4)		1.30	1.31	1.31

(1) The Rod Block Monitor (RBM) trip setpoints are determined by the equation shown in Table 3.2.5 of the Technical Specifications.

(2) The current analyses for MCPR Operating Limits do not include 7X7 fuel. On this basis further evaluation of MCPR operating limits is required before 7X7 fuel can be used in Reactor Power Operation.

(3) For the duration of pump trip and stability testing.

(4) K_f factors are not applied during the pump trip and stability testing.

REFERENCES

1. A. A. F. Ansari, et al., Vermont Yankee Cycle 9 Core Performance Analysis, YAEC-1275, August 1981.

2. General Electric Standard Application for Reactor Fuel (GESTARII), NEDE-24011-P-A-5, GE Company Proprietary, August 1982.

3. D. M. VerPlanck, Methods for the Analysis of Boiling Water Reactors Steady State Core Physics, YAEC-1238, March 1981.

4. E. E. Pilat, Methods for the Analysis of Boiling Water Reactors Lattice Physics, YAEC-1232, December 1980.

5. S. P. Schultz and K. E. St.John, Methods for the Analysis of Oxide Fuel Rod Steady-State Thermal Effects (FROSSTEY) Code/Model Description Manual, YAEC-1249P, April 1981.

6. S. P. Schultz and K. E. St.John, Methods for the Analysis of Oxide Fuel Rod Steady-State Thermal Effects (FROSSTEY) Code Qualification and Application, YAEC-1265P, June 1981.

7. D. C. Albright, H2ODA: An Improved Water Properties Package, YAEC-1237, March 1981.

8. Appendix A to Operating License DPR-28 Technical Specifications and Bases for Vermont Yankee Nuclear Power Station, Docket No. 50-271.

9. A. A. F. Ansari, Methods for the Analysis of Boiling Water Reactors: Steady-State Core Flow Distribution Code (FIBWR), YAEC-1234, December 1980.

10. A. A. F. Ansari, R. R. Gay, and B. J. Gitnick, FIBWR: A Steady-State Core Flow Distribution Code for Boiling Water Reactors - Code Verification and Qualification Report, EPRI NP-1923, Project 1754-1 Final Report, July 1981.

11. General Electric Company, GEXL Correlation Application to BWR 2-6 Reactors, NEDE-25422, GE Company Proprietary, June 1981.

12. A. A. F. Ansari and J. T. Cronin, Methods for the Analysis of Boiling Water Reactors: A Systems Transient Analysis Model (RETRAN), YAEC-1233, April 1981.

13. EPRI, RETRAN - A Program for One-Dimensional Transient Thermal-Hydraulic Analysis of Complex Fluid Flow Systems, CCM-5, December 1978.

14. A. A. F. Ansari, K. J. Burns, and D. K. Beller, Methods for the Analysis of Boiling Water Reactors: Transient Critical Power Ratio Analysis (RETRAN-TCPYA01), YAEC-1299P, March 1982.

15. J. M. Holzer, Methods for the Analysis of Boiling Water Reactors Transient Core Physics, YAEC-1239P, August 1981.

16. C. J. Paone, et al., Rod Drop Accident Analysis for Large Boiling Water Reactors, NEDO-10527, March 1972.

17. R. C. Stirn, et al., Rod Drop Accident Analysis for Large Boiling Water Reactors Addendum No. 1, Multiple Enrichment Cores With Axial Gadolinium, NEDO-10527, Supplement 1, July 1972.

18. D. Radcliffe and R. E. Bates, "Reduced Notch Worth Procedure", SIL-316, November 1979.

19. R. C. Stirn, et al., Rod Drop Accident Analysis for Large Boiling Water Reactor Addendum No. 2 Exposed Cores, NEDO-10527, Supplement 2, January 1973.

20. Letter, FVY 82-21, dated February 25, 1982, E. W. Jackson to R. C. Haynes, Director of USNRC Region I, "Cycle IX Startup Test Report".

21. Loss-of-Coolant Accident Analysis for Vermont Yankee Nuclear Power Station, NEDO-21697, August 1977, as amended.